Designing Novel 1,2,3- and 1,2,4-Triazoles for Coordination Complexes and Frameworks

A Dissertation Presented for the

Doctor of Philosophy

Degree

The University of Tennessee, Knoxville

Brianna Celiese Hughes

August 2015

Copyright © 2015 by Brianna Celiese Hughes.

All rights reserved.

DEDICATION

To the linkers in my life – those who connect me to others and expand my vision and life to be full of happiness and laughter – I love you and am so thankful for the times we've spent together. Let's face it, without y'all I wouldn't be where I am today. Well, maybe, just wouldn't have had a blast along the way!

To the metals – my center to the framework of my life – I love you. Knowing that unending support was only a phone call away helped me through this reaction I've undergone the past 5 years. Thanks for being the best family a girl could ask for.

To the counteranions – thanks for pushing me when I was ready to give up, for counteracting the charges that came full force during the past few years. I've come to love you as family and appreciate each and every one of you. Could not have made it these past five years without the new friendships I've made.

To JACS Daniel – you're my pride and joy. Inspired by chemistry and received in Tennessee, your name will be a constant reminder of who I am and where I come from when I leave the University of Tennessee.

ACKNOWLEDGEMENTS

I would like to acknowledge Dr. David M. Jenkins for being a mentor during my time at the University of Tennessee. My knowledge as a chemist has been pushed and stretched with his guidance and support that has allowed me to grow, not only in knowledge, but also in character. Thank you for the motivation to finish the journey of graduate school.

I would also like to thank those who have been there through thick and thin, whether they had a choice or not, my current and past group members. Thanks to Preeti Chandrachud (little one), Derek Mull, Luke Keller, Kristina Vailonis, and Joe DeJesus. And to past members, Dr. Chi-Linh Do-Tanh, Dr. Zheng Lu, thank you. Special thanks to Dr. Heather M. Bass, Dr. S. Alan Cramer, and Dr. Christopher R. Murdock for guidance in the lab, and friendships that I'd be lost without.

ABSTRACT

Triazoles are versatile ligands that form a variety of compounds and extended materials within the field of coordination chemistry. The reactions of triazoles with metals lead to the synthesis of homoleptic complexes, coordination polymers and metal-organic frameworks (MOFs). These triazole compounds and materials have been employed for a variety of applications in chemistry ranging from nanomaterials to anion recognition.

The synthesis of tris(1,2,3-triazolyl)borate completed and complemented the initial research began by Trofimenko in 1966. This ligand was used in metal reactions and found to form both homoleptic complexes and coordination polymers. The connectivity of the tris(1,2,3-triazolyl)borate varied dependent on the transition metal employed.

The success of incorporating a triazole onto a borate ligand led to further work utilizing novel triazole derivatives. By combining a borane with a 1,2,3-triazole, a borate-nitrenium that has an overall neutral charge was synthesized. Nitrenium ligands are the nitrogen analog of Arduengo's N-heterocyclic carbene and have only recently been explored. Although initial attempts to synthesize a metal complex with the monodentate neutral nitrenium ligands were unsuccessful, these potential complexes could influence our understanding of transition metal bonds.

Metal-organic frameworks were initially synthesized with carboxylates as the organic linkers connected to the metal centers of the scaffold. Recently, triazoles and tetrazoles have been utilized as an alternative for the formation of porous MOFs. The gate-opening effect of some breathing MOFs has been successfully shown with the inclusion of a bis-triazole linker with a rotating central moiety. By extending the central moiety from a phenyl ring to a biphenyl unit on the bis-triazole linker, we were able to demonstrate three separate states of rotation (open/open, open/closed, closed/closed) within three separate MOFs. These separate states were observed through single crystal X-ray diffraction and were the first example of an isostructurally designed family of gate-based breathing MOFs.

Spin-crossover has been shown in iron MOFs by incorporating triazoles and tetrazoles within the organic linker. A family of mixed triazole/tetrazole as well as bis-tetrazole ligands were synthesized and tested with metal salts. A coordination polymer was synthesized with these ligands.

TABLE OF CONTENTS

Chapter 1 Introduction 1

Chapter 2 Synthesis of Di-, Tri-, and Tetrasubstituted Borate Ligands and Their Metal Complexes 10

Abstract 11

Introduction 12

Results and Discussion 14

Conclusion 27

Experimentals 27

Chapter 3 Synthesis Towards a Monodentate Nitrenium Ligand 34

Abstract 35

Introduction 35

Results and Discussion 38

Conclusion 41

Experimentals 45

Chapter 4 Isostructural Design for 2D Breathing MOFs with Aryl Gates 49

Abstract 50

Introduction 51

Results and Discussion 55

Conclusion 77

Experimentals 78

Chapter 5 Preparation of a Coordination Polymer From Mixed Triazole/Tetrazole Ligands 83
Abstract 84
Introduction 84
Results and Discussion 89
Conclusion 94
Experimentals 96
Chapter 6 Conclusions 100
Chapter Summaries 101
Dissertation Summation 104
Potential Future Directions 105
List of References 107
Vita 119

LIST OF TABLES

Table 2.1. Comparison between metal complexes with 1 and analogous complexes with tripodal ligands. 23

Table 3.1. Conditions of metal reactions attempted with ligands 3 and 4. 43

LIST OF FIGURES

Figure 1.1. Various binding modes of 1,2,3-triazoles (top line) and 1,2,4-triazoles (bottom line) with metal ions (M). Dash line separates triazoles (left) from triazolates (right). 3

Figure 1.2. Variations of Trofimenko's initial tris(pyrazolyl)borate shown with one nitrogen (1N) up to four nitrogens (4N) with the year they were published (left). One binding possibility of the tris(pyrazolyl)borate with a metal center (right). 4

Figure 1.3. Carbene (top left) with analogous nitrene (top right). The resonances of nitrenium cation are shown on the bottom. 6

Figure 1.4. Single crystal X-ray structure of Liang's coordination polymer (left) and X-ray crystal structure of Yaghi's porous metal-organic framework (right). 7

Figure 2.1. Tripodal borate ligands with various numbers of nitrogens in heterocylces. The date shows first synthesis of complexes (or ligand). Horizontal double arrows show regioisomers, only one of which is the thermodynamic product. HC = homoleptic complexes and CP = coordination polymers that can be formed with the ligand. 13

Figure 2.2. ESI/MS of di(1,2,3-triazolyl)borate (A) and tetra(1,2,3-triazolyl)borate ligand (B). Inset shows the highlight of the observed peak. 17

Figure 2.3. X-ray crystal structure of extended lattice of $Na(HB(C_2H_2N_3)_3)$, 1. Blue, gray, olive, orange, and white ellipsoids (50% probability) represent N, C, B, Na, and H respectively. All hydrogen atoms except the one bound to boron have been omitted for clarity. 19

Figure 2.4. X-ray crystal structures of Fe (2), Co (3), and Ni (4) complexes. Blue, gray, olive, and white ellipsoids (50% probability) represent N, C, B, and H, respectively while red, yellow, and pink are Fe, Co, and Ni, respectively. Solvent molecules and all hydrogen atoms except the one bound to boron have been omitted for clarity. 21

Figure 2.5. Labeled drawings to accompany Table 2.1. A. Tris(1,2,3-triazolyl)borate complexes. B. Tris(pyrazolyl)borate complexes. C. Tris(1,2,4-triazolyl)borate complexes. 22

Figure 2.6. X-ray crystal structure of Cd coordination polymer (5). Blue, gray, olive, white and aqua coordinate with N, C, B, H, and Cd, respectively. All hydrogen atoms except the one bound to boron have been omitted for clarity. 24

Figure 2.7. PXRD of 5, showing experimental in red and simulated pattern in black. 25

Figure 3.1. N-heterocyclic carbene-type ligands including *p*-block elements (E) with potential bonding to a transition metal center (M). 36

Figure 3.2. Crystal structure of 4 with C, N, and B in black, light blue, and light purple respectively. All hydrogens have been removed for clarity. 42

Figure 3.3. Crystal structure of the dimer of 3 with C, N, and B in black, light blue, and light purple respectively. All hydrogens have been removed for clarity. 44

Figure 4.1. Graphical depiction of a subunit (aryl ring) of the semirigid linker rotating to open and close the pore. Where (a) represents the width of a single subunit, and (b) represents the additional width of extended subunits added to the linker. Green spheres represent metal centers or secondary building units (SBUs), and gray and purple components represent rigid and flexible portions of the ligand, respectively. 54

Figure 4.2. (A) Crystal structure of 3 showing the silver connectivity. (B) Crystal structure of 3 showing silver chains along the *y* axis. (C) Crystal structure of 3 viewed orthogonal to the *y* axis showing the 2D sheet topology. Purple, light blue, black, green, and red spheres represent Ag, N, C, Cl, O, respectively. All hydrogen atoms have been omitted for clarity. 60

Figure 4.3. Crystal structure of 4 shown orthogonal to the *y* axis showing the 2D sheet topology. Royal blue, light blue, black, green, and red spheres represent Cu, N, C, Cl, O, respectively. All hydrogen atoms have been omitted for clarity. 61

Figure 4.4. Crystal structures viewed orthogonal to the *y* axis showing fused-tube topology (A) 5 and (B) 6. Purple, light blue, black, green, and red spheres represent Ag, N, C, Cl, O, respectively. All hydrogen atoms have been omitted for clarity. 63

Figure 4.5. PXRD pattern for 5: experimental (red) and simulated (black).....65

Figure 4.6. PXRD pattern for 6: experimental (red) and simulated (black).....66

Figure 4.7. PXRD patterns showing changes to 5 (A) and 6 (B) as a function of evaporation time. 5 (A) can be resolvated with DMA to give the same PXRD pattern. 67

Figure 4.8. PXRD study for 4, showing changes as a function of evaporation time. Black represents 0 h and increases up to purple at 6 h, with a 1 h time increment. 68

Figure 4.9. PXRD pattern overlay for 5 (red) and 6 (blue) after desolvation in air for 6 h. 69

Figure 4.10. IR measurements as function of evaporation time for 5 (A) and 6 (B) (ROYGBIV as each hour increases starting from 0 h to 6 h). 71

Figure 4.11. IR study for 4, showing changes as a function of evaporation time. (ROYGBIV as each hour increases, starting from 0 h to 6 h). 72

Figure 4.12. Full solid state ^{13}C CP-MAS NMR spectrum of 4 (A) and 5 (B). Inset shows highlighted crystal structure with labeled C atoms. Asterisks denote spinning sidebands. 74

Figure 4.13. SSNMR for 3, with spinning sidebands denoted by asterisks. 75

Figure 4.14. SSNMR for 6, with spinning sidebands denoted by asterisks. 76

Figure 5.1. A d^6 iron(II) ion undergoing a spin-state transition as a function of temperature. 86

Figure 5.2. Schematic representation of a SCO MOF. Red circles represent Fe^{II} sites, blue circles represent the triazole/tetrazole ligand, and the shaded spheres show the change in pore size. 90

Figure 5.3. Crystal structure of 8 with carbon, nitrogen, carbon/nitrogen (locations of the triazole/tetrazolate cycles of the ligand are idealized since two types of the sites were equally disordered by symmetry), and copper in white, royal blue, light purple, and aqua. All hydrogen atoms have been removed for clarity. 95

LIST OF SCHEMES

Scheme 2.1 Synthesis of tris(1,2,3-triazolyl)borate ligand, 1, and synthesis of HCs and CP from 1.....15

Scheme 3.1. Synthesis of neutral nitrene precursors.....40

Scheme 4.1. Synthesis of di-MTZ^{Biph} (2).....57

Scheme 4.2. Synthesis of silver and copper frameworks.....58

Scheme 5.1. Various reactions to synthesize mixed triazole/tetrazole (4 and 5) and bistetrazole ligands (6 and 7).....91

CHAPTER 1
INTRODUCTION

Triazoles have been used extensively by coordination chemists since their discovery in the late 19th century.[1] Though 1,2,3-triazoles were initially discovered in 1899[2] and 1,2,4-triazoles briefly mentioned in 1885,[3] these organic N-heterocycles were not thoroughly explored until decades later.[1, 4] The versatility of triazoles is demonstrated by their prevalence in diverse fields of chemistry such as pharmacological compounds,[1a, 5] coordination polymers,[1b, 6] and metal-organic frameworks.[1b, 6a, 7]

The latter two classes of materials can be synthesized by incorporating triazoles at the ends of organic linkers to bind a metal center to form an extended framework. Depending on the protonation and substituents of the triazole, both 1,2,3-triazoles and 1,2,4-triazoles can bind to metals (Figure 1.1).[1b] These different binding modes of the triazoles can yield diverse connectivities in coordination polymers and metal-organic frameworks. Their high chemical stability and heteroaromatic character are advantageous for preparing these robust materials.[1b, 1d]

One example that highlights the triazole's versatility is its substitution for a pyrazole in tris(azolyl)borates (Figure 1.2).[8] Tris(azolyl)borates are also known as scorpionate ligands, as described by Trofimenko, allowing for two groups to coordinate to a metal ion while the third "stings" the metal ion by arching over.[9] With the additional nitrogen (from the triazole) present in the borate compared to the pyrazole, a multitude of binding modes can occur with metal ions to form frameworks. By synthesizing tris(triazolyl)borates and combining these ligands with metal salts, both homoleptic complexes and coordination polymers can be synthesized with varying metal centers.[8c, d, 10]

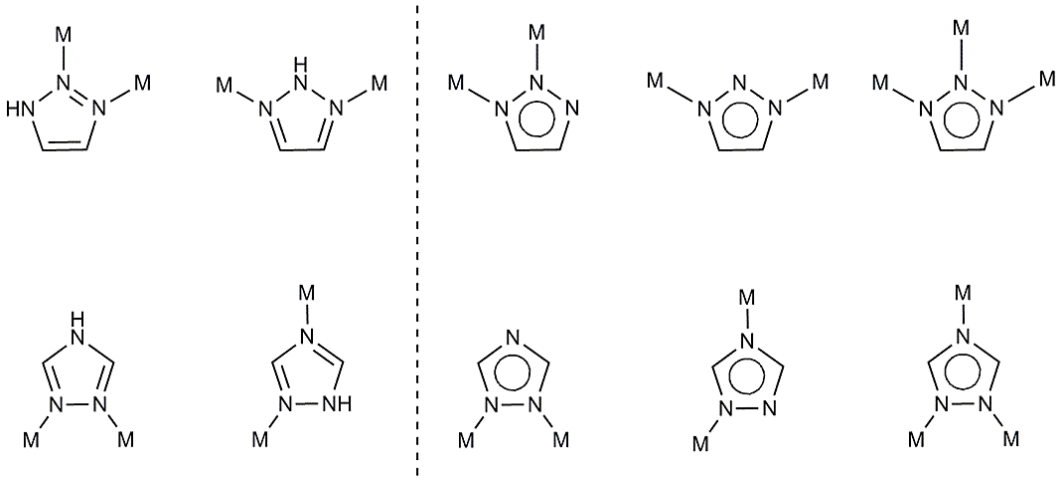


Figure 1.1. Various binding modes of 1,2,3-triazoles (top line) and 1,2,4-triazoles (bottom line) with metal ions (M). Dash line separates triazoles (left) from triazolates (right).

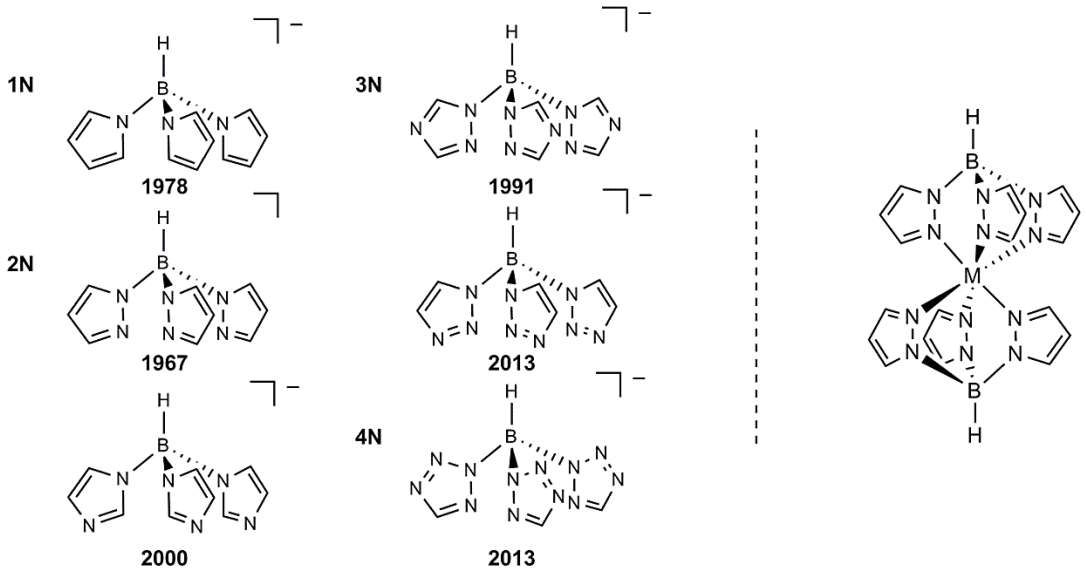


Figure 1.2. Variations of Trofimenko's initial tris(pyrazolyl)borate shown with one nitrogen (1N) up to four nitrogens (4N) with the year they were published (left). One binding possibility of the tris(pyrazolyl)borate with a metal center (right).

In addition to azolylborates, recently, 1,2,3-triazoles have been demonstrated to be an alternative to the well-known N-heterocyclic carbene[11] by forming a nitrene or nitrenium ion (Figure 1.3).[4, 12] A nitrene is the nitrogen counterpart of the carbene, simply replacing the central carbon with a nitrogen atom. The nitrenium ion has been examined by Gandelman and coworkers since 2011, who demonstrated that chelating arms on the triazolium ring help form a bond between a metal ion and the central nitrogen.[12b]

Although these ligands could contribute to coordination complexes, as mentioned previously, triazoles may also be incorporated as ligands for extended frameworks and coordination materials. Coordination polymers (CPs) can be described as "A coordination compound with repeating coordination entities extending in one, two, or three dimensions."[13] CPs are infinite systems made with metal ions and organic linkers that are linked via a coordination bond.[14] A CP can also be repeated in two or three dimensions, therefore making an extended coordination compound known as a coordination network.[13] Within this coordination network subset are metal-organic frameworks (MOFs), which also contain potential voids (Figure 1.4).[15] Major MOF researchers described these materials in such a way as to include the numerous systems that are both static and dynamic.[13]

Metal-organic frameworks are synthesized in a combinatorial approach, by varying metal salts, metal to ligand ratio, solvent, temperature, and time a variety of frameworks are made possible. MOFs are characterized as possessing coordination

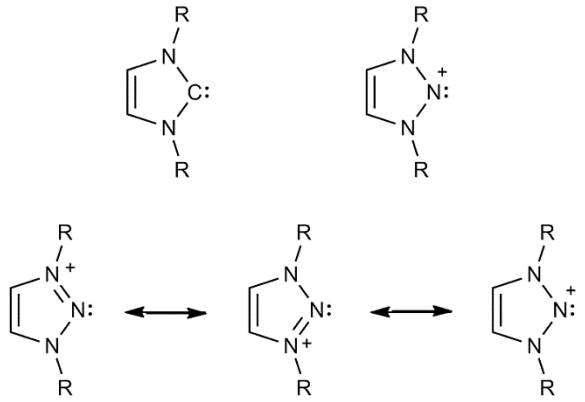
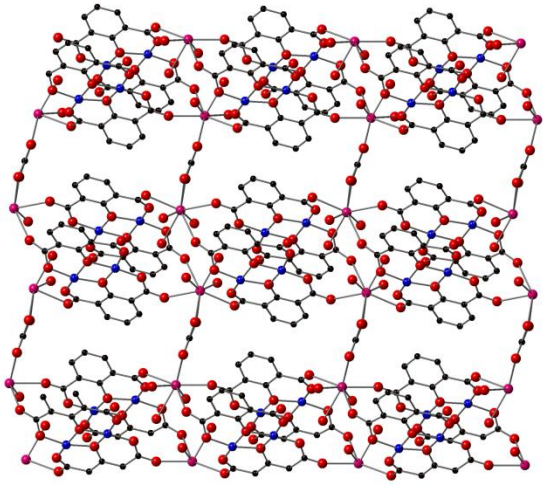
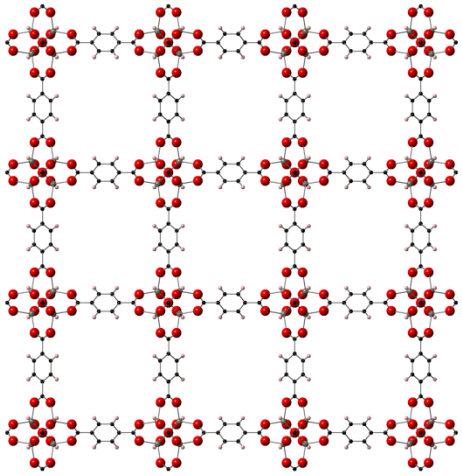


Figure 1.3. Carbene (top left) with analogous nitrene (top right). The resonances of nitrenium cation are shown on the bottom.



Coordination Polymer



Metal-Organic Framework

Figure 1.4. Single crystal X-ray structure of Liang's coordination polymer (left) and X-ray crystal structure of Yaghi's porous metal-organic framework (right).

bonds between organic linkers and metal ions that create a robust crystalline framework that can then be tailored to achieve specific properties.[16] Static frameworks maintain their original robust, porous crystalline structure[16-17] while dynamic frameworks can "breathe" or open/close at the pore of the structure. Numerous mechanisms of breathing have been identified by MOF chemists some of which include flexing at the metal-ligand interface or a rotation of the organic linker.[18]

Dynamic MOFs have rapidly increased in number with many different routes to breathing have been described.[19] These methods include multiple dimensions and fall into three categories as defined by Kitagawa: one dimensional coordination polymers that form a rhombus in the remaining dimensions, two dimensional coordination polymer layers connected through a flexible ligand, and three dimensional interpenetrating networks.[19] Other methods to modify the breathing in these frameworks include a gate effect,[18j, k] allowing the ligand to rotate thus opening and closing the pores, or incorporating spin-crossover properties.[1b, 19-20]

One mechanism that has been proposed for MOF breathing is spin-crossover (SCO). SCO occurs when metal ions change between spin states (high spin and low spin) under external perturbations such as temperature, pressure, or light.[21] Not only has SCO been showcased in small metal complexes, but recent research has focused on supramolecular chemistry by incorporating this property within crystalline molecular networks.[20a, 22] These materials allow for the reversible absorption of guest molecules within the pores of the framework switching on, or off, the SCO process.[21a, 23]

We explored the many binding modes of triazoles through coordination chemistry and their incorporation into new frameworks. Homoleptic complexes, metal-organic frameworks and coordination polymers have been synthesized and characterized utilizing 1,2,3-triazoles or 1,2,4-triazoles. The synthesis of our triazolylborate completed a family of tris(azolyl)borates that had previously been synthesized.[10c] Building on the azolylborate concept, we explored the synthesis of a monodentate neutral nitrenium ion. Finally, by incorporating a 1,2,4-triazole in a biphenyl linker, the gate effect was successfully shown in two dimensional metal-organic frameworks. These MOFs were the first of an isostructurally designed family of gate-based breathing MOFs, in which all possible breathing states were observed through single crystal X-ray diffraction. Lastly, breathing MOFs can also be synthesized by incorporating spin crossover properties. We synthesized a variety of mixed triazole/tetrazole and tetrazole ligands to explore spin crossover MOFs.

CHAPTER 2
SYNTHESIS OF DI-, TRI-, AND TETRASUBSTITUTED BORATE LIGANDS AND THEIR METAL COMPLEXES

A version of this chapter was originally published by Brianna C. Hughes, Zheng Lu, and David M. Jenkins:

Hughes, Brianna C.; Lu, Zheng; Jenkins, David M. “The final unadorned tris(azolyl)borate: finishing what Trofimenko started in 1966.” *Chem. Comm.* **2014**, *50*, 5273-5275.

All work presented herein is the work of Brianna Hughes with assistance in crystallography by Zheng Lu.

Abstract

The final addition to the tris(azolyl)borate ligand family, tris(1,2,3-triazolyl)borate, has been synthesized. The sodium salt of the ligand forms a complex polymeric structure where both N2 and N3 bind to crystallographically independent sodium ions. Depending on the divalent transition metal, tris(1,2,3-triazolyl)borate forms either molecular homoleptic complexes or coordination polymers. Other variants, di- and tetra(1,2,3-triazolyl)borate ligands, will also be discussed although they were not successfully isolated and purified.

Introduction

Since the introduction of tris(pyrazolyl)borate by Trofimenko in 1966,[8a] tripodal azolyl borate ligands have revolutionized the field of coordination chemistry.[8g, h, 9c, 24] Since his initial reports, variants of tris(azolyl)borates with substituents on the carbons have served as auxiliary ligands in a remarkable breadth of research including catalysis,[8g, 25] small molecule activation,[25d, 26] and bioinorganic mimics.[8g, 25d, 27] What Trofimenko may not have suspected is that his synthetic strategy of mixing simple five-membered N-heterocycles with alkali metal borohydrides would be modified to afford a wide range of simple tripodal ligands where nitrogen atoms are placed on each position on the five-membered ring (Figure 2.1).

While tris(pyrazolyl)borate often yields octahedral homoleptic complexes (HCs) with two ligands bound to a metal center and tris(imidazolyl)borate can form coordination polymers (CPs) (Figure 2.1),[8g-k, 8m] from a structural perspective, the more interesting cases are ambidentate tris(azolyl)borate ligands, which require three or more nitrogen atoms in each ring. The most widely studied ligand of this type is tris(1,2,4-triazolyl)borate which normally binds to a metal center in the same manner as tris(pyrazolyl)borate leading to HCs with metals such as Fe, Co, Ni, and Zn (Figure 2.1).[8d, 10b, 28] Janiak and Youm have demonstrated that these molecular complexes can be building blocks for forming larger CPs.[8c, 29] Finally, earlier this year Winter and

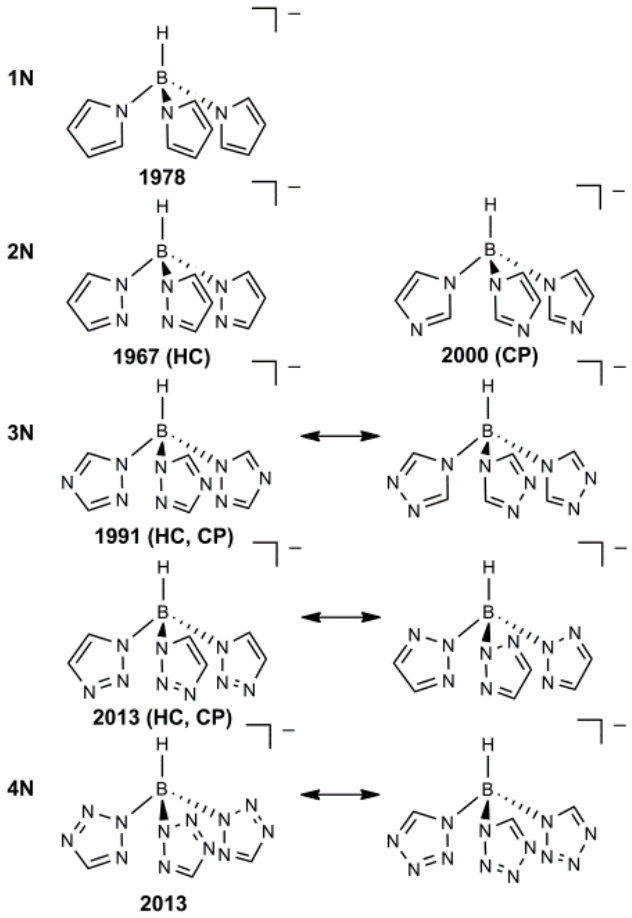


Figure 2.1. Tripodal borate ligands with various numbers of nitrogens in heterocylces. The date shows first synthesis of complexes (or ligand). Horizontal double arrows show regioisomers, only one of which is the thermodynamic product. HC = homoleptic complexes and CP = coordination polymers that can be formed with the ligand.

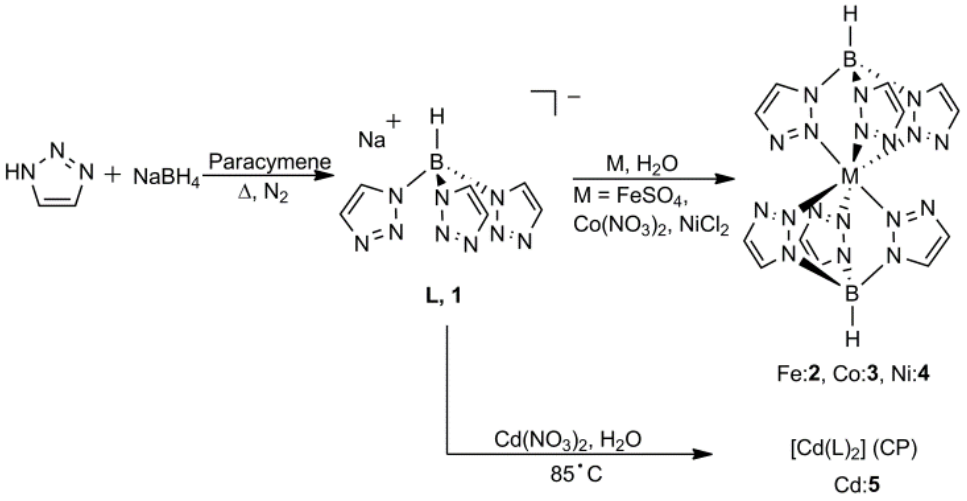
coworkers reported the synthesis of tris(1,2,3,5-tetrazolyl)borate, but did not report any transition metal complexes or CPs (Figure 2.1).[30]

Despite the immense diversity of tris(azolyl)borate ligands that have been synthesized, the simplest 1,2,3-triazole variation of this classic ligand motif has never been prepared (Figure 2.1, fourth from top on left). While a handful of accounts have reported a variant, tris(1,2,3-benzotriazolyl)borate, neither simple HCs, nor CPs have been crystallographically characterized with that tripodal ligand.[8e, f, 8l, 31] We sought to rectify this glaring omission and synthesize tris(1,2,3-triazolyl)borate and its first complexes.

Results and Discussion

Our synthetic strategy for tris(1,2,3-triazolyl)borate was derived from the preparation of analogous tris(azolyl)borates.[8a, b, 24] Under a nitrogen atmosphere, sodium borohydride and 1,2,3-triazole were mixed in a 1 : 4 ratio in paracymene. The resulting heterogeneous mixture was stirred vigorously at 180˚C for one week. After cooling to room temperature, the resulting white solid was collected and washed with toluene and hexanes. To remove trace impurities, the solid was stirred in tetrahydrofuran and the supernatant was decanted. The white solid was dried, yielding pure **1** in a 90.4% yield (Scheme 2.1).

Scheme 2.1 Synthesis of tris(1,2,3-triazolyl)borate ligand, 1, and synthesis of HCs and CP from 1.



In order to be complete, other synthetic methods were attempted to synthesize both the di- and tetra(1,2,3-triazolyl)borate ligands. Their syntheses were also derived from analogous azolyl borates.[8a, b, 24] The di(1,2,3-triazolyl)borate was made under nitrogen atmosphere, with a ratio of 1 : 3 sodium borohydride and 1,2,3-triazole in toluene. This mixture was allowed to stir vigorously for three days at 90℃. The reaction was cooled and a sticky off-white solid was collected and washed with toluene and hexanes (Figure 2.2). Methods to isolate and purify this borate included crystallization techniques with water as the solvent, as well as multiple toluene washes, to no avail.

As for the tetra(1,2,3-triazolyl)borate ligand, a ratio of 1 : 5 for sodium borohydride and 1,2,3-triazole in hexyl ether was used. This solution was heated to 228℃, and had an additional 3 equivalents of 1,2,3-triazole added after three days to continue for one week. The triazole was added to ensure enough of this reactant was present for the reaction to continue to completion, as the triazole has a boiling point of 90℃ and could be boiled off at such high temperatures. After cooling to room temperature, a sticky off-solid was removed from solution and washed with toluene and hexane (Figure 2.2). Similar to the di(1,2,3-triazolyl)borate, methods to isolate and purify this borate included crystallization techniques with water as the solvent, as well as multiple toluene washes, to no avail.

Tris(1,2,3-triazolyl)borate (**1**) was characterized by solution NMR (^{1}H, ^{13}C, and ^{11}B) and single crystal X-ray diffraction. Solution NMR demonstrates that **1** has three-

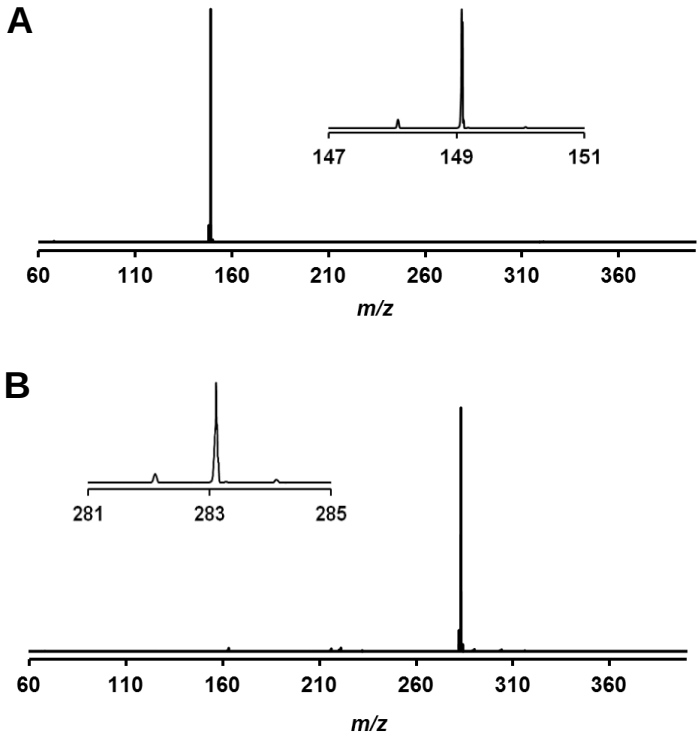


Figure 2.2. ESI/MS of di(1,2,3-triazolyl)borate (A) and tetra(1,2,3-triazolyl)borate ligand (B). Inset shows the highlight of the observed peak.

fold symmetry and resonances are consistent with similar tris(azolyl)borates.[8b, 10b, 32] X-ray crystallography shows **1** has two distinct sodium atoms, designated Na1 and Na2, that are each coordinated by six nitrogens from the tris(1,2,3-triazolyl)borate ligand (Figure 2.3). Na1 is coordinated to six N2 atoms from two separate tris(1,2,3-triazolyl)borates. Each Na1–N2 has a consistent bond length of 2.495(1) Å with cis bond angles of 77.19(3)° for N2–Na1–N2'. Na2 is coordinated to six N3 atoms, and unlike Na1, these bonds are formed from six separate tris(1,2,3-triazolyl)borates. The individual Na2–N3 bond distances are each 2.522(1) Å with cis bond angles of 81.91(5)°. Thus, each tris(1,2,3-triazolyl)borate coordinates with four separate sodium centers, one Na1 and three Na2, which forms an extended lattice structure.

Since tris(1,2,3-triazolyl)borate is ambidentate, a variety of structures are possible based on the choice of metal and its oxidation state. To determine which binding motif would occur for each metal center, we investigated reactions with different metal salts, including examples with Mg, Mn, Fe, Co, Ni, Zn, Pd, Ag, Cd, Sn, Eu, and Hg. From these screening reactions, we identified four metals, Fe, Co, Ni, and Cd that easily yielded HCs or CPs with **1**. Fe, Co, and Ni salts led to HCs (**2**, **3**, and **4**, respectively), while a Cd salt afforded a CP (**5**). These metal complexes of Fe, Co, and Ni were synthesized with a metal to ligand ratio of 1 : 2 in water at room temperature. The Cd CP was also prepared in a metal to ligand ratio of 1 : 2 in an aqueous reaction at 85 °C. All of these reactions afforded crystals suitable for single crystal X-ray diffraction.

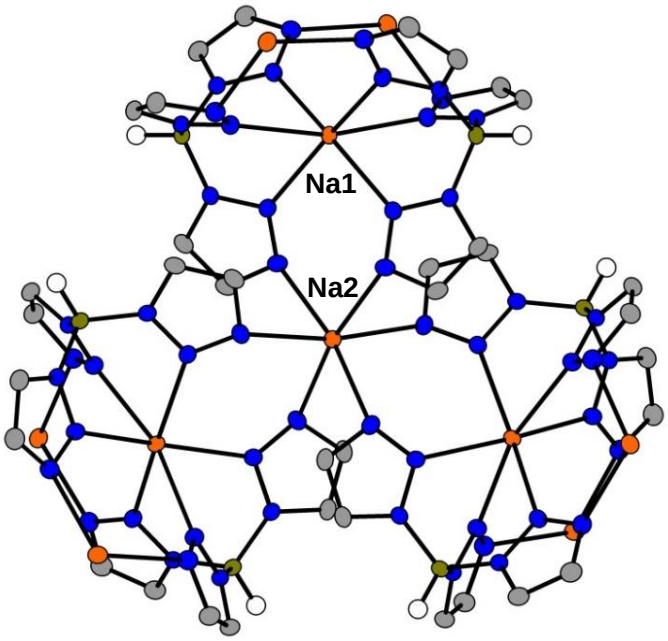


Figure 2.3. X-ray crystal structure of extended lattice of $Na(HB(C_2H_2N_3)_3)$, 1. Blue, gray, olive, orange, and white ellipsoids (50% probability) represent N, C, B, Na, and H respectively. All hydrogen atoms except the one bound to boron have been omitted for clarity.

Each HC with Fe, Co, and Ni, crystallizes in the $R\bar{3}$ space group and has an octahedral geometry. The two tridentate ligands adopt a mutually staggered conformation coordinating to six N2 atoms around the metal ion (Figure 2.4). The bond distances of our Fe, Co, and Ni complexes are comparable to the bond lengths of the well-known tris(pyrazolyl)borate ligand complexes and the tris(1,2,4-triazolyl)borate ligand complexes with the same respective metals (Figure 2.5 and Table 2.1).[10b, 28, 33]

Homoleptic tris(pyrazolyl)borate complexes of Fe are reported to undergo spin-crossover,[33c] so we investigated **2** for this phenomenon. When comparing the low spin data (Table 2.1) with our Fe complex, we can conclude that **2** is also in the low-spin state, due to its similar bond lengths and angles, as well as the typical red color of the crystals.[33c] To bolster our assignment of **2** as a low spin complex, we also obtained a CP/MAS ^{13}C NMR spectrum, which showed two peaks at 135.70 and 139.43 ppm, which is in agreement with the two separate carbons crystallographically observed.

With Cd a CP is formed that is distinct from both the first row complexes, as well as, previously made Cd complexes with similar tripodal ligands.[34] Single crystal X-ray diffraction shows that the Cd binds to **1** through the N3 atoms (Figure 2.6) and the bond lengths range from 2.341(1) Å to 2.354(1) Å. Each Cd center is surrounded by six separate tripodal ligands in the same manner as Na2 in the crystal structure of **1**, which means that **5** has the same topology as the structure of **1**, but without the encapsulated Na1. Powder X-ray diffraction (PXRD) was also taken in order to confirm the cadmium CP structure (Figure 2.7).

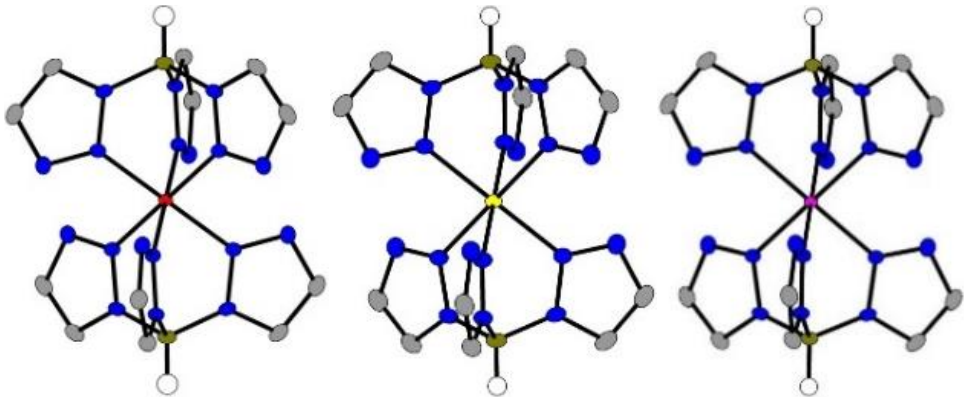


Figure 2.4. X-ray crystal structures of Fe (2), Co (3), and Ni (4) complexes. Blue, gray, olive, and white ellipsoids (50% probability) represent N, C, B, and H, respectively while red, yellow, and pink are Fe, Co, and Ni, respectively. Solvent molecules and all hydrogen atoms except the one bound to boron have been omitted for clarity.

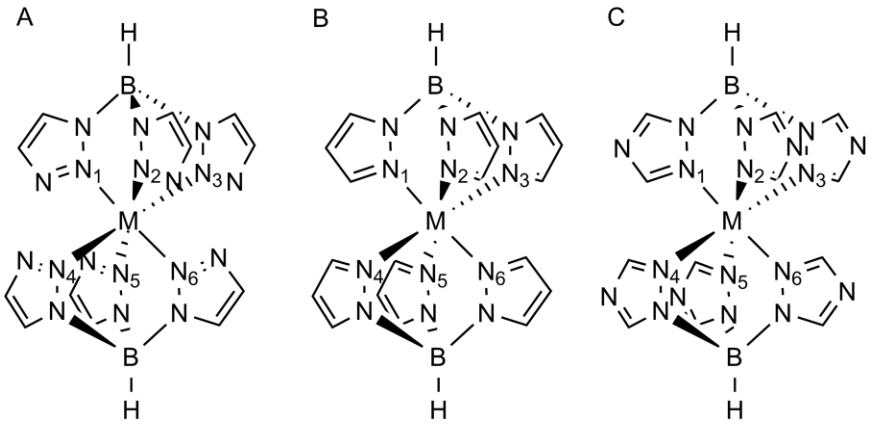


Figure 2.5. Labeled drawings to accompany Table 2.1. A. Tris(1,2,3-triazolyl)borate complexes. B. Tris(pyrazolyl)borate complexes. C. Tris(1,2,4-triazolyl)borate complexes.

Table 2.1. Comparison between metal complexes with 1 and analogous complexes with tripodal ligands.

	Fe			Co			Ni		
	2	**2b**	**2c**	**3**	**3b**	**3c**	**4**	**4b**	**4c**
Ligand	1,2,3-triazolyl	pyrazolyl	1,2,4-triazolyl	1,2,3-triazolyl	pyrazolyl	1,2,4-triazolyl	1,2,3-triazolyl	pyrazolyl	1,2,4-triazolyl
Space Group	$R\bar{3}$	$P\bar{1}$	Cmca	$R\bar{3}$	$P2_1/n$	Cmca	$R\bar{3}$	$P2_1/n$	Cmca
Bond Lengths (Å)									
M-N(1)	1.957(1)	1.987(1)	1.994	2.102(1)	2.133(7)	2.128	2.067(9)	2.088(2)	2.079(3)
M-N(2)	1.957(1)	1.977(1)	1.994	2.102(1)	2.130(7)	2.121	2.067(9)	2.098(2)	2.095(2)
M-N(3)	1.957(1)	1.978(1)	1.992	2.102(1)	2.120(7)	2.128	2.067(9)	2.090(3)	2.089(2)
M-N(4)	1.957(1)	1.980(1)	1.992	2.102(1)	2.133(8)	2.128	2.067(9)	2.087(2)	2.082(3)
M-N(5)	1.957(1)	1.977(1)	1.994	2.102(1)	2.128(8)	2.121	2.067(9)	2.104(3)	2.095(2)
M-N(6)	1.957(1)	1.983(1)	1.994	2.102(1)	2.140(7)	2.128	2.067(9)	2.091(2)	2.089(2)
Bond Angles (average in ˚)									
Cis (intra)	88.52(4)	88.40(7)	87.91	86.19(5)	85.5(5)	85.27	87.13(4)	86.7(8)	86.19(7)
Cis (inter)	91.48(4)	91.60(8)	92.09	93.81(5)	94.5(3)	94.73	92.87(4)	93.2(8)	93.80(6)
Trans	180.00(5)	178.74(4)	180	180.00(5)	177.3(3)	180	180.00(6)	178.4(4)	179.58(4)

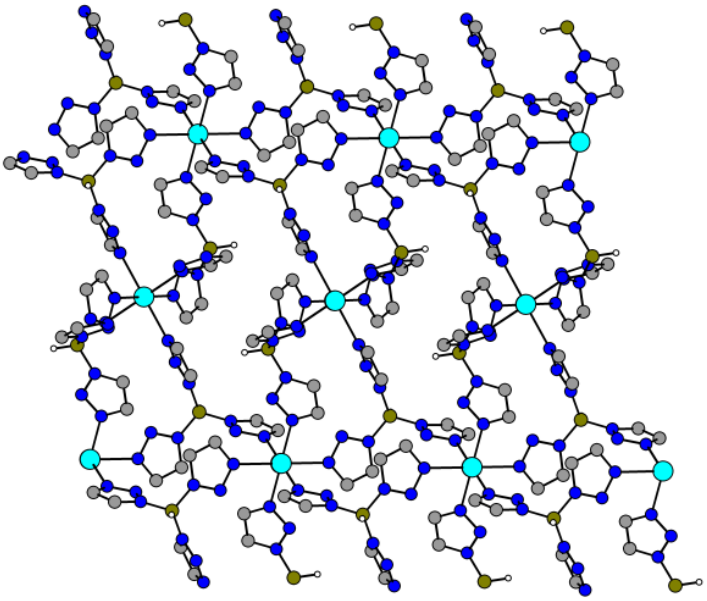


Figure 2.6. X-ray crystal structure of Cd coordination polymer (5). Blue, gray, olive, white and aqua coordinate with N, C, B, H, and Cd, respectively. All hydrogen atoms except the one bound to boron have been omitted for clarity.

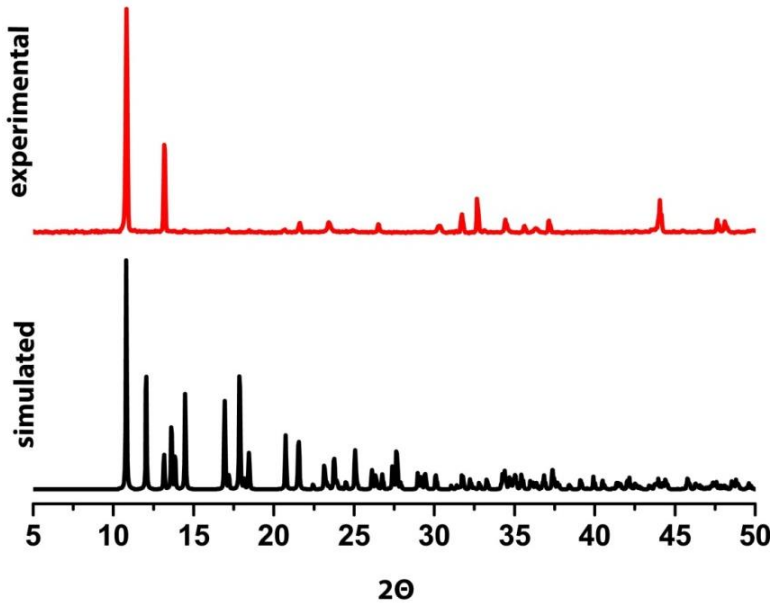


Figure 2.7. PXRD of 5, showing experimental in red and simulated pattern in black.

While no corresponding Cd CP has been synthesized with a tris(azolyl)borate ligand, two comparisons to this structure are worthwhile. First, Ellis and coworkers reported a Cd HC with tris(pyrazolyl)borate, where the crystal structure is isostructural to our previously mentioned monomers with Fe, Co, and Ni. The Cd–N2 bond lengths for Ellis' Cd structure ranged from 2.282(5) Å to 2.371(6) Å.[34] Second, Bu's boron imidazolate framework (BIF), BIF-6, has an analogous ligand, the tris(imidazolyl)borate framework, showing similar connectivity with Cu as the metal center instead of Cd.[35] Given the ambidentate nature of tris(1,2,3-triazolyl)borate, we have determined that at least for Cd, the ligand behaves more like an imidazolate than a pyrazolate.

To compare the effect of binding through N3 versus N2, we obtained a cross-polarization magic-angle-spinning (CP-MAS) ^{13}C NMR spectrum of **5**, which showed three resonances at 126.94, 131.28, and 133.40 ppm. Careful observation of the crystal structure of **5** shows six distinct carbon sites, which explains why more than two resonances are observed. These peak positions in **5** are shifted upfield versus **2**, which can be attributed to the different binding motifs between the Fe complex (N2 binding) and Cd CP (N3 binding). For comparison, Marchetti and coworkers synthesized an octahedral Cd complex with tris(4-bromo-1H-pyrazol-1-yl)borate, which had resonances at 137.0 and 141.2 ppm for the C3 and C5 atoms and a resonance at 93.5 ppm for the bromine substituted C4.[36]

Conclusion

In conclusion, we have synthesized tris(1,2,3-triazolyl)borate, the final unadorned member of the tripodal family of tris(azolyl)borates. In addition, the di- and tetra(1,2,3-triazolyl)borate ligands were also synthesized, although these ligands were not completely isolated and purified. The sodium variant of tris(1,2,3-triazolyl)borate was characterized by multi-nuclear NMR and single crystal X-ray diffraction. This ambidentate ligand forms octahedral metal complexes on Fe, Co, or Ni that are isostructural to their tris(pyrazolyl)borate and tris(1,2,4- triazolyl)borate counterparts. However, upon investigation of a second row transition metal, Cd, we were able to synthesize a CP that binds to the metal through the N3 atoms that is similar to BIFs that have been formed with tris(imidazolyl)borates. These initial results suggest that by exploring a variety of metals and reaction conditions, it will be possible to prepare additional HCs and CPs with this new ambidentate tripodal ligand.

Experimentals

All reagents were purchased from commercial vendors and used without purification. Solution ^{1}H, $^{13}C\{^{1}H\}$, and ^{11}B NMR spectra were recorded at ambient temperature on a Varian Mercury 300 MHz, Bruker Advance 400 MHz, or Varian VNMRS 500 MHz, narrow-bore broadband system. ^{1}H and $^{13}C\{^{1}H\}$ NMR chemical

shifts were referenced to the residual solvent. ^{11}B chemical shifts are reported relative to an external standard of neat BF_3•OEt_2. Solid ^{13}C CP-MAS NMR samples were recorded on a Varian Inova 400 MHz spectrometer and referenced to an external adamantane sample. All mass spectrometry analyses were conducted at the Mass Spectrometry Center located in the Department of Chemistry at the University of Tennessee. The ESI/MS analyses were performed using a QSTAR Elite quadrupole time-of-flight (QTOF) mass spectrometer with an electrospray ionization source from AB Sciex (Concord, Ontario, Canada). Sample solutions of ligand (**1, 6** and **7**) for mass spectrometry were prepared in acetonitrile. Infrared spectra were collected on a Thermo Scientific Nicolet iS10 with a Smart iTR accessory for attenuated total reflectance. Thermogravimetric analysis data were collected on a TA Instruments TGA Q50 under N_2. Carbon, hydrogen, and nitrogen analyses were obtained from Atlantic Microlab, Norcross, GA.

Synthesis of Na(HB($C_2H_2N_3$)$_3$) (L), (1). Sodium borohydride ($NaBH_4$) (0.138 g, 3.62 mmol) and 1,2,3-triazole (1.00 g, 14.5 mmol) were combined in a 50 mL round bottom flask with paracymene (15 mL) and stirred. The reaction was heated to 180 °C for one week during which time a white solid formed. The reaction mixture was cooled to room temperature and the white solid was collected on a 60 mL fine sintered-glass frit and was washed with toluene (3 x 10 mL) and hexanes (3 x 10 mL). The solid was moved to a 20 mL scintillation vial with tetrahydrofuran (10 mL) and stirred for 4 h. After allowing the solid to settle, the solvent was decanted. Additional THF (5 mL) was added

and this mixture was then filtered using a medium sintered glass frit, leaving the pure white solid product that was dried under reduced pressure (0.782 g, 90.4% yield). Crystals suitable for single crystal X-ray diffraction were grown by slow evaporation from water. ^{1}H NMR (DMSO-$_{d6}$, 499.74 MHz): δ 7.76 (s, 3H), 7.56 (s, 3H), 5.23 (br, 1H). ^{1}H NMR (D_2O, 499.74 MHz): δ 7.78 (s, 3H), 7.76 (s, 3H). ^{13}C NMR (DMSO-*d_6*, 125.67 MHz): δ 131.68, 127.27. ^{13}C NMR (D_2O, 125.67 MHz): δ 132.17, 127.74. ^{11}B NMR (DMSO-*d_6*, 128.42 MHz): δ -1.36. IR (neat): 3137, 2457, 1664, 1477, 1421, 1278, 1227, 1194, 1123, 1096, 1061, 1024, 958, 867, 806, 740, 700 cm^{-1}. HR-ESI-MS (*m*/*z*): $[L]^-$ $C_6N_9H_7B$ 216.0924 (calcd.); 216.0916 (found).

Synthesis of Fe(L)$_2$, (2). Iron(II) sulfate pentahydrate (0.0303 g, 1.04 mmol) and **1** (0.0450 g, 2.08 mmol) were added to separate 20 mL scintillation vials and dissolved with 5 mL and 15 mL of water, respectively. The solution of **1** was then pipetted slowly into the iron sulfate solution and left at room temperature. After 3 d, red block crystals had formed (0.0399 g, 78.7% yield). CP-MAS ^{13}C NMR (100.53 MHz) δ 139.43, 135.70. IR (neat): 3117, 2916, 2517, 1472, 1436, 1376, 1288, 1262, 1204, 1189, 1134, 1098, 1058, 1034, 961, 794, 783, 740, 683, 647 cm^{-1}. Anal. Calcd. for $C_{12}H_{14}B_2N_{18}Fe$: C, 29.54; H, 2.89; N, 51.68. Found: C, 29.23; H, 2.98; N, 50.60.

Synthesis of Co(L)$_2$, (3). Cobalt(II) nitrate hexahydrate (0.0303 g, 1.04 mmol) and **1** (0.0450 g, 2.08 mmol) were added to separate 20 mL scintillation vials and dissolved with 3 mL and 6 mL of water, respectively. The solution of **1** was then pipetted slowly

into the metal solution and left at room temperature. After 3 d, yellow block crystals had formed (0.0337 g, 65.9% yield). IR (neat): 3174, 2500, 1473, 1438, 1284, 1249, 1190, 1133, 1060, 1032, 961, 812, 767, 736, 687 cm^{-1}. Anal. Calcd. for $C_{12}H_{14}B_2N_{18}Co$: C, 29.36; H, 2.87; N, 51.36. Found: C, 29.46; H, 2.78; N, 51.08.

Synthesis of $Ni(L)_2$, (4). Nickel(II) chloride hexahydrate (0.0247 g, 1.04 mmol) and **1** (0.0450 g, 2.08 mmol) were added to separate 20 mL scintillation vials and dissolved with 3 mL and 6 mL of water, respectively. The solution of **1** was then pipetted slowly into the metal solution and left at room temperature. After 3 d, pink block crystals had formed (0.0355 g, 69.5% yield). IR (neat): 3263, 3155, 3140, 2561, 2174, 1688, 1647, 1476, 1443, 1296, 1262, 1209, 1140, 1071, 1040, 967, 890, 771, 732 cm^{-1}. Anal. Calcd. for $C_{12}H_{14}B_2N_{18}Ni$: C, 29.37; H, 2.88; N, 51.38. Found: C, 29.53; H, 2.79; N, 51.13.

Synthesis of $Cd(L)_2$, (5). Cadmium(II) nitrate tetrahydrate (0.0321 g, 1.04 mmol) and **1** (0.0450 g, 2.08 mmol) were added to separate 20 mL scintillation vials and dissolved with 10 mL of water each. The solution of **1** was added to the metal solution by pipette. The vial was then heated to 85 °C overnight in an aluminum heating block. Colorless needle crystals were formed and collected using a Buchner funnel and filter paper (0.0522g, 95.3% yield). CP-MAS ^{13}C NMR (100.53 MHz) δ 133.40, 131.28, 126.94. IR (neat): 3364, 3134, 2476, 1650, 1482, 1422, 1286, 1279, 1227, 1214, 1204, 1121,

1105, 1094, 1069, 1021, 971, 878, 788, 760, 742, 728, 694 cm^{-1}. Anal. Calcd. for $C_{12}H_{14}B_2N_{18}Cd$: C, 26.48; H, 2.59; N, 46.31. Found: C, 25.74; H, 2.60; N, 44.84.

Synthesis of $Na(HB(C_2H_2N_3)_2)$, (6). Sodium borohydride ($NaBH_4$) (0.110 g, 2.90 mmol) and 1,2,3-triazole (0.600 g, 8.70 mmol) were combined in a 50 mL round bottom flask with toluene (15 mL) and stirred. The reaction was heated to 90 °C for three days during which time an off-white sticky solid formed. The reaction mixture was cooled to room temperature and the off-white solid was collected on a 60 mL fine sintered-glass frit and was washed with toluene (3 x 10 mL) and hexanes (3 x 10 mL). ^{1}H NMR (DMSO-$_{d6}$, 499.74 MHz): δ 7.56 (s, 1H), 7.49 (s, 0.4H), 7.424 (t, 2H). HR-ESI-MS (*m*/*z*): $[L]^-$ $C_4N_6H_6B$ 149.0747 (calcd.); 149.0666 (found).

Synthesis of $Na(HB(C_2H_2N_3)_4)$, (7). Sodium borohydride ($NaBH_4$) (0.0647 g, 1.70 mmol) and 1,2,3-triazole (0.600 g, 8.70 mmol) were combined in a 50 mL round bottom flask with hexyl ether (15 mL) and stirred. The reaction was heated to 228 °C for three days, and 0.600 g of additional 1,2,3-triazole was added. The reaction continued stirring for the remainder of a week during which time an off-white sticky solid formed. The reaction mixture was cooled to room temperature and the off-white solid was collected on a 60 mL fine sintered-glass frit and was washed with toluene (3 x 10 mL) and hexanes (3 x 10 mL). ^{1}H NMR (DMSO-$_{d6}$, 499.74 MHz): δ 7.75 (s, 1H), 7.62 (s, 1H), 7.54(s, 1H). HR-ESI-MS (*m*/*z*): $[L]^-$ $C_8N_{12}H_8B$ 283.1088 (calcd.); 283.0831(found).

X-ray Structure Determinations. X-ray diffraction measurements were performed on single crystals coated with Paratone oil (Hampton Research) and mounted on glass fibers or nylon cryoloops (Hampton Reasearch). Each crystal was frozen under a stream of N_2 while data were collected on a Bruker SMART APEXII three circle diffractometer equipped with a CCD area detector and operated at 1,800 W power (45 kV, 40 mA) to generate Mo Kα radiation (λ = 0.71073 Å). A matrix scan using at least 12 centered reflections was used to determine initial lattice parameters. Reflections were merged and corrected for Lorenz and polarization effects, scan speed, and background using SAINT 4.05. Absorption corrections, including odd and even ordered spherical harmonics were performed using SADABS, if necessary. Space group assignments were based upon systematic absences, *E* statistics, and successful refinement of the structure. The structures were solved by direct methods with the aid of successive difference Fourier maps, and were refined against all data using the SHELXTL 5.0 software package.

Powder X-ray experiments. Powder X-ray diffraction (PXRD) data was collected using a Panalytical Empyrean θ-2θ diffractometer in reflectance Bragg-Brentano geometry. Cu-Kα radiation (λ = 1.5406 Å; 1,800 W, 45 kV, 40 mA) was focused using a planar Gobel Mirror riding the Kα line. Diffracted radiation was detected using a PIXcel3d detector [(6° 2θ sampling width) equipped with a Ni monochrometer]. All samples were mounted onto a zero background quartz plate fixed on a sample holder by dropping powders and then leveling the sample surface. The best counting statistics were

achieved by using a 0.0131º 2θ step scan from 4 – 50° with an exposure time of 81.6 s per step and a revolution spin rate of 4 s.

CHAPTER 3
SYNTHESIS TOWARDS A MONODENTATE NITRENIUM LIGAND

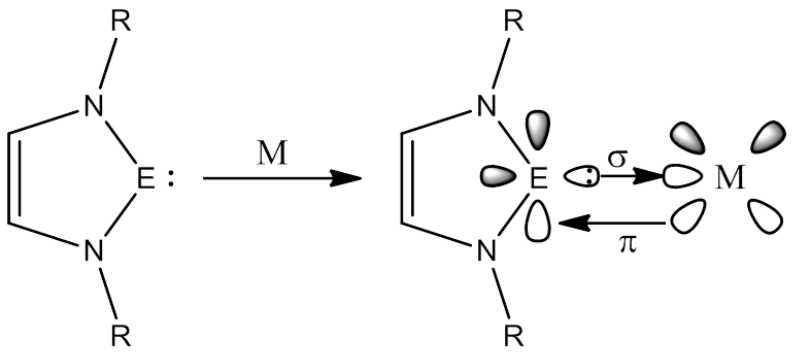
All work presented herein is the work of Brianna Hughes with assistance from a Research Experience for Undergraduates (REU) participant, Asmita Shrestha.

Abstract

The all nitrogen analogue of N-heterocyclic carbenes (NHCs) is still relatively unexplored long after the initial discovery of NHCs by Arduengo. Various main group elements, except nitrogen, have since replaced the center carbon on the carbene, including many from Groups 13-15, and these have proven beneficial in transition metal coordination chemistry. To date, only chelating nitrenium ions have been synthesized. This initial investigation searches for a monodentate neutral nitrene ligand and reports the findings thus far.

Introduction

Since the initial discovery and success of N-heterocyclic carbenes (NHCs) by Arduengo,[37] numerous analogs have been explored (Figure 3.1).[38] Atoms from Groups 13-15 have replaced the central carbon within the carbene, allowing for different features to be associated dependent on the atom used; for example, Groups 13 and 14 are nucleophilic in nature while the atoms from Group 15 have electrophilic properties.[38a-e, 39] The use of silylenes (silicon as the central atom in the carbene) has recently shown to provide facile routes to synthesize complex silacyclic compounds that



Where E =

Anionic	Neutral	Cationic
B	C	N
Al	Si	P
Ga	Ge	As
In	Sn	Sb
Tl	Pb	Bi

Figure 3.1. N-heterocyclic carbene-type ligands including *p*-block elements (E) with potential bonding to a transition metal center (M).

could in turn be developed into the sila pharmaceutical industry.[40] Incorporating a boron within the N-heterocycle allowed for lithium boryl complexes to be achieved, which opened up a new synthetic route to other metal boryl complexes, that could potentially lead to lithium halide elimination.[38a] Despite these advances, the nitrogen analog has barely been explored.

The challenge of incorporating nitrogen into a carbene is the cationic nature of the nitrenium analog. The ease of binding to a metal center is therefore hindered, and alterations to the nitrenium ligand must be made to overcome this problem. Gandelman and coworkers incorporated a chelating ligand that allowed the central nitrogen of the nitrenium ligand to effectively bind to a metal center.[12b] With a pincer-type system, both Rh^{I} and Ru^{II} complexes were synthesized and characterized employing the first nitrenium ion as a free ligand. Further research with the nitrenium ligand included a nitrenium-Ni complex that integrated a cyclam within the nitrenium ligand.[12a] Gandelman and coworkers later showcased the pincer-type nitrenium ions bound to several metals including Mo^{0}, Ru^{0}, Rh^{III}, Pd^{II}, and Ag^{I}.[4] Nevertheless, these nitrenium ligands required an additional binding site within the ligand, and thus a monodentate example has yet to be investigated.

We sought to prepare a monodentate neutral nitrenium ligand, thus alleviating the cationic charge associated with previously mentioned examples. This can be achieved by incorporating a borane on an arm of the nitrenium ligand, counterbalancing the positive charge formerly seen, as well as contributing as a directing group to the central nitrogen. The synthesis of azolyl borates has been studied extensively, dating

back to the original azolyl borates by Trofimenko in 1966.[8a, b, 8g, h, 9c, 24] However, utilizing boranes on 1,2,3-triazoles (essentially preparing a borate) has only recently been explored by Shi and coworkers in 2009.[41] This group discovered that triazole-boranes have improved stability of the N-B bond, as well as possessing stability towards air, moisture, and heat. Thus, including a borane within the nitrenium ion would allow for a neutral monodentate ligand to be prepared. While we have yet to be successful in this endeavor, this chapter describes our progress towards this goal.

Results and Discussion

The first step to synthesize novel neutral nitrene ligands was to develop a family of 1,2,3-triazole pieces to then combine with different borane sources. Initial reactions included the addition of a methyl group or an isopropyl group onto the triazole source. Triethyl borane and triphenyl borane were tested as the two borane sources. Once these neutral nitrene ligands were confirmed by NMR and X-ray crystallography, a variety of metal complexation reactions were attempted.

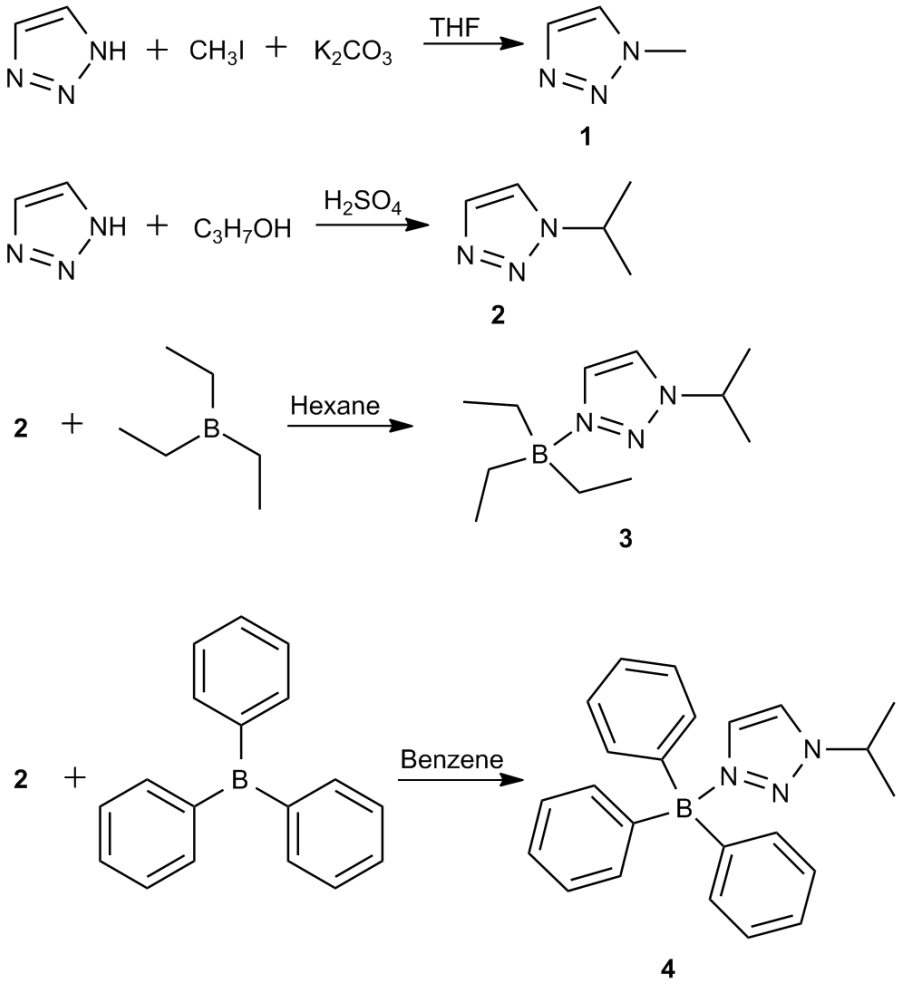
1-methyl-1,2,3-triazole (**1**) was synthesized following a previous procedure[42] wherein tetrahydrofuran (THF) and 1,2,3-triazole were added together and allowed to stir. Potassium carbonate and methyl iodide were added and the resulting mixture was allowed to stir for three hours at room temperature. The extra solvent was removed

under reduced pressure and the product was collected as a yellow liquid in a 29.7% yield (Scheme 3.1).

1-isopropyl-1,2,3-triazole (**2**) was synthesized through a modification from the method of Koren.[43] 1,2,3-triazole and sulfuric acid were combined in a flask and isopropyl alcohol (IPA) was then added drop-wise. The resulting mixture was allowed to stir for 40 hours. This solution was then added to ice and the pH was changed to neutral by the addition of potassium hydroxide. The resulting solution was then extracted with methylene chloride, and the organic layer was dried over magnesium sulfate. The solvent was removed under reduced pressure and the product was collected as a pure clear liquid in 57.4% yield (Scheme 3.1).

Once these initial triazole fragments were synthesized, the next step was the addition of a borane source in order to complete the process of making a neutral nitrenium ligand. 1-isopropyl-1,2,3-triazole (**2**) was added to hexane in air free conditions and allowed to stir. Triethyl borane was then added to the solution and was allowed to stir at room temperature overnight. The resulting solution was concentrated under reduced pressure and the pure product, 1-(1-isopropyl-1,2,3-triazole)triethyl borate, was collected as a clear liquid in a 96% yield (**3**, Scheme 3.1). Under similar conditions, 1-(1-isopropyl-1,2,3-triazole)triphenyl borate (**4**) was synthesized with the addition of triphenyl borane in benzene to **2** in benzene in air free conditions. The solution was allowed to stir at room temperature until a precipitate formed. After 30 minutes, a white solid precipitated out and volatiles were then removed under reduced

Scheme 3.1. Synthesis of neutral nitrene precursors.



pressure. The residue was washed with benzene and the residual solvent was removed under reduced pressure. The pure product, 1-(1-isopropyl-1,2,3-triazole)triphenyl borate, was collected as an off-white solid (59.7% yield) (**4**, Scheme 3.1). **4** also crystallized through desolvation in THF and vapor diffusion with pentane (Figure 3.2).

The resulting nitrenium ligands (**3** and **4**) were then combined with a variety of metals ranging from nickel, palladium and platinum (Table 3.1). Unfortunately, these reactions were unsuccessful in producing a metal complex.

With one particular metal reaction however, **3** with palladium(II) iodide in THF, a crystal structure was obtained from the solution allowing to sit at room temperature. Instead of a metal complex as expected, two ligands of **3** combined to form a dimer-like complex shown in Figure 3.3. This structure was also characterized by ^{1}H, as well as ^{13}C NMR.

Conclusion

N-heterocyclic carbenes (NHCs) have been an asset in varying fields of chemistry. Thus it comes as no surprise that varying analogs of NHCs have been explored. As the nitrogen counterpart, nitrenium ligands have only recently been researched as a potential ligand that can be used in a variety of applications similar to that of NHCs. This work showed recent attempts at synthesizing a monodentate neutral nitrenium ligand as well as metal complex reactions attempted thus far.

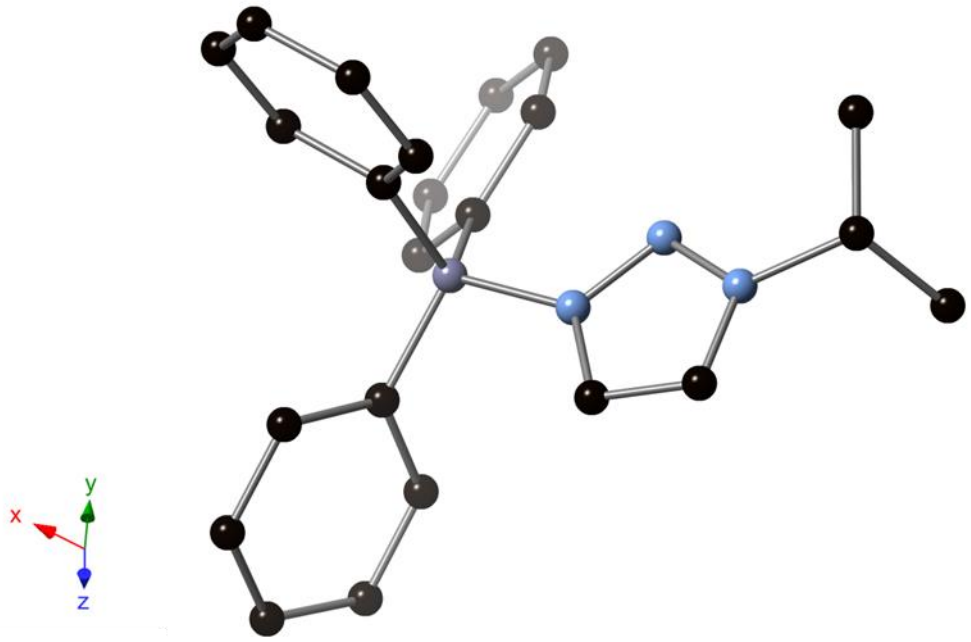


Figure 3.2. Crystal structure of 4 with C, N, and B in black, light blue, and light purple respectively. All hydrogens have been removed for clarity.

Table 3.1. Conditions of metal reactions attempted with ligands 3 and 4.

Ligand	Metal	Solvent*	Ratio (M:L)	Temperature (˚C)
3	PdI_2	THF	1:2	50, 60, RT
		Benzene-*d*	1:2	RT and 50
		ACN	1:2	60
	Tris(dibenzylideneacetone)dipalladium(0)	THF	1:4	RT
		Benzene-*d*	1:4	RT
		Toluene	1:4	70
	Dichlorobis(benzonitrile)platinum(II)	Benzene-*d*	1:2	50
		ACN	1:2	60
	NiI_2	THF	1:2	60 and RT
		ACN	1:2	60
4	PdI_2	THF	1:2	RT
		Toluene	1:2	70
		Benzene-*d*	1:2	RT
	CoI_2	Benzene	1:2	70
	$FeBr_2$	Benzene	1:2	RT
	$CrCl_2$	Benzene	1:2	RT

* : THF = tetrahydrofuran, ACN = acetonitrile

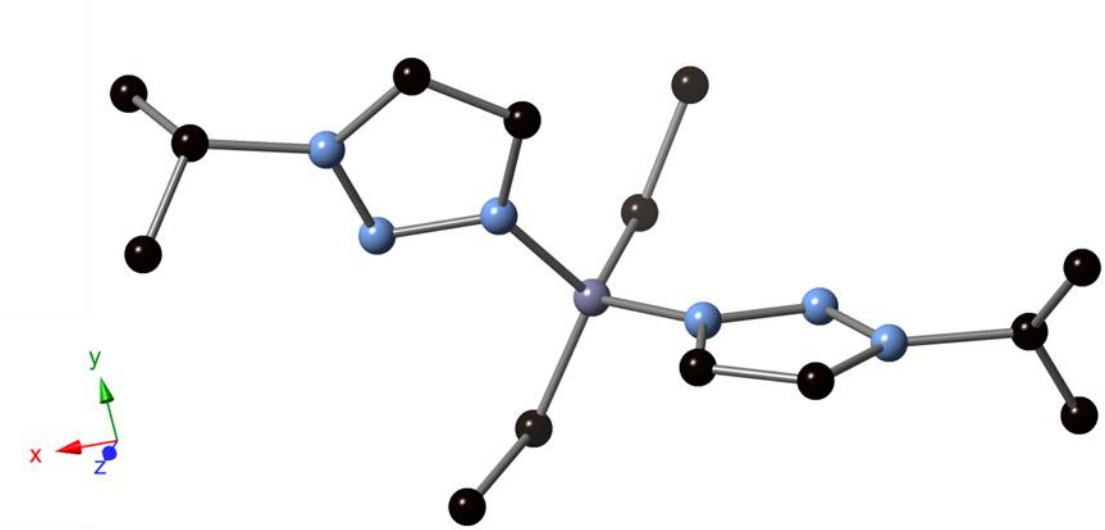


Figure 3.3. Crystal structure of the dimer of 3 with C, N, and B in black, light blue, and light purple respectively. All hydrogens have been removed for clarity.

Experimentals

Reactions with borane reagents were performed under a dry nitrogen atmosphere with the use of either a drybox or standard Schlenk techniques. Solvents were dried on an Innovative Technologies (Newburgport, MA, USA) Pure Solv MD-7 Solvent Purification System and degassed by three freeze-pump-thaw cycles on a Schlenk line to remove O_2 prior to use. Acetonitrile-d_3, chloroform-d, dimethysulfoxide-d_6, and tetrahydrofuran-d_8 were degassed by three freeze-pump-thaw cycles prior to drying over activated molecular sieves. These NMR solvents were then stored under N_2 in a glovebox. All reagents were purchased from commercial vendors and used without purification. Solution ^{1}H, $^{13}C\{^{1}H\}$, and ^{11}B NMR spectra were recorded at ambient temperature on a Varian Mercury 300 MHz, Bruker Advance 400 MHz, or Varian VNMRS 500 MHz, narrow-bore broadband system. ^{1}H and $^{13}C\{^{1}H\}$ NMR chemical shifts were referenced to the residual solvent. ^{11}B chemical shifts are reported relative to an external standard of neat BF_3•OEt_2. All mass spectrometry analyses were conducted at the Mass Spectrometry Center located in the Department of Chemistry at the University of Tennessee. The DART analyses were performed using a JEOL AccuTOF-D time-of-flight (TOF) mass spectrometer with a DART (direct analysis in real time) ionization source from JEOL USA, Inc. (Peabody, MA, USA). The ESI/MS analyses were performed using a QSTAR Elite quadrupole time-of-flight (QTOF) mass spectrometer with an electrospray ionization source from AB Sciex (Concord, Ontario,

Canada). Sample solutions of ligands (**1** and **2**) for mass spectrometry were prepared in acetonitrile. Infrared spectra were collected on a Thermo Scientific Nicolet iS10 with a Smart iTR accessory for attenuated total reflectance. Carbon, hydrogen, and nitrogen analyses were obtained from Atlantic Microlab, Norcross, GA.

Synthesis of 1-methyl-1,2,3-triazole, $C_3H_5N_3$ (1).[42] To a round bottom flask, 7.5 mL of tetrahydrofuran (THF) was added followed by addition of 1,2,3-triazole (0.500 g, 7.24 mmol) and the solution was allowed to stir. Potassium carbonate (2.00 g, 14.5 mmol) and methyl iodide (0.675 mL, 10.9 mmol) were added and allowed to stir at room temperature for 3 hrs. The reaction was then filtered on a 60 mL fine sintered-glass frit, and the filtrate was collected. The filtrate was then concentrated by removing solvent by reduced pressure, and the product was collected as a yellow liquid (0.1786 g, 29.7% yield). ^{1}H NMR ($CDCl_3$, 300.1 MHz): δ 7.67 (s, 1H), 7.52 (s, 1H), 4.09 (s, 3H). ^{13}C NMR ($CDCl_3$, 300 MHz): δ 134.09, 124.34, 36.55.

Synthesis of 1-isopropyl-1,2,3-triazole, $C_5H_9N_3$ (2).[43] 1,2,3-triazole (0.690 g, 10.0 mmol) and 7 mL of sulfuric acid were combined in a 25 mL Erlenmeyer flask. Isopropyl alcohol (0.580 mL, 11.0 mmol) was added drop-wise to the solution and allowed to stir for 40 hrs. The solution was then added to crushed ice (40 g) and allowed to stir. Potassium hydroxide was added to the solution until a neutral pH was reached. The resulting solution was extracted with methylene chloride (3 x 40 mL). The organic layer was dried over magnesium sulfate, and solvent was removed under reduced pressure.

The product was collected as a pure liquid (0.656 g, 57.4% yield). ^{1}H NMR (DMSO-d_6, 300.1 MHz): δ 8.15 (s, 1H), 7.69 (s, 1H), 4.82 (sept, J = 6.7 Hz, 1H), 1.47 (d, J = 6.7, Hz, 6H). ^{1}H NMR (THF-d_8, 300.1 MHz): δ 7.30 (s, 1H), 7.04 (s, 1H), 4.32 (sept, 1H), 1.03 (d, J = 6.7 Hz, 6H). ^{1}H NMR ($CDCl_3$, 300.1 MHz): δ 7.62 (s, 1H), 7.53 (s, 1H), 4.85 (sept, 1H), 1.52 (d, J = 6.8 Hz, 6H). IR (neat): 3122, 2983, 2983, 1649, 1456, 1392, 1372, 1351.52, 1299, 1285, 1234, 1222, 1203, 1159, 1132, 1113, 1071, 1019, 951, 885, 783, 734, 707, 636 cm^{-1}.

Synthesis of 1-(1-isopropyl-1,2,3-triazole)triethyl borate, $C_6H_{15}BC_5H_9N_3$ (3). IPA triazole (0.429 g, 3.86 mmol) was added to hexane (2.00 mL) in air free conditions, followed by addition of triethyl borane (4.05 mL, 4.05 mmol). The resulting solution was allowed to stir at room temperature overnight and was then concentrated under reduced pressure. The pure product was collected as a clear liquid (0.775 g, 96% yield). ^{1}H NMR (C_6D_6, 300.1 MHz): δ 7.33 (s, 1H), 6.20 (s, 1H), 3.70 (sept, 1H), 1.26 (t, J = 7.3 Hz, 9H), 1.15 (q, 6H), 0.70 (d, J = 6.7 Hz, 6H). ^{13}C NMR ($CDCl_3$, 125.66 MHz): δ 129.52, 121.62, 54.32, 21.73, 15.89, 10.67. ^{11}B NMR ($CDCl_3$, 128.42 MHz): δ 1.58. IR (neat): 3148, 2985, 2937, 2900, 2860, 2812, 1514, 1457, 1395, 1374, 1312, 1268, 1247, 1148, 1086, 1069, 1047, 894, 780, 716, 653 cm^{-1}.

Synthesis of 1-(1-isopropyl-1,2,3-triazole)triphenyl borate, $C_6H_{15}BC_5H_9N_3$ (4). Triphenyl borane (0.300 g, 1.23 mmol) was added to 1 mL benzene in a 20 mL vial, while IPA triazole (0.101 g, 1.23 mmol) was added to a separate 20 mL vial with 1 mL

benzene in air free conditions. The solution of IPA triazole was added to the solution of triphenyl borane and allowed to stir at room temperature. After 30 minutes, a white solid precipitated out. The volatiles were then removed under reduced pressure. The residue was then washed with benzene (3 x 10 mL) and residual solvent was removed under reduced pressure. The pure product was collected as an off-white solid (0.2316 g, 59.7% yield). ^{1}H NMR (CD_3CN, 300.1 MHz): δ 8.05 (s, 1H), 7.66 (s, 1H), 7.15 (m, 15H), 4.91 (s, 1H), 1.58 (s, 6H). ^{1}H NMR (THF-d_8, 499.74 MHz): δ 8.18 (s, 1H), 7.71 (s, 1H), 7.16 (dd, J = 8.1, 1.6 Hz, 5H), 7.05 (m, 10H), 4.92 (sept, J = 6.6 Hz, 1H), 1.59 (d, J = 6.7 Hz, 6H). ^{13}C NMR (THF-d_8, 499.74 MHz): δ 135.53, 133.83, 129.01, 127.04, 125.22, 124.45, 56.56, 22.53. Anal. Calcd. for $C_6H_{15}BC_5H_9N_3$: C, 78.20; H, 6.85; N, 11.89. Found: C, 78.34; H, 6.88; N, 12.01.

CHAPTER 4
ISOSTRUCTURAL DESIGN FOR 2D BREATHING MOFS WITH ARYL GATES

A verison of this chapter is currently in submission for publication on 5-19-15 by Brianna C. Hughes, Christopher R. Murdock, and David M. Jenkins.

Hughes, Brianna C.; Murdock, Christopher R.; Jenkins, David M. “Isostructual Design for 2D Breathing MOFs with Aryl Gates.”

All work presented herein is the work of Brianna Hughes with assistance in crystallography by Christopher R. Murdock.

Abstract

A series of breathing two-dimensional metal-organic frameworks (MOFs) was synthesized with group 11 metals and semirigid ligands that bind in a *syn* conformation. The modular synthetic approach allows the pore to be expanded based on the number of aryl rings on the linker. Each aryl ring can act independently as a rotating gate as a function of guest molecules. For the two aryl ring system, all three states (open/open, open/closed, and closed/closed) are observed by single crystal X-ray diffraction (SCXRD). By uniting solid state spectroscopic and diffraction techniques, including powder X-ray diffraction (PXRD), solid-state ^{13}C cross-polarization magic-angle spinning (CP-MAS) NMR, and IR, the changing solvation and associated ring rotation can be monitored in the bulk material. This combined spectroscopic approach for determining

gate opening is critical as larger breathing MOFs are synthesized for potential chromatographic applications.

Introduction

Breathing MOFs are functional materials that combine crystallinity with softness.[18b, 18d-f] These materials' softness (multiple stable states) as a function of guest has led to initial studies that focused on gas adsorption.[18a, 18f, 18n, 44] More recent research has expanded to include the intriguing possibility that these breathing materials can act as the stationary phase in chromatographic separations.[45] Denayer and De Vos have demonstrated separations utilizing MIL-53 and MIL-47 with mixtures of styrene and ethylbenzene, xylene isomers, as well as ortho-substituted aromatics.[45]

To understand the impact guests have on the breathing structure, detailed studies involving powder X-ray diffraction (PXRD) and single crystal X-ray diffraction (SCXRD) have been performed on MIL-47.[46] As organic molecules were loaded into the framework, the host-guest interactions were monitored. Jacobsen and coworkers illustrated that as the shape of the guest molecules change from flat benzene to a more spherical cyclohexane, MIL-47 deforms through cooperative rotation of octahedral chains together with progressive bending of the channel walls.[46] The guest molecules were packed in two columns inside each channel of the MIL-47 framework. Unlike previous deformations (translation of the octahedral chains with no rotation), the twisting

deformation shown with these guest molecules results from an adaptation of the framework for specific guest molecule packing. Therefore, the impact the guest species has on the MOF could have a significant impact on its separation properties.

If breathing MOFs are to be applied effectively as stationary phases for separations, both rational synthetic strategies and effective characterization of breathing in the bulk material must be achieved. These two issues, while distinct, are interrelated due to the manner in which most breathing MOFs are synthesized. The breathing occurs at the "kneecap" of the material, which is the flexing point.[17b, 18b, 18e, f, 47] The "kneecap" is often at the metal-ligand interface, such as the octahedral chains in MIL-47, which limits the rational design of new systems and makes spectroscopic characterization more complex.[18e, f, 48] To alleviate this limitation, researchers have proposed putting the hinge solely on the ligand itself.[17b, 18h, i, 49] Ligand-based breathing can be accomplished via a double-hinged screw mechanism or through employing a "gate" on an anisotropic MOF.[18c, 18g-j, 18l-n] The gate effect allows for the linker to rotate based on the solvent present, thus opening or closing the pore. The gate approach has the additional advantage of easier spectroscopic scrutiny since the rest of the MOF will be static.[18j]

This gate effect was pioneered by Kitagawa and coworkers who prepared a cadmium coordination polymer (CP) in which the aryl ring could rotate as a function of hydration.[18k] This CP was characterized and monitored through SCXRD.[18k] Although this CP showed the gate effect by an opening and closing of the pores, it was also

accompanied by a contraction of the layering distances as the solvent was removed, making spectroscopic characterization more problematic.[18k]

Our previous research showcased a 2D framework wherein a phenyl ring moiety on the linker rotates and blocks the pore as a function of guest.[18j] The backbone was comprised of a bidentate semirigid linker in a *syn* conformation with a phenyl ring subunit that rotated between parallel and perpendicular positions as a function of guest solvent. Crucially, no other portion of the MOF shifted as a function of breathing. This allowed the position of the aryl ring to be correlated between single crystal X-ray measurements and ^{13}C cross-polarization magic-angle-spinning (CP-MAS) NMR spectroscopy.[18j] Unlike other spectroscopic techniques (IR, PXRD), ^{13}C CP-MAS NMR can be employed to deduce the position of the gate as a function of guest, which makes this a particularly powerful tool.

To see why advances in spectroscopic characterization are so critical, consider the case of an isostructural gate 2D MOF system with multiple aryl rings (Figure 4.1). As the number of aryl rings (n) increase, not only will the pore size broaden ($a+(b)_n$), but the permutations for rotated rings will also proliferate. When n is 0, there are only two options for ring position, open and closed. Assuming orientation does not matter, when n is 1, three combinations are possible: open/open, open/closed, and closed/closed. Yet, when n is 2, six ring rotation combinations are now possible. While single crystal X-ray diffraction is clearly possible when n is 0 or 1, this technique will not be feasible for all combinations as n increases. With these expanded aryl ring systems, the

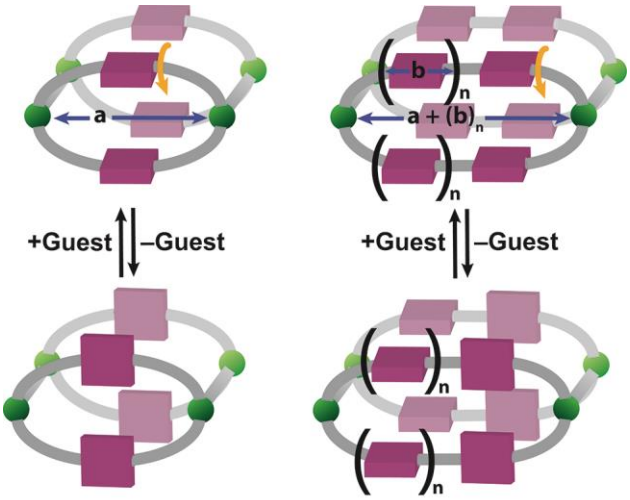


Figure 4.1. Graphical depiction of a subunit (aryl ring) of the semirigid linker rotating to open and close the pore. Where (a) represents the width of a single subunit, and (b) represents the additional width of extended subunits added to the linker. Green spheres represent metal centers or secondary building units (SBUs), and gray and purple components represent rigid and flexible portions of the ligand, respectively.

complexity for both synthesis and characterization clearly increases as n increases. Therefore, spectroscopic methods will need to be developed to determine each aryl ring position.

We have synthesized a series of breathing 2D sheet MOFs with group 11 metals and semirigid ligands that are arranged in a *syn* conformation. The modular nature of these 2D breathing MOFs allows additional aryl rings to be added to the linker showcasing the first isoreticular set of gate-based breathing MOFs. Single crystal X-ray diffraction studies conclusively show that all three combinations of open and closed ring positions are possible, although these measurements were not all obtained on the same MOF. Solid state spectroscopic and diffraction measurements, including ^{13}C CP-MAS NMR, IR, and PXRD, could allow for monitoring of the ring rotation in the bulk material. Our objective was to employ these bulk measurements to assign a breathing state that was not previously directly observed by SCXRD. While the spectroscopic results are not conclusive, we believe that this multi-faceted approach will be essential for larger breathing MOFs.

Results and Discussion

We have previously reported the synthesis of the double-hinged ligand, 4,4'-(1,4-(xylene)diyl)bis(1,2,4-triazole) (di-MTZ^{Ph}) and have expanded the synthetic methodology by incorporating a biphenyl moiety as the central unit between the triazoles.[18j] The

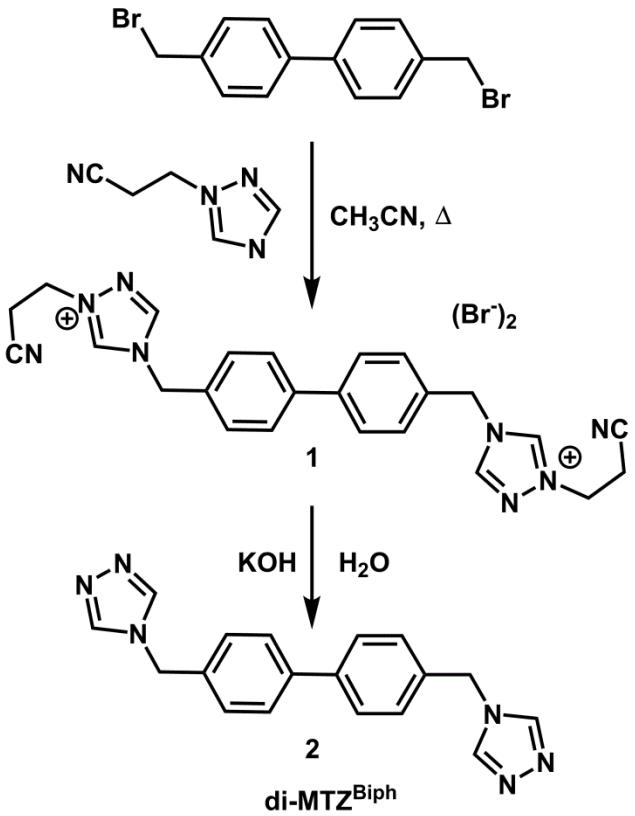
addition of 1,2,4-triazole-1-propanenitrile to 4,4'-bis(bromomethyl)-1,1'-biphenyl led to the formation of intermediate **1** in 84% yield (Scheme 4.1). Addition of potassium hydroxide cleaved the protecting group which generated the product, 4,4′-(4,4'-bi-tolyl)-bis(1,2,4-triazole), **2** (di-MTZ^{Biph}), in 85% yield. The ligand, di-MTZ^{Biph}, was further purified via recrystallization from water.

Previously reported results with di-MTZ^{Ph} and 4,4'-(1,4-(trans-2-butene)diyl)bis(1,2,4-triazole) demonstrated that multiple copper MOFs can be synthesized by varying the reaction conditions, including solvent, metal-to-ligand ratio, and starting metal salt.[18i,18j] Consequently, a combinatorial approach was employed that varied these conditions for our new ligand.

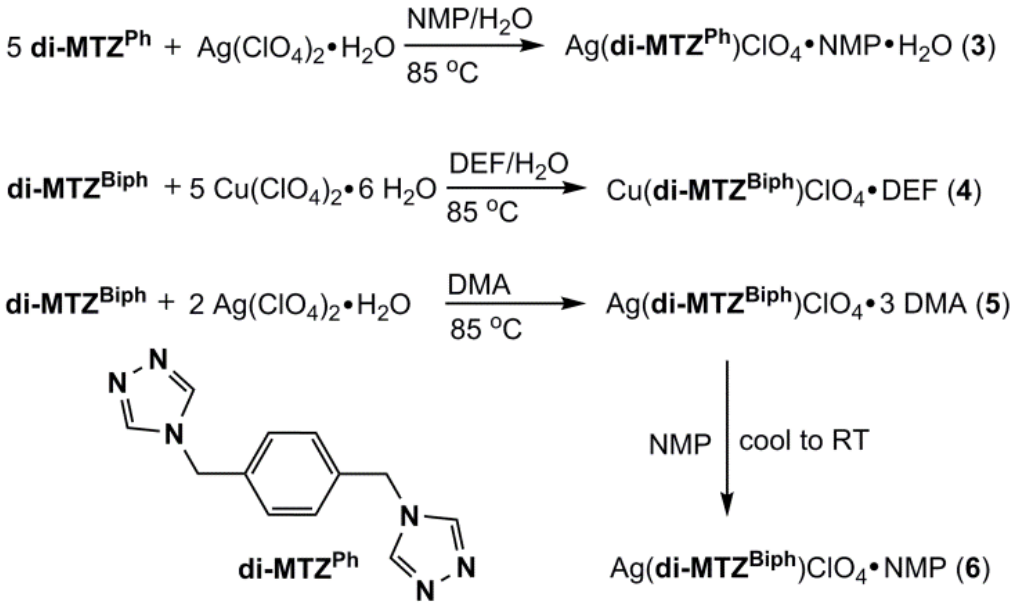
Initial reaction conditions focused on forming a silver 2D MOF with the original di-MTZ^{Ph} ligand that would be complementary to the copper MOFs that we previously reported.[18j] The addition of five equivalents of di-MTZ^{Ph} and one equivalent of silver perchlorate to a mixture of N-methyl-2-pyrrolidone (NMP) and water led to the formation of [Ag(di-MTZ^{Ph})(ClO_4)] • NMP • H_2O (**3**) (Scheme 4.2). Colorless needle crystals suitable for X-ray diffraction were obtained after heating the reaction mixture for 3 h at 85℃.

We were successful in preparing 2D MOFs with the expanded ligand di-MTZ^{Biph} with both copper and silver. The addition of one equivalent of di-MTZ^{Biph} to five equivalents of copper perchlorate to a mixture of *N*,*N*-diethylformamide (DEF) and water led to the formation of [Cu(di-MTZ^{Biph})(ClO_4)] • DEF (**4**) (Scheme 4.2). The framework

Scheme 4.1. Synthesis of di-MTZ^{Biph} (2).



Scheme 4.2. Synthesis of silver and copper frameworks.



was collected as colorless needles after heating for 24 h at 85 ℃. One equivalent of di-MTZ^{Biph} and two equivalents of silver perchlorate in *N*,*N*-dimethylacetamide (DMA) yielded [Ag(di-MTZ^{Biph})(ClO_4)] • 3 DMA (**5**) (Scheme 4.2). In order to obtain crystalline **5**, the solution was heated for 24 h at 85 ℃ then pipetted to a clean vial. As the reaction mixture was cooled, colorless needles suitable for X-ray diffraction were formed. Notably, the addition of various solvents during the reactions allowed structural variation of the MOFs to form. Upon the addition of 2 mL of NMP to **5** as it was cooling, [Ag(di-MTZ^{Biph})(ClO_4)] • NMP (**6**) was obtained as colorless needles suitable for X-ray diffraction (Scheme 4.2).

Single crystal XRD of **3** showed that each tetrahedral Ag(I) center is coordinated to four triazole ligands (Figure 4.2A). Adjacent silver atoms are bridged by two triazole ligands to form an equatorial plane, which results in a linear chain of silver atoms (Figure 4.2B).

The semirigid ligand shows a *syn* conformation that forms a 2D layered structure, like those previously reported with copper and this ligand (Figure 4.2C).[18j] This framework exhibits an open state, only one of two positions possible for a one aryl ring system. Due to the bridging triazole ligands between the silver centers in an alternating manner, the overall topology is a 2D sheet MOF. This framework incorporates guest molecules of NMP with perchlorate anions packed between the sheet layers.

Single crystal XRD of **4** revealed the same coordination with the copper(I) centers bridged by the triazole ligands, resulting in a 2D MOF similar to **3** (Figure 4.3).

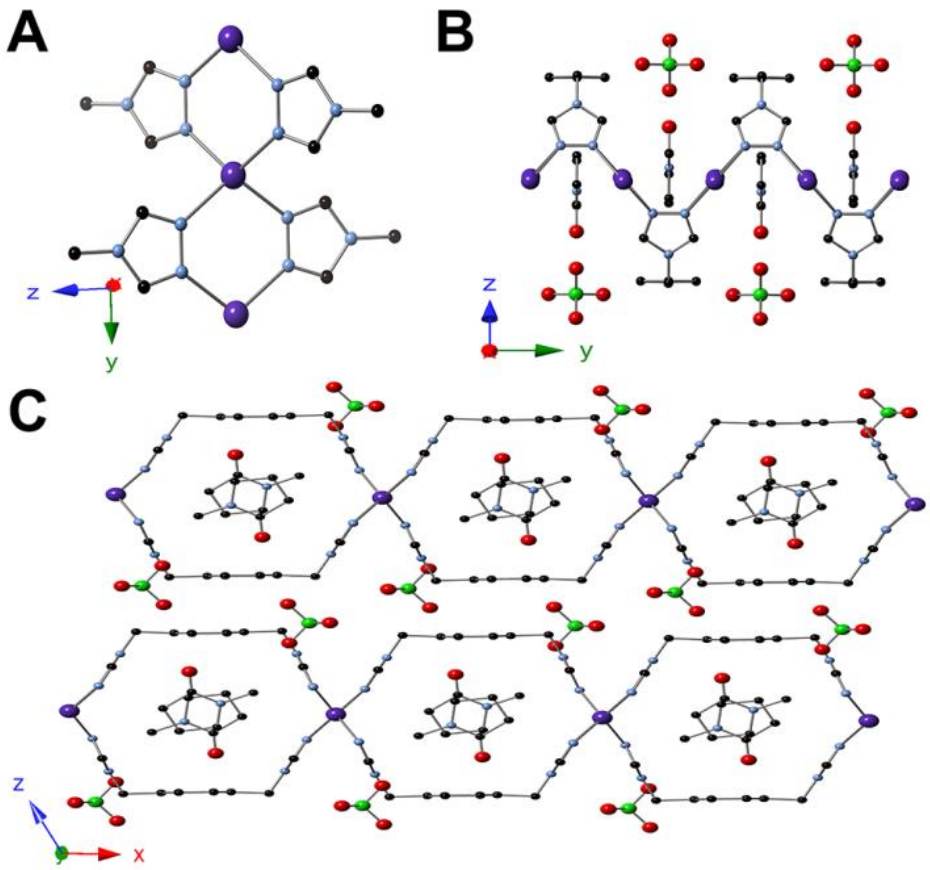


Figure 4.2. (A) Crystal structure of 3 showing the silver connectivity. (B) Crystal structure of 3 showing silver chains along the *y* axis. (C) Crystal structure of 3 viewed orthogonal to the *y* axis showing the 2D sheet topology. Purple, light blue, black, green, and red spheres represent Ag, N, C, Cl, O, respectively. All hydrogen atoms have been omitted for clarity.

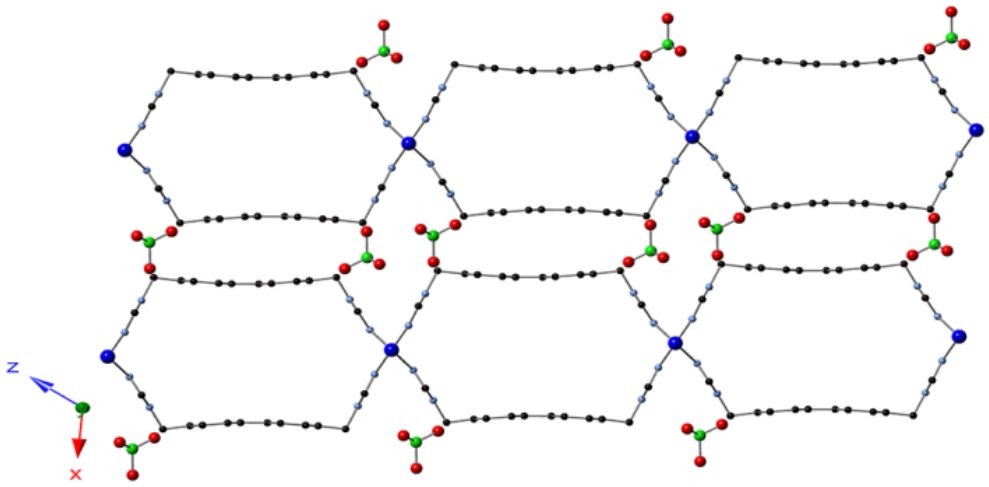


Figure 4.3. Crystal structure of 4 shown orthogonal to the *y* axis showing the 2D sheet topology. Royal blue, light blue, black, green, and red spheres represent Cu, N, C, Cl, O, respectively. All hydrogen atoms have been omitted for clarity.

In framework **4**, the phenyl rings within the triazole linker are both parallel to one another (open/open state) which results in layers that are stacked through extensive π-π interactions. Like in **3**, the perchlorate anions are found in between the 2D sheet layers of the framework. Although DEF molecules are present and confirmed through CHN analysis, the DEF molecules could not be corroborated through single crystal X-ray analysis.

In silver MOF **5**, the topology is similar to **4**; however, ligand-based breathing causes a notable difference in the structure. Both the phenyl rings within the triazole linker are rotated by 35.4°, resulting in a partially perpendicular orientation (closed/closed state) compared to that of the tubes (Figure 4.4A). This allows for four DMA solvent molecules to be within the pores of the extended framework, as well as additional solvent molecules between the layers of the framework. As in **4**, the perchlorate anions are situated in between the 2D sheets of the framework.

The structure of **6** was topologically identical to that of **5** – consisting of Ag(I) centers bridged by two triazole ligands to form a fused-tube structure – but there was one major structural change (Figure 4.4B). The orientation of one of the phenyl rings had rotated to a parallel position compared to that in **5**, while the other is at 90.0° resulting in an open/closed state. This rotation allows for the migration of solvent within the pore between the rotated and non-rotated phenyl rings. Notably, **3** has the same guest solvent, but in that case the rings are parallel. The perchlorate anions have not moved with a change in guest solvent, from DMA to NMP, between **5** and **6**.

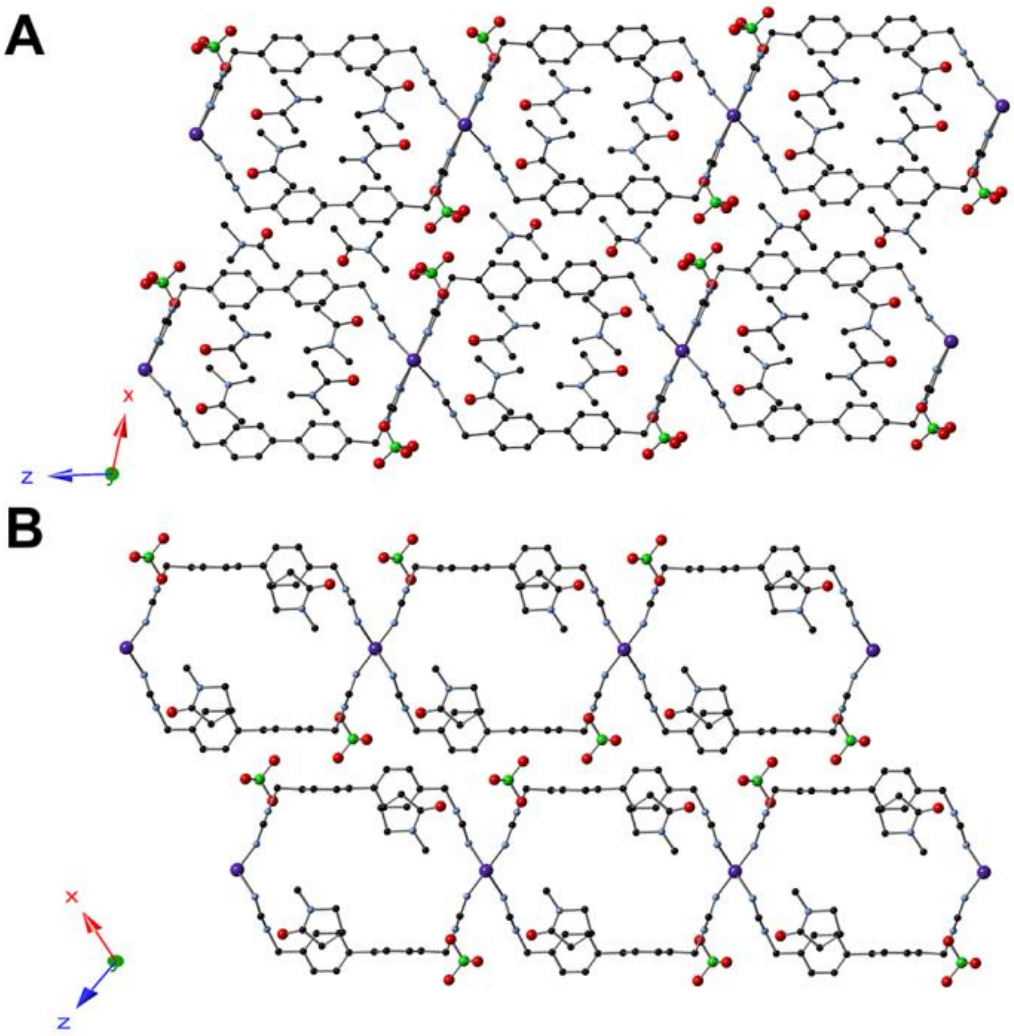


Figure 4.4. Crystal structures viewed orthogonal to the *y* axis showing fused-tube topology (A) 5 and (B) 6. Purple, light blue, black, green, and red spheres represent Ag, N, C, Cl, O, respectively. All hydrogen atoms have been omitted for clarity.

A comparison of the X-ray structures of **4**, **5**, and **6** demonstrates that each permutation of the aryl ring positions (parallel versus perpendicular) is measurable. Nevertheless, as the number of rings in the system increase, it will become progressively challenging to directly determine their positions with crystallography. Furthermore, 2D MOFs **5** and **6** are not static as a function of guest. Consequently, we undertook a detailed spectroscopic investigation of **5** and **6** as a function of solvation; **4** was also analyzed for comparison.

Initial measurements focused on determining the position of the aryl rings in **5** and **6** as the solvent was evaporating. Without solvent in the pores, **5** and **6** should converge to the same framework, as they consist of the same metal center and linker. Initial PXRD patterns were collected and matched the calculated data from the actual single crystal structure (Figures 4.5 and 4.6, respectively). PXRD measurements were then taken as a function of time for **5** and **6** over the course of 6 hours (Figure 4.7). This PXRD study was also performed with **4**, which showed no change as solvent was evaporated over the 6 h time period (Figure 4.8).

Evaporation tests with **5** demonstrated that within one hour there was an obvious change in the powder pattern, and after 2 hours the pattern no longer altered. To determine if the process was reversible, the sample was resolvated by adding DMA (the original solvent). Resolvation at room temperature yielded a PXRD pattern that did not match the original, but heating the sample at 85℃ for 6 h (i.e. original reaction conditions) was successful in demonstrating reversible solvation (Figure 4.7A). Therefore, the aryl rings on **5** can rotate as a function of guest reversibly. In the case of

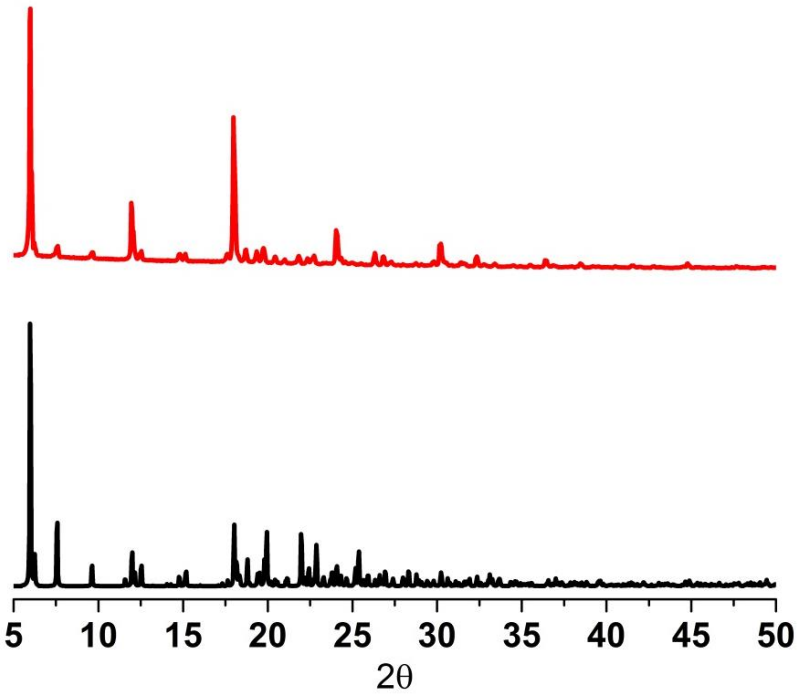


Figure 4.5. PXRD pattern for 5: experimental (red) and simulated (black).

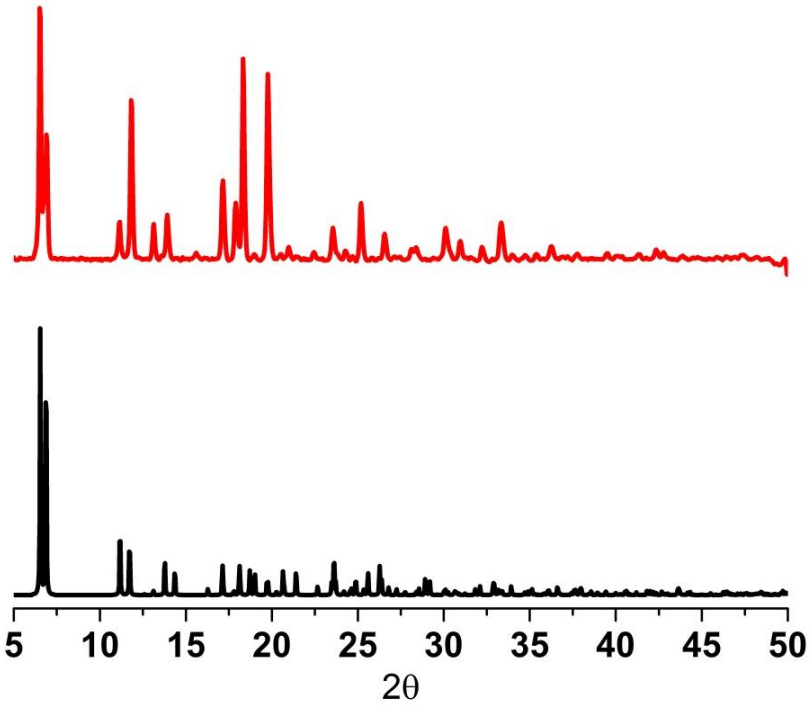


Figure 4.6. PXRD pattern for 6: experimental (red) and simulated (black).

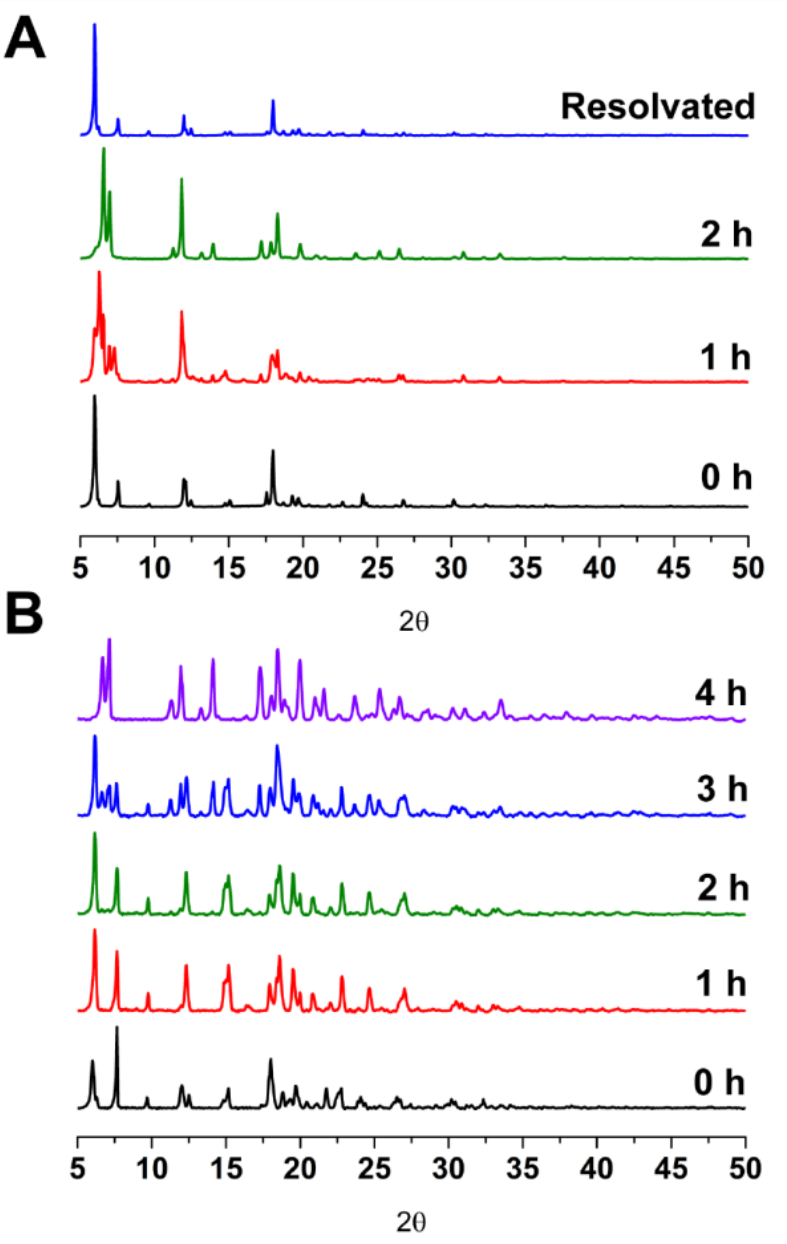


Figure 4.7. PXRD patterns showing changes to 5 (A) and 6 (B) as a function of evaporation time. 5 (A) can be resolvated with DMA to give the same PXRD pattern.

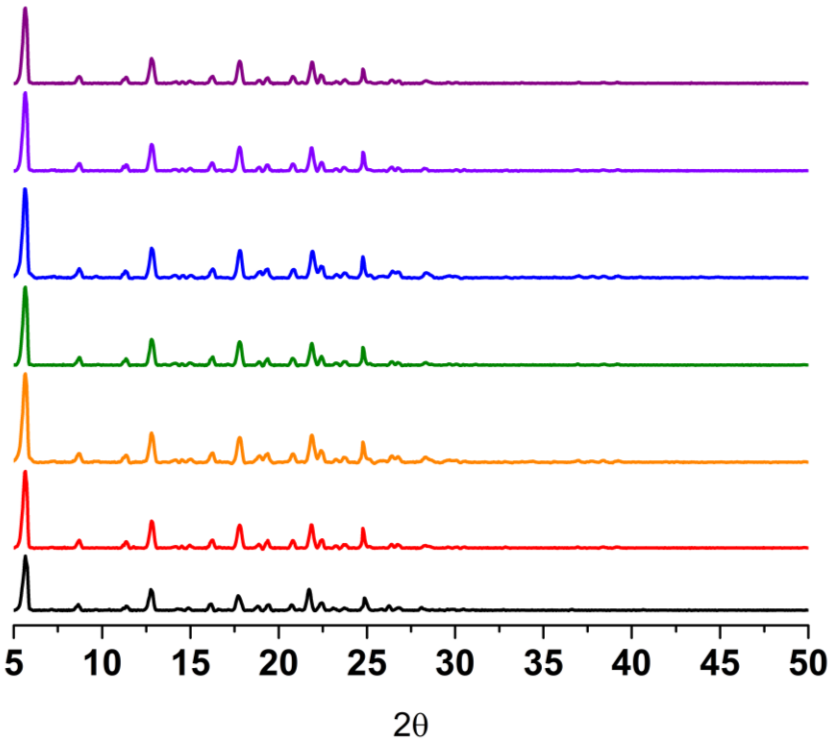


Figure 4.8. PXRD study for 4, showing changes as a function of evaporation time. Black represents 0 h and increases up to purple at 6 h, with a 1 h time increment.

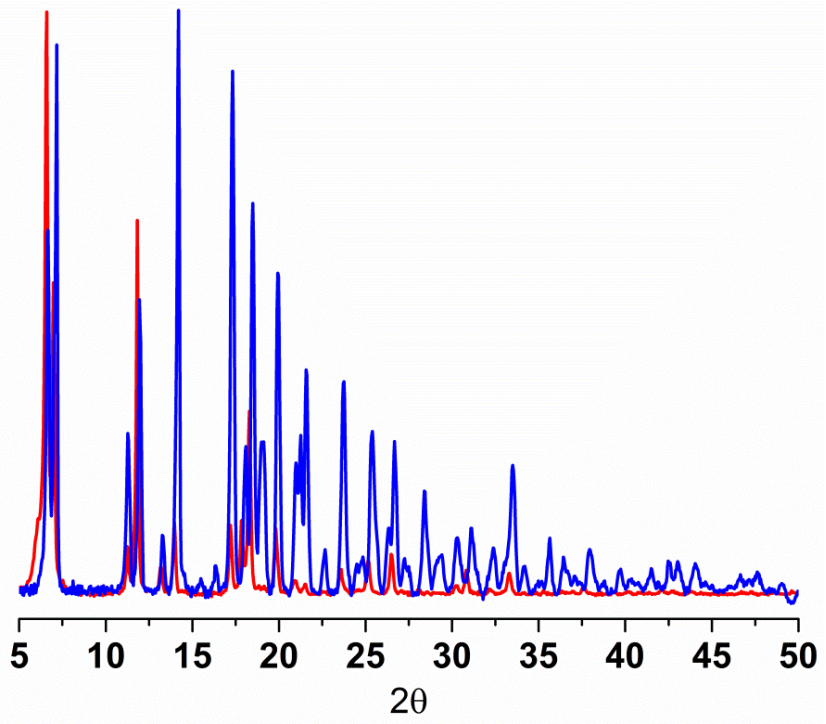


Figure 4.9. PXRD pattern overlay for 5 (red) and 6 (blue) after desolvation in air for 6 h.

6, evaporation proceeded over 4 h (Figure 4.7B), but unlike **5**, resolvation did not yield the initial powder pattern. A comparison of the desolvated powder patterns showed strong correlation with peaks that matched at 6.6, 7.0, 11.3, 11.9, 13.2, and 14.0 2θ (Figure 4.9). Since the parallel ring position should be the lowest energy position due to π-π stacking, it is probable that **5** and **6** have merged to form a structure similar to **4**.

To further monitor the evaporation of solvent within **5** and **6**, infrared spectroscopy (IR) was employed. As with the PXRD study, **5** and **6** were both initially analyzed between 0 h to 6 h and allowed to rest in air between the measurements (Figure 4.10). For **5**, the IR data showed a decrease of peaks around 3470 and 1630 cm^{-1} for DMA as each hour passed up until hour 6 (Figure 4.10A). For **6**, the data showed a decrease of peaks around 2925 and 1667 cm^{-1} for NMP up until hour 2 and no further changes were made in the spectra (Figure 4.10B). These spectra confirm that as these frameworks are exposed to air, solvent molecules are being removed via evaporation. Evaporation in **4** was also measured, and showed appropriate decreasing peaks for the solvent (Figure 4.11).

Although IR measurements confirm that the solvent is evaporating and PXRD shows that the change is reversible in **5**, neither of the techniques confirms that the aryl rings in **5** or **6** rotate to a parallel mode when solvent is removed. Solid state NMR (SSNMR); however, should distinguish aryl ring rotations if a related MOF is structurally elucidated. Fortunately, **4** has its aryl rings in the fully parallel position (open/open state) which allows for a direct comparison. In addition, previous studies showed that

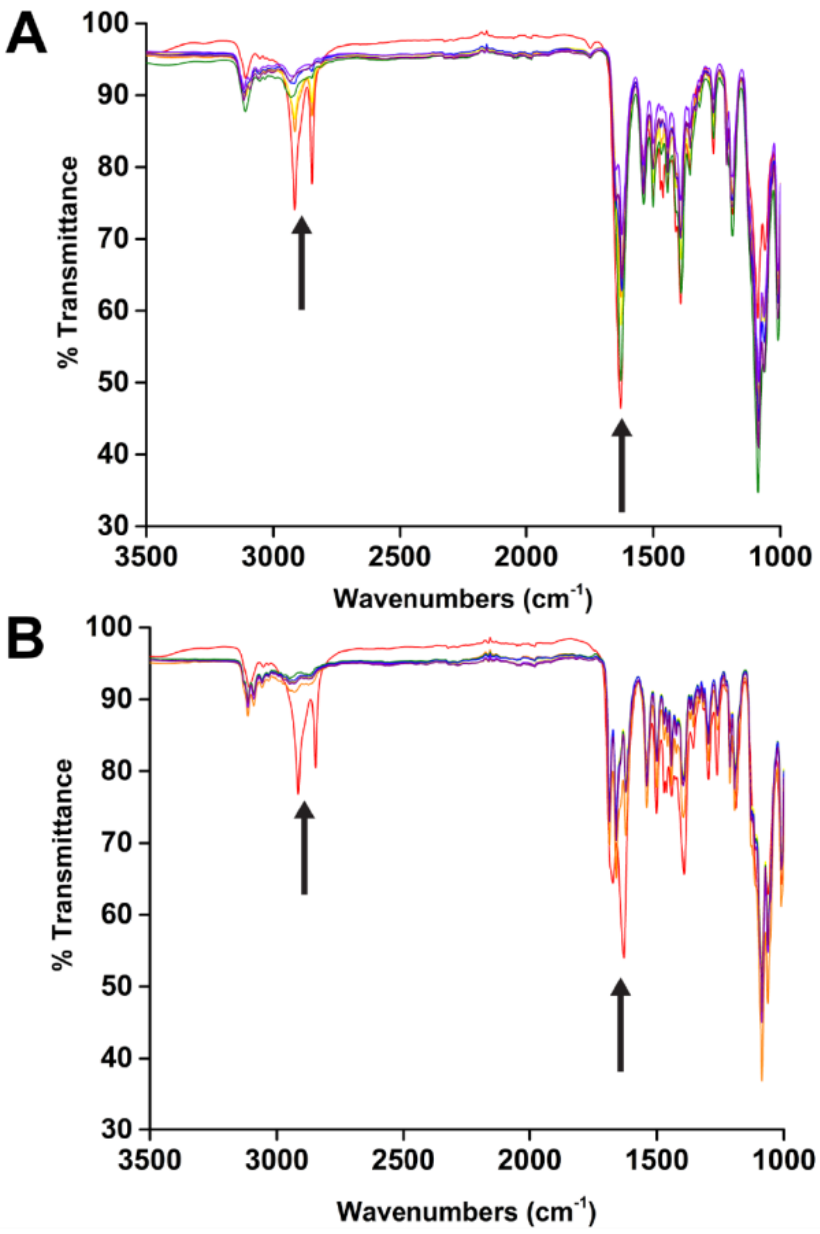


Figure 4.10. IR measurements as function of evaporation time for 5 (A) and 6 (B) (ROYGBIV as each hour increases starting from 0 h to 6 h).

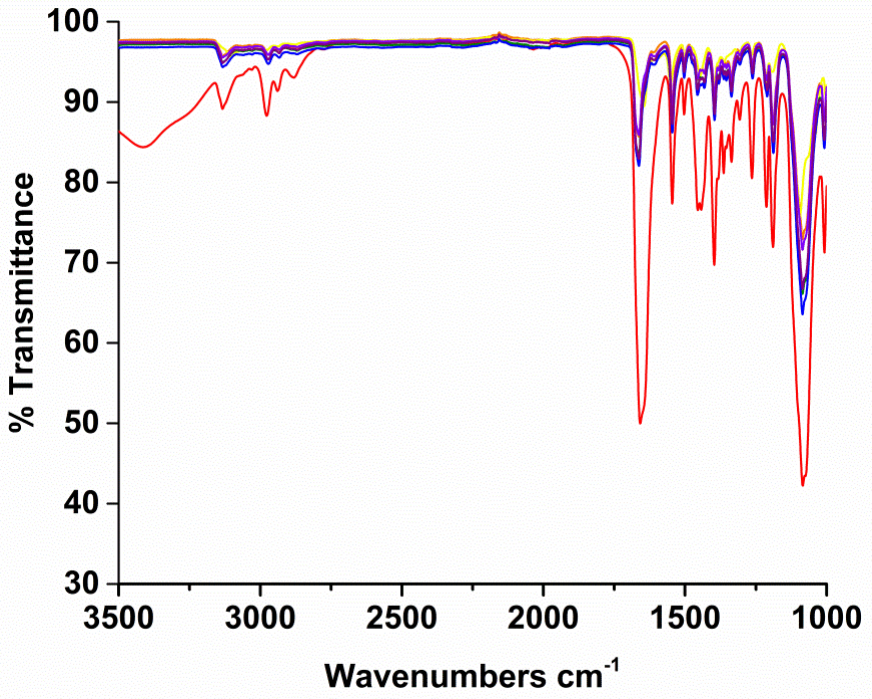


Figure 4.11. IR study for 4, showing changes as a function of evaporation time. (ROYGBIV as each hour increases, starting from 0 h to 6 h).

although solvent was evaporating from the framework, the actual structure of **4** remained in the open/open state.

In order to correctly assign the carbon peak positions in the frameworks, the ^{13}C peak positions for **2** must be assigned in the solution state NMR spectrum. Heteronuclear multiple-bond correlation (HMBC) spectra was collected for **2** in DMSO-d_6 along with standard 1D ^{1}H and ^{13}C NMR spectra, which allowed for the absolute assignments of all the distinct carbons within the ligand. These resonances were then confirmed through ^{13}C cross-polarization magic-angle-spinning (CP-MAS NMR).

Once the ^{13}C NMR spectrum of **2** had been successfully assigned, we were able to compare **2**'s resonances to those of **4** and **5** (Figure 4.12). The solvents within the frameworks can be detected by NMR analysis and correlate with the solvents that were employed during their synthesis. Although the structure of **4** has both phenyl rings from the ligand completely flat (open/open state) and **5** has both phenyl rings partially rotated (closed/closed state), the ^{13}C resonances attributed of the biphenyl ring nearly matched in the ^{13}C CP-MAS NMR. This result suggests that the phenyl rings in **5** have rotated to a parallel position after evaporation of solvent. The long time scale that is necessary (6 h) to complete the ^{13}C CP-MAS NMR experiment in conjunction with our IR and PXRD studies allow to deduce that most of the DMA has evaporated. Without these DMA molecules interacting with the aryl rings in **5**, the closed/closed state could therefore alter to the open/open state of **4**. ^{13}C CP-MAS NMR spectrums for **3** and **6** were also completed (Figure 4.13 and 4.14, respectively).

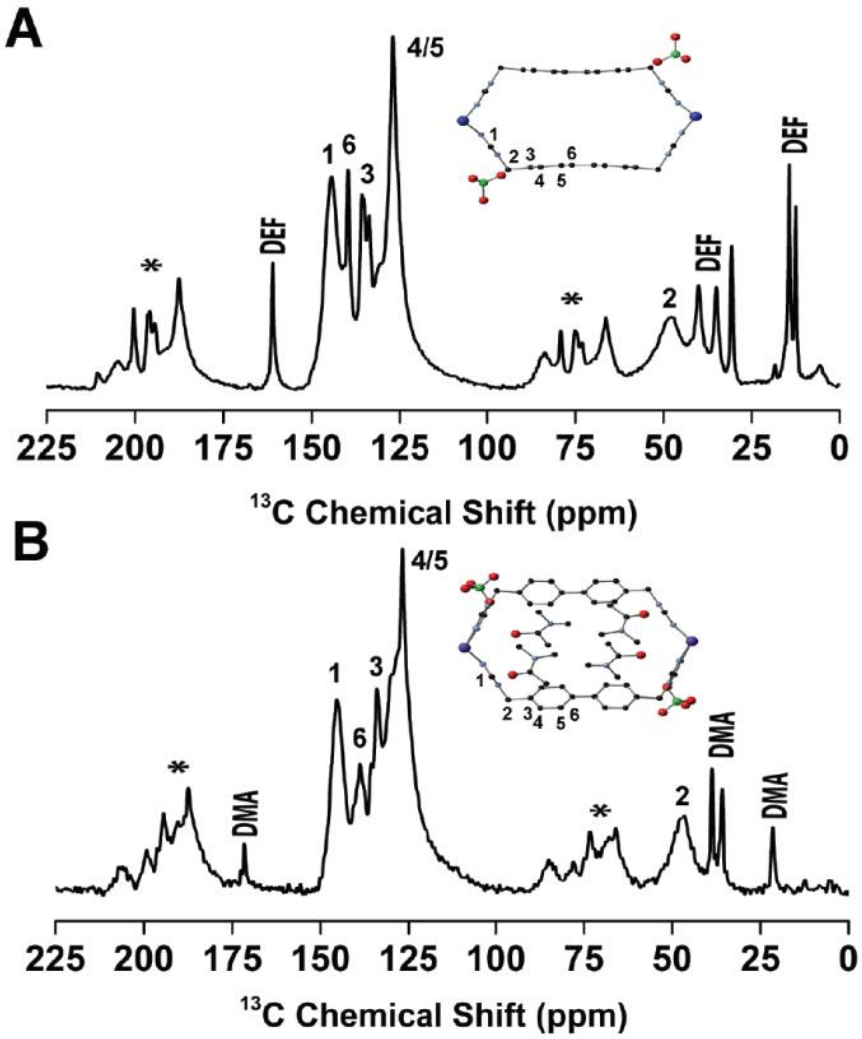


Figure 4.12. Full solid state ^{13}C CP-MAS NMR spectrum of 4 (A) and 5 (B). Inset shows highlighted crystal structure with labeled C atoms. Asterisks denote spinning sidebands.

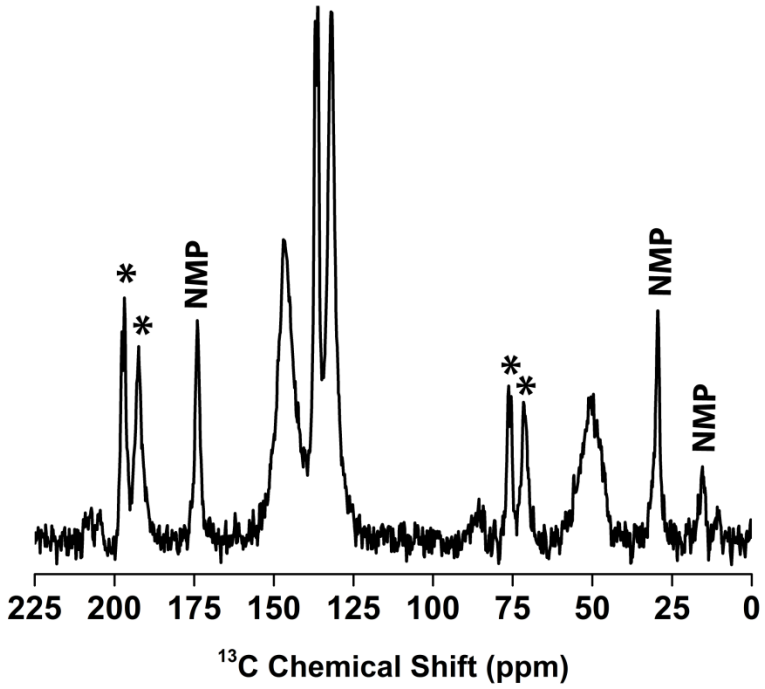


Figure 4.13. SSNMR for 3, with spinning sidebands denoted by asterisks.

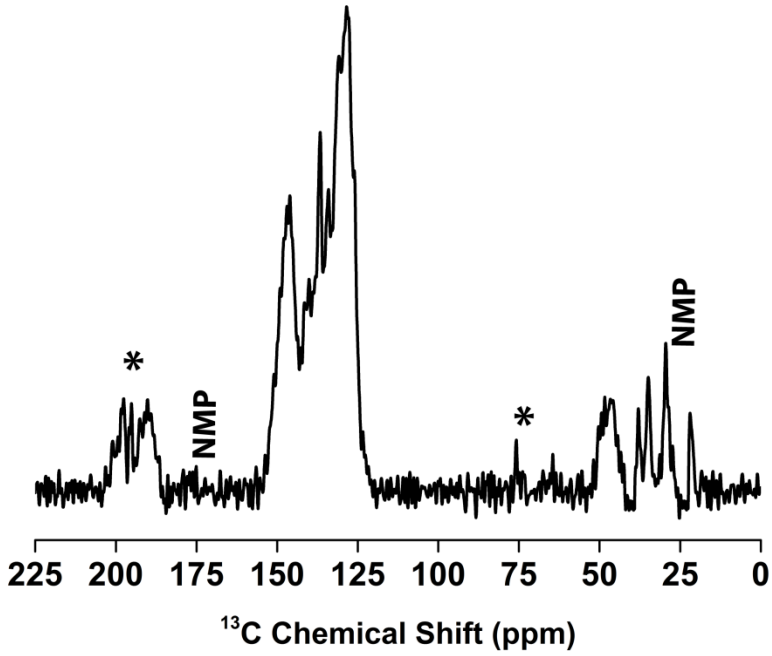


Figure 4.14. SSNMR for 6, with spinning sidebands denoted by asterisks.

Conclusion

A series of breathing two-dimensional metal-organic frameworks was synthesized utilizing group 11 metals and semirigid bis(1,2,4-triazole)ligands that are arranged in a *syn* conformation. The modular synthetic approach allows for increasing numbers of aryl rings between the triazole moieties which expands the widths of the pores. In addition to the larger pores, each aryl ring can act independently as a rotating gate as a function of guest. Three separate X-ray structures of the MOFs showcased the three possible outcomes: two rings parallel, one ring parallel and one ring perpendicular, and two rings perpendicular. This set of MOFs is the first isoreticular set of gate-based breathing MOFs.

Because X-ray measurements of each permutation will become unfeasible as the number of rings increases, spectroscopic methods must be developed. Solid state spectroscopic and diffraction measurements, including PXRD, IR and SSNMR, suggest that the aryl rings rotate as a function of guest. Despite observing changes in the IR, SSNMR, and PXRD with the loss of solvent in **5** and **6**, enough spectroscopic differences persist that we cannot completely confirm that the expected fully parallel state of the silver MOF, which is analogous to copper MOF **4**, was the only breathing mode. In addition to synthesizing linkers with more aryl rings, future research directions for these 2D extended frameworks include functionalizing the aryl rings to improve separations in chromatographic applications.

Experimentals

The compound 1,2,4-triazole-1-propanenitrile, 4,4'-(1,4-(xylene)diyl)bis(1,2,4-triazole) (**di-MTZ^{Ph}**), and [Cu(di-MTZ^{Ph})(ClO_4)] • DMA • H_2O (**7**), were prepared as described previously.[1] All other reagents were purchased from commercial vendors and used without purification. ^1H and $^{13}C\{^1H\}$ NMR spectra were recorded at ambient temperature on a Varian Mercury 300 MHz or a Varian VNMRS 500 MHz narrow-bore broadband system. ^1H and ^{13}C NMR chemical shifts were referenced to the residual solvent. Solid ^{13}C CP-MAS NMR samples were recorded on a Varian Inova 400 MHz spectrometer and referenced to an external adamantane sample. All mass spectrometry analyses were conducted at the Mass Spectrometry Center located in the Department of Chemistry at the University of Tennessee. The ESI/MS analyses were performed using a QSTAR Elite quadrupole time-of-flight (QTOF) mass spectrometer with an electrospray ionization source from AB Sciex (Concord, Ontario, Canada). Infrared spectra were collected on a Thermo Scientific Nicolet iS10 with a Smart iTR accessory for attenuated total reflectance. Thermogravimetric analysis data were collected on a TA Instruments TGA Q50 under N_2. Carbon, hydrogen, and nitrogen analyses were obtained from Atlantic Microlab, Norcross, GA.

Synthesis of 4,4'-[4,4'-bitolyl]bis-(1-(2-cyanoethyl)-1,2,4-triazolium) dibromide, 1. 4,4'-bis(bromomethyl)-1,1'-biphenyl (2.00 g, 0.00588 mol) was added to a 100 mL round bottom flask which had 1,2,4-triazole-1-propanenitrile (1.437 g, 0.0118 mol) and the

mixture was diluted with acetonitrile (40 mL). The reaction was heated to reflux for 24 h, followed by cooling the reaction to rt and washing the precipitate with diethyl ether (30 mL), and then dried under reduced pressure. The crude white solid was then washed with acetonitrile (3 x 30 mL) and dried under reduced pressure to yield the pure product (2.75 g, 84.1 % yield). ^{1}H NMR (DMSO-d_6, 499.72 MHz) δ 10.40 (s, 2H), 9.51 (s, 2H), 7.78 (d, J = 8.3 Hz, 4H), 7.63 (d, J = 8.2 Hz, 4H), 5.65 (s, 4H), 4.74 (t, J = 6.3 Hz, 4H), 3.25 (t, J = 6.3 Hz, 4H). ^{13}C{^{1}H} NMR (DMSO-d_6, 125.66 MHz): δ 144.97, 143.38, 139.92, 133.01, 129.56, 127.32, 117.71, 50.21, 47.25, 17.31. IR (neat): 3101, 3032, 3018, 2982, 2254, 1820, 1584, 1519, 1500, 1439, 1419, 1393, 1381, 1367, 1341, 1297, 1215, 1182, 1143, 1068, 1043, 1024, 1005, 980, 965, 916, 849, 833, 816, 787, 756, 708 cm^{-1}. ESI/MS (m/z): $[M\text{-}Br]^{+}$ 503.11, $[M\text{-}2Br]^{2+}$ 212.14. Anal. Calcd. for $C_{24}H_{24}Br_2N_8$: C, 49.33; H, 4.14; N, 19.18. Found: C, 49.31; H, 4.08; N, 18.90.

Synthesis of 4,4′-(4,4'-bitolyl)bis(1,2,4-triazole), 2 (di-MTZ^{Biph}). Potassium hydroxide (1.17 g, 0.0208 mol) and **1** (2.90 g, 0.00521 mol) were added to a 50 mL Erlenmeyer flask containing 25 mL of water. After 24 h, the product precipitated from solution as a white powder and was filtered and washed with water (3 x 50 mL), acetonitrile (3 x 50 mL), and tetrahydrofuran (3 x 50 mL). The pure product was dried under reduced pressure to yield 1.40 g (85.2 % yield). ^{1}H NMR (DMSO-d_6, 499.72 MHz) δ 8.65 (s, 4H), 7.66 (d, J = 7.7 Hz, 4H), 7.38 (d, J = 7.8 Hz, 4H), 5.32 (s, 4H). ^{13}C{^{1}H} NMR (DMSO-d_6, 125.66 MHz): δ 143.27, 139.25, 136.05, 128.29, 127.12, 47.21. IR (neat): 3089, 3029, 2962, 1664, 1613, 1522, 1500, 1458, 1439, 1403, 1378, 1361, 1336, 1316, 1207, 1179,

1169, 1074, 1006, 976, 967, 950, 889, 854, 833, 796, 755, 746, 712, 693 cm^{-1}. Anal. Calcd. for $C_{16}H_{14}N_6$: C, 68.34; H, 5.10; N, 26.56. Found: C, 67.80; H, 5.18; N, 25.77.

Synthesis of [Ag(di-MTZ^{Ph})(ClO_4)] • NMP • H_2O, 3. Silver(II) perchlorate monohydrate (0.0331 g, 0.0147 mmol) and **di-MTZ^{Ph}** (0.0177 g, 0.0735 mmol) were added to separate 4 mL scintillation vials and dissolved in 1 mL of water and 2 mL of NMP, respectively. The vials were heated to 85 °C for 30 min in an aluminum heating block, followed by mixing of the solutions and additional heating. After heating for 3 h, colorless needles formed and were isolated and washed with water and acetone to yield the pure product (35.2 mg, 84.8 % yield). IR (neat): 3587, 3115, 1678, 1622, 1540, 1501, 1453, 1423, 1404, 1337, 1295, 1210, 1194, 1168, 1089, 1014, 984, 960, 928, 892, 832, 811, 748, 715, 678, 653, 635 cm^{-1}. Anal. Calcd. for $C_{12}H_{14}ClAgN_6O_4$•DMA: C, 36.16; H, 4.11; N, 17.36. Found: C, 36.36; H, 4.12; N, 17.34.

Synthesis of [Cu(di-MTZ^{Biph})(ClO_4)] • DEF, 4. Copper(II) perchlorate hexahydrate (0.0136 g, 0.0367 mmol) and **di-MTZ^{Biph}** (0.0232 g, 0.0735 mmol) were added to separate 4 mL scintillation vials and dissolved in 1 mL of water and 2 mL of DEF, respectively. The vials were heated to 85 °C for 30 min in an aluminum heating block, followed by mixing of the solutions and additional heating. After heating for 24 h, colorless needles formed and were isolated and washed with water and acetone to yield the pure product (2.40 mg, 13.1 % yield). IR (neat): 3618, 3133, 2968, 2917, 2870, 2838, 1661, 1605, 1545, 1503, 1455, 1432, 1396, 1380, 1355, 1336, 1307, 1262, 1210,

1189, 1085, 1008, 973, 942, 859, 819, 754, 703, 684 cm^{-1}. Anal. Calcd. for $C_{18}H_{16}ClCuN_6O_4$•DEF: C, 47.59; H, 4.69; N, 16.89. Found: C, 47.59; H, 4.63; N, 16.84.

Synthesis of [Ag(di-MTZ^{Biph})(ClO_4)] • 3DMA, 5. Silver(II) perchlorate monohydrate (0.0331 g, 0.0147 mmol) and **di-MTZ^{Biph}** (0.0232 g, 0.0735 mmol) were added to separate 4 mL scintillation vials and dissolved in 1 mL of DMA and 2 mL of DMA, respectively. The vials were heated to 85 °C for 30 min in an aluminum heating block, followed by mixing of the solutions and additional heating. After heating for 24 h, the solution was pipetted to another 4 mL scintillation vial and allowed to cool to rt. Colorless needles formed after cooling and were isolated and washed with acetone to yield the pure product (23.0 mg, 59.7 % yield). IR (neat): 3123, 1703, 1542, 1501, 1444, 1389, 1356, 1185, 1083, 1006, 864, 803, 751, 693 cm^{-1}. Anal. Calcd. for $C_{18}H_{16}ClAgN_6O_4$: C, 41.28; H, 3.08; N, 16.05. Found: C, 41.16; H, 3.23; N, 15.76.

Synthesis of [Ag(di-MTZ^{Biph})(ClO_4)] • NMP, 6. Silver(II) perchlorate monohydrate (0.0331 g, 0.0147 mmol) and **di-MTZ^{Biph}** (0.0232 g, 0.0735 mmol) were added to separate 4 mL scintillation vials and dissolved in 1 mL of DMA and 2 mL of DMA, respectively. The vials were heated to 85 °C for 30 min in an aluminum heating block, followed by mixing of the solutions and additional heating. After heating for 24 h, the solution was pipetted to a 20 mL vial and 2 mL of heated (85 °C) NMP was added while solution was still hot, and allowed to cool to rt. Colorless needles formed after cooling.

IR (neat): 3109, 2932, 1673, 1629, 1537, 1501, 1443, 1392, 1356, 1296, 1263, 1189, 1088, 1062, 1009, 982, 932, 890, 850, 807, 751, 704, 646 cm^{-1}.

CHAPTER 5
PREPARATION OF A COORDINATION POLYMER FROM MIXED TRIAZOLE/TETRAZOLE LIGANDS

All work presented herein is the work of Brianna Hughes with assistance in crystallography by Zheng Lu.

Abstract

A variety of ligands incorporating mixed triazole/tetrazole and bistetrazoles were synthesized. With these ligands numerous metal combinations to form metal-organic frameworks were carried out. The formation of a coordination polymer with a mixed triazole/tetrazole ligand occurred and was characterized via single crystal X-ray diffraction along with spectroscopic methods and gas adsorption.

Introduction

Metal-organic frameworks (MOFs) allow for flexibility of pore sizes based on the organic linkers used.[18b, 50] This can adjust for high surface areas and the ability to absorb and desorb gases repeatedly, which indicates the versatility of these porous materials for gas separation and purification.[44e, 51]

To make multi-functional MOFs, consideration of spin-crossover metal-organic frameworks was proposed. Spin-crossover materials have the ability to change properties, such as metal-ligand bond length, dependent of an external force such as

pressure or temperature.[52] This external perturbation can cause a spin transition to occur, which will affect the metal-ligand bond distance of the framework.[1b, 53] Thus, developing these spin-crossover materials could create new membranes for the use of gas separation that would separate a three component gas mixture with one membrane.

Spin-crossover (SCO) occurs when small deviations in energy cause the valence d-electrons of a transition metal to change spin multiplicity.[52a, 54] For example, in an octahedral ligand field, the d-orbitals split into the t_{2g} and e_g subsets and may exist in either a high-spin (HS) or low-spin (LS) state for d^4 to d^7 configurations (Figure 5.1). The activation energy barrier to overcome these spin state transitions can occur as a function of temperature, light, or pressure.[52b] The critical temperature of a spin-crossover material occurs when there is an equilibrium of LS and HS metal centers.[52c]

Spin-crossover leads to changes in a material's physical properties, including magnetic moment, metal-ligand bond distances, and electronic transition energies.[53c] The changes in metal-ligand bond distance are of primary interest to potentially use spin-crossover materials in separations of gases. For example, comparing metal-ligand bond distances of LS states to HS states for Fe^{II} in an octahedral ligand field, changes can be between 0.15 and 0.18 Å in the HS state compared to the LS state.[52c]

The largest class of spin-crossover materials occurs in octahedral iron(II) complexes that are coordinated to nitrogenous heterocyclic ligands.[1b] The first example of a two- and three-dimensional spin-crossover compound utilized a bis-triazole ligand within the material.[52b] This finding led to a focus on the use of 1,2,4-triazoles as ligands

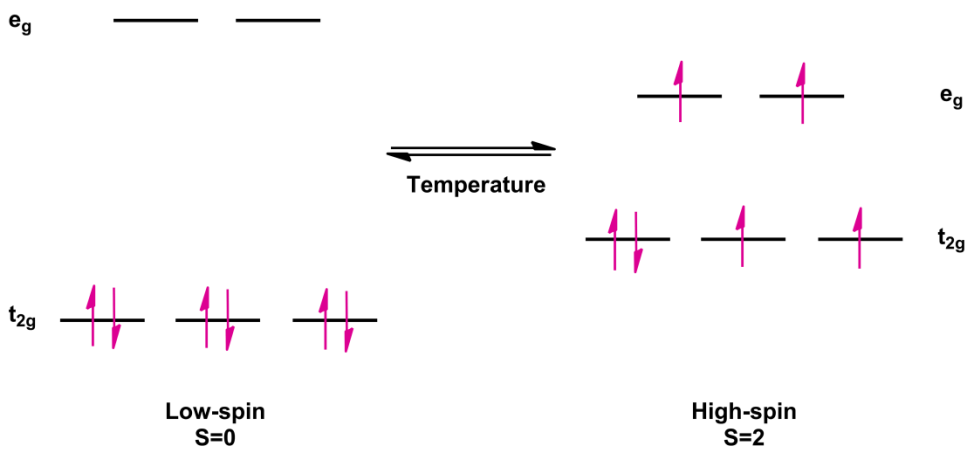


Figure 5.1. A d^6 iron(II) ion undergoing a spin-state transition as a function of temperature.

for SCO materials. Employing 1,2,4-triazoles as ligands has also been shown to raise the critical temperature (where the spin transition occurs) to near room temperature, improving upon the low temperatures of previously reported MOFs with pyridine linkers.[52b]

Kepert and coworkers synthesized the first porous spin-crossover framework, which consisted of a double penetrated two-dimensional rhombic grid constructed with the linkage of Fe^{II} centers by azpy, *trans*-4,4'-azopyridine units.[55] Crystals were collected of $Fe_2(azpy)_4(NCS)_4 \cdot (EtOH)$, as well as $Fe_2(azpy)_2(NCS)_2$. The ethanol within the framework formed H-bonds with the sulfur atoms of the thiocyanate ligands bound to the Fe-2, but not with the thiocyanate ligands bound to the Fe-1, allowing for the desolvation to affect the spin state of the iron. Thus, spin-crossover occurs when these bonds are broken at the Fe-2 site, allowing for a different conformation of the framework and different spin state of the iron. Above 150 K, both Fe^{II} sites are in the high-spin state where S = 2; while below 150 K, half of the Fe^{II} sites are present in the low-spin state, Fe-1 is S = 2 and Fe-2 becomes S = 0. The critical temperature for this synthesized framework is 150 K due to the spin state change at this temperature. Other solvents, such as methanol or isopropanol, have also been used within the framework and spin-crossover still occurs with desolvation making materials like these useful to the field of molecular sensing.[55]

Spin-crossover materials may also exhibit a magnetic hysteresis. A hysteresis occurs when the low-spin to high-spin transition temperature is higher than the high-spin to low-spin transition temperature. This, in turn, creates a memory effect within the

system.[52c] Kepert[56] and Kitagawa[57] both prepared separate spin-crossover MOFs utilizing Prussian Blue analog sheets linked by a pyrazine unit to create a three-dimensional structure. For Kepert's MOF, either Fe or Ni was used for the cyanide linkages, while Pt was used for Kitagawa's MOF. Both of these newly synthesized MOFs were found to undergo spin-crossover at ambient temperatures and displayed a magnetic hysteresis. Kitagawa's MOF was studied for guest adsorption properties. Gases such as N_2 and O_2 have no effect on the spin state, but others such as water, alcohols, and five or six-membered rings actually stabilize the high-spin state. The low-spin state was only stabilized with CS_2. When these guest gases or molecules were desorbed, the framework retained its spin-state, creating a memory function.

Kepert's MOF also exhibited a memory function after the guest was desorbed with the Ni MOF. Kepert continued analyzing the Ni framework and studied the gas adsorption capabilities.[56] Kitagawa's MOF was shown only to adsorb CO_2 at 298 K and the spin-state was unchanged,[57] while Kepert's MOF showed adsorption properties that were dependent on the spin state of the framework. Less N_2 was taken up in the low-spin state due to the decreased pore size, while CO_2 adsorption was favored in the low-spin state at low loadings and the high-spin state at high loadings. The adsorption of these gases had little effect on the transition temperature. Also, the gases were only released from the framework by changing the spin state. Kepert's framework showed a 13% change in cell volume, which contributed to the change in adsorption isotherms for the gases mentioned above. This was the first example that a change in spin state could affect these isotherms at a single temperature.[56]

We proposed synthesizing iron(II) SCO MOFs employing 1,2,3-triazoles and 1,2,3,4-tetrazoles as bridging ligands. These MOFs are expected to exhibit a change in surface area, pore size due to the property of spin-crossover, and metal-ligand bond distances (changing as a function of spin state), which makes them ideal for complex gas separation. Figure 5.2 illustrates the metal-ligand bond distance change when a framework undergoes spin-crossover. Tuning the ligands and reaction conditions will allow for MOFs to have a variety of pore sizes, enabling these spin-crossover MOFs to be used in gas separating applications that focus on differing kinetic diameters of gases.

Having the ability to adjust pore sizes based on spin-crossover MOFs would allow for different gases to be separated by using their unique kinetic diameters. These frameworks would also be analyzed via gas adsorption measurements at both high-spin and low-spin states in order to determine the pore sizes and, therefore, the potential applications for that particular MOF.

Results and Discussion

We synthesized ligands with rigid bistetrazoles or a triazole/tetrazole combination to allow our frameworks to have porosity suitable for gas separation applications. The ligands were chosen (Scheme 5.1) to allow the frameworks to have the necessary qualifications needed to be considered a MOF. Reaction 1 (Scheme 5.1) was carried

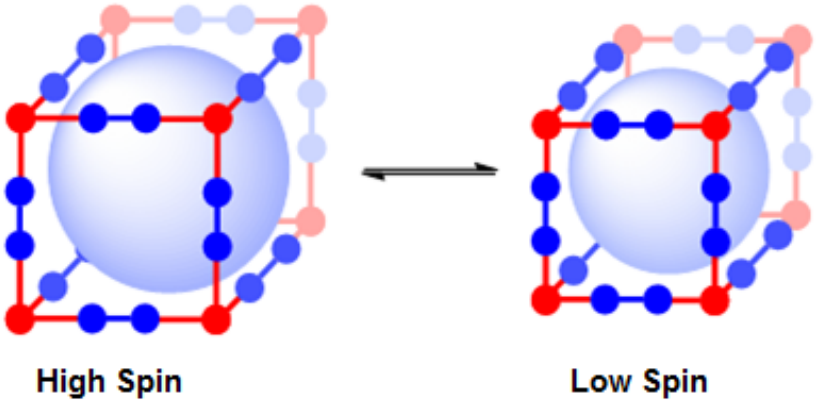
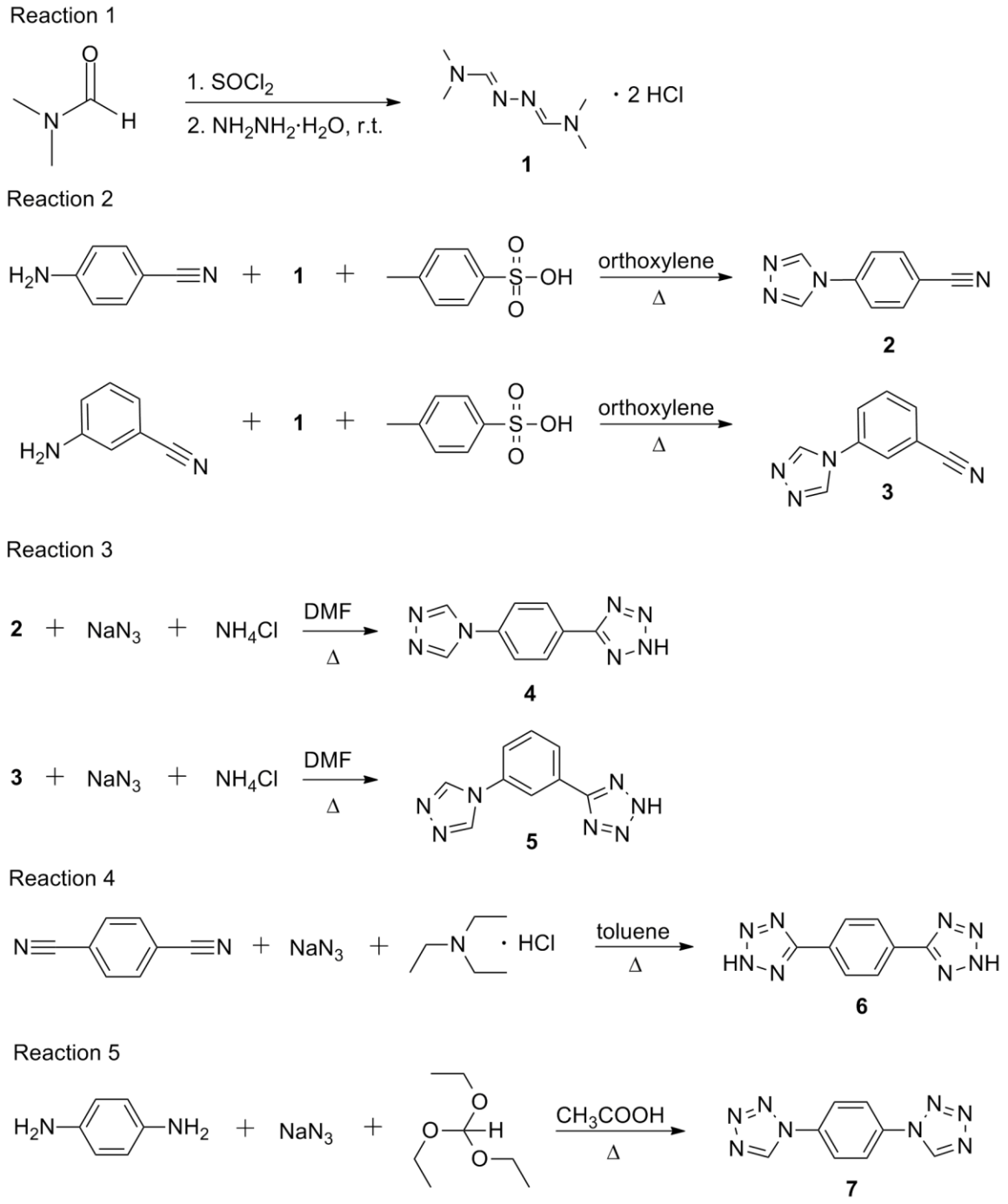


Figure 5.2. Schematic representation of a SCO MOF. Red circles represent Fe^{II} sites, blue circles represent the triazole/tetrazole ligand, and the shaded spheres show the change in pore size.

Scheme 5.1. Various reactions to synthesize mixed triazole/tetrazole (4 and 5) and bistetrazole ligands (6 and 7).



out by chilling DMF and carefully pipetting thionyl chloride and hydrazine hydrate into the solution. Solid formation of methanehydrazonamide (**1**) occurred after a few days.[58] After obtaining **1**, it was refluxed with 4-aminobenzonitrile and *para*-toluenesulfonic acid in orthoxylene until the desired product precipitated out (Scheme 5.1, Reaction 2). For Reaction 3 (Scheme 5.1), 4-(4H-1,2,4-triazol-4-yl)benzonitrile (**2**) reacted with sodium azide and ammonium chloride in *N*,*N*-dimethylmethanamide (DMF) with heat to synthesize 5-(4-[1,2,4]Triazol-4-yl-phenyl)-*2H*-tetrazole in a yield of 99% (**4**).[59] The meta-substituted ligand, 5-(3-[1,2,4]Triazol-4-yl-phenyl)-2*H*-tetrazole (**5**), was prepared by the same method. The first bistetrazole ligand (**6**) was prepared by refluxing 1,4-dicyanobenzene, sodium azide, and triethylamine hydrochloride in toluene as seen in Reaction 4 (Scheme 5.1). The solution was dissolved in NaOH solution then acidified using HCl, thus causing the product, 1,4-di(2*H*-tetrazol-5-yl)benzene, to precipitate out with a yield of 93%.[53d] The second bistetrazole ligand, 1,4-di(1*H*-tetrazol-1-yl)benzene (**7**) was made by heating sodium azide, *para*-phenylenediamine, and triethylorthoformate for 3 hours, then cooling to room temperature. Upon reaching room temperature, water was added (Scheme 5.1, Reaction 5).[53e] Isolated **7** was synthesized and had a yield of 54%. All ligands were characterized by ^{1}H and ^{13}C NMR and FT-IR.

Once our ligand library was developed, each ligand could proceed to MOF synthesis. MOF synthesis typically uses a combinatorial approach, which includes slightly altering variables such as metal to ligand ratio, temperature, length of reaction time, solvent, and counter-anion. These slight changes to reaction conditions affect the

connectivity of the MOF.[60] When favored reaction conditions are met single crystals will form, which is critical for characterization. Crystal growth of these frameworks can be promoted by varying techniques, such as slow diffusion or super saturation.[61]

Most of the ligands we synthesized (**4**-**6**) are neutral (all but **5** have been synthesized before),[10-12] but can be deprotonated in basic conditions or in the presence of metal ions to form an anionic ligand, which would lead to the formation of a neutral MOF. Neutral MOFs are beneficial in that there are no anions within the pores, allowing for gas adsorption to occur more readily. However, **7** is solely a neutral ligand while the Fe has a "+2" charge; this implies that in order to balance the charge, anions must be present in the framework by either being bound to the metal center or present in the pores. These anions vary depending upon the iron salt used in the reaction and include: chloride, sulfate, perchlorate, or thiocyanate. Due to the presence of these anions and their position in the MOF, stability and porosity can be greatly affected. Also depending on the anion present, the framework could change its spin state.[52b]

Small scale reactions with **4**-**7** enabled a wide variety of variables to be tested to determine optimal conditions for formation of crystalline materials. Promising results came from the reaction forming Cu coordination polymer (CP) **8** by a 1 : 5 metal to ligand ratio with **4** and copper(II) nitrate with a solvent mixture of DMF and water, and a temperature of 85 °C overnight. Blue crystals were collected from these reaction conditions. The PXRD data indicated a change from **4**, and displayed a promising peak between 0-10° on the 2θ scale. In addition, FT-IR spectroscopy indicated a shift from the ligand fingerprint to the MOF structure, which potentially indicates that the ligand

was bound to the metal center. A TGA displayed a 71.95% weight loss around 150 °C. Single crystal X-ray data was also collected (Figure 5.3). Comparing our results with the literature pointed to an isostructural Cu-MOF by Domasevitch and coworkers, only differing in the identity of the counter-anion present within the pores.[59] Unfortunately, this CP was determined to be nonporous and no other reaction conditions provided significant results with these particular ligands.

Conclusion

Presently, gas separation methods use membrane materials such as zeolites and polymers. Unfortunately, these materials have limitations, such as their tendency to fluctuate under pressure and their short life span. MOFs provide an alternative as they are porous materials with a high surface area. These frameworks can also exhibit size and shape selectivity with guest molecules. This property can be emphasized by the function of spin-crossover. Previous spin-crossover MOFs have shown that changing the spin state of the Fe^{II} present in the framework affects the metal-ligand bond distance. Thus, these spin-crossover frameworks may be used for gas separation methods by separating multi-component gas mixtures using one material. With the synthesis of mixed triazole/tetrazole and bistetrazole ligands, efforts to create metal-organic frameworks with spin-crossover led to a coordination polymer with copper. This

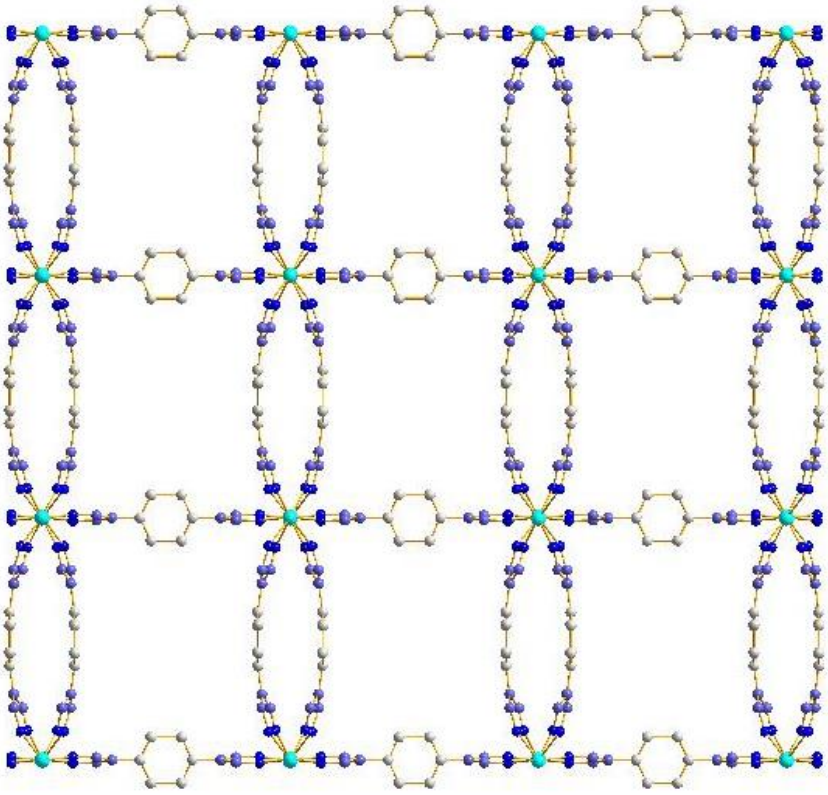


Figure 5.3. Crystal structure of 8 with carbon, nitrogen, carbon/nitrogen (locations of the triazole/tetrazolate cycles of the ligand are idealized since two types of the sites were equally disordered by symmetry), and copper in white, royal blue, light purple, and aqua. All hydrogen atoms have been removed for clarity.

CP was characterized through single crystal X-ray crystallography, among other methods. Unfortunately, no other coordination polymers or MOFs were synthesized. The use of neutral ligands with spin-crossover materials would still be highly advantageous for the application of gas separation today.

Experimentals

The compounds methanehydrazonamide (**1**),[58] 4-(4H-1,2,4-triazol-4-yl)benzonitrile (**2**),[10] 5-(4-[1,2,4]Triazol-4-yl-phenyl)-*2H*-tetrazole (**4**),[59] 1,4-di(2*H*-tetrazol-5-yl)benzene (**6**),[53d] and 1,4-di(1*H*-tetrazol-1-yl)benzene (**7**),[53e] were all prepared from the literature. All reagents were purchased from commercial vendors and used without further purification. Solution ^{1}H and $^{13}C\{^{1}H\}$ spectra were recorded at ambient temperature on a Varian Mercury 300 MHz or Varian VNMRS 500 MHz, narrow-bore broadband system. ^{1}H and $^{13}C\{^{1}H\}$ NMR chemical shifts were referenced to the residual solvent. All mass spectrometry analyses were conducted at the Mass Spectrometry Center located in the Department of Chemistry at the University of Tennessee, Knoxville. The ESI/MS analyses were performed using a QSTAR Elite quadrupole time-of-flight (QTOF) mass spectrometer with an electrospray ionization source from AB Sciex (Concord, Ontario, Canada). Sample solutions of ligands **4**-**6** for mass spectrometry were prepared in acetonitrile. Infrared spectra were collected on a Thermo Scientific Nicolet iS10 with a Smart iTR accessory for attenuated total reflectance. Thermogravimetric analysis data were collected on a TA Instruments TGA

Q50 under N_2. Carbon, hydrogen, and nitrogen analyses were obtained from Atlantic Microlab, Norcross, GA.

Synthesis of 3-(4H-1,2,4-triazol-4-yl)benzonitrile, $C_9H_6N_4$, 3. 3-aminobenzonitrile (15.3 g, 0.130 mol), **1** (35.9 g, 0.143 mol), and *para*-toluenesulfonic acid (1.24 g, 6.49 mmol) were added to a 1000 mL round bottom flask. 150 mL of orthoxylene was added and the resulting mixture was set up to reflux overnight at a temperature of 140 °C. The brown solid in the reaction was then broken up before cooling to room temperature. This solid was then filtered through a 150 mL medium sintered-glass frit and washed with (2x50 mL) each of toluene, methylene chloride, and sodium bicarbonate as well as (2x30 mL) each of water and tetrahydrofuran. Any further impurities were removed by stirring in water, filtering and washing with tetrahydrofuran. The resulting solid was then dried under reduced pressure (14.7 g, 66.3 % yield). ^{1}H NMR (DMSO-$_{d6}$, 300.1 MHz): δ 9.21 (s, 1H), 8.09 (d, *J* = 8.0 Hz, 1H), 7.90 (d, *J* = 7.7 Hz, 1H), 7.77 (t, *J* = 7.9 Hz, 1H), 3.35 (s, 1H).

Synthesis of 5-(3-[1,2,4]Triazol-4-yl-phenyl)-2*H*-tetrazole, $C_9H_7N_6$, 5. *Meta*-toluenesulfonic acid (**3**) (3.79 g, 22.3 mmol), sodium azide (1.81 g, 27.9 mmol), and ammonium chloride (1.42 g, 26.6 mmol) were combined in a 250 mL round bottom flask with dimethylformamide (DMF) (75 mL) and stirred. The reaction was heated to 110 °C for one night. The reaction mixture was cooled to room temperature and added to 600 mL of water. Addition of acetic acid to pH = 4 was then carried out. The reaction

mixture was then collected in a 150 mL fine sintered-glass frit and washed with 25 mL each of water, ethanol, and ethyl ether. The white solid product was then dried under reduced pressure (4.31 g, 90.6 % yield). ^{1}H NMR (DMSO-$_{d6}$, 300.1 MHz): δ 9.22 (s, 1H), 8.32 (s, 1H), 8.06 (d, *J* = 7.4 Hz, 1H), 7.92 (d, *J* = 7.6 Hz, 1H), 7.80 (t, *J* = 7.9 Hz, 1H). IR (neat): 3126, 3065, 2427, 1849, 1622, 1592, 1574, 1533, 1509, 1484, 1414.93, 1295, 1267, 1248, 1180, 1146, 1100, 1068, 1041, 1011, 973, 955, 889, 862, 812, 755, 744, 711, 686, 671, 658 cm^{-1}. Anal. Calcd. for $C_9H_7N_7$: C, 50.70; H, 3.31; N, 45.99. Found: C, 49.73; H, 3.15; N, 45.20.

Synthesis of Cu CP 8. **4** (7.90 mg, 0.0368 mmol) was added to 2 mL DMF in a 4 mL scintillation vial. This vial was then sonicated and heated at 85 °C to result in a clear solution. Copper(II) nitrate (1.80 mg, 0.00735 mmol) was added to 2 mL water in a 4 mL scintillation vial. The solution of the metal was then added slowly via pipette to the solution of the ligand. The resulting solution was then heated at 85 ℃ overnight. Blue crystals suitable for X-ray crystallography formed.

X-ray Structure Determinations. X-ray diffraction measurements were performed on single crystals coated with Paratone oil (Hampton Research) and mounted on glass fibers or nylon cryoloops (Hampton Reasearch). Each crystal was frozen under a stream of N_2 while data were collected on a Bruker SMART APEXII three circle diffractometer equipped with a CCD area detector and operated at 1,800 W power (45 kV, 40 mA) to generate Mo Kα radiation (λ = 0.71073 Å). A matrix scan using at least

12 centered reflections was used to determine initial lattice parameters. Reflections were merged and corrected for Lorenz and polarization effects, scan speed, and background using SAINT 4.05. Absorption corrections, including odd and even ordered spherical harmonics were performed using SADABS, if necessary. Space group assignments were based upon systematic absences, *E* statistics, and successful refinement of the structure. The structures were solved by direct methods with the aid of successive difference Fourier maps, and were refined against all data using the SHELXTL 5.0 software package.

Solving **8** led to an uncertainty in carbon and nitrogen determination as one N-heterocycle was a triazole and the opposite was a tetrazole. These atoms were denoted as a separate color (light purple) in the crystal structure.

Powder X-ray experiments. Powder X-ray diffraction (PXRD) data was collected using a Panalytical Empyrean θ-2θ diffractometer in reflectance Bragg-Brentano geometry. Cu-Kα radiation (λ = 1.5406 Å; 1,800 W, 45 kV, 40 mA) was focused using a planar Gobel Mirror riding the Kα line. Diffracted radiation was detected using a PIXcel3d detector [(6° 2θ sampling width) equipped with a Ni monochrometer]. All samples were mounted onto a zero background quartz plate fixed on a sample holder by dropping powders and then leveling the sample surface. The best counting statistics were achieved by using a 0.0131º 2θ step scan from 4 – 50° with an exposure time of 81.6 s per step and a revolution spin rate of 4 s.

CHAPTER 6
CONCLUSIONS

Chapter Summaries

Previous work with azolyl borates showed both homoleptic complexes and coordination polymers; however, there was a missing tris-azolyl borate that had never been prepared, the tris(1,2,3-triazolyl)borate ligand. Tris(1,2,3-triazolyl)borate was synthesized to explore metal reactions that could lead to homoleptic complexes and coordination polymers. Tris(1,2,3-triazolyl)borate exhibited two separate bonding characteristics through binding in the sodium salt when analyzed via single crystal X-ray diffraction. Initial work showed the formation of both homoleptic complexes as well as coordination polymers by utilizing a tris(1,2,3-triazolyl)borate ligand with varying metal salts. First row transition metals, including Fe, Ni, and Co, reacted with our triazolyl borate to give homoleptic complexes. The inclusion of Cd, a larger metal center, led to a different binding through the tris(1,2,3-triazolyl)borate and contributed to the formation of a coordination polymer. Thus with the synthesis and completion of Trofimenko's original work on azolyl borate ligands, new homoleptic complexes and a coordination polymer were made by the missing link, the tris(1,2,3-triazolyl)borate.

Since incorporating an azolyl, or triazolyl in particular, onto a borate ligand has previously been successful, further work included formation of borate nitrenium ligands. Nitrenium ligands, which utilize the 1,2,3-triazole, are the nitrogen analog of Arduengo's N-heterocyclic carbene, and have only recently been explored. By interchanging the central carbon for nitrogen, Gandelman and coworkers prepared a chelating ligand that allowed the central nitrogen of the nitrenium ligand to bind to the metal center. In an

attempt to overcome the need for chelating arms on the nitrenium ligand, a monodentate neutral nitrenium ligand could be synthesized that may improve binding to a cationic metal center. By combining a borane with a 1,2,3-triazole, a borate-nitrenium that has an overall neutral charge can be synthesized. Two separate neutral nitrenium ligands were made with either ethyl groups or phenyl groups on the borate moiety. These ligands were combined with various metals in a series of reactions, but no metal complexes were successfully synthesized. Nevertheless, utilizing a monodentate neutral nitrenium ligand on a metal center could be a highly impactful endeavor if realized.

The development of metal-organic frameworks (MOFs) has flourished since their discovery in the late 1990s. MOFs can be prepared in a combinatorial manner, by reacting a metal salt and a linker to form an extended porous framework. Triazoles and tetrazoles have been incorporated in linkers as an alternative to the heavily researched carboxylates within framework formation of porous metal-organic frameworks. The first porous stable MOFs prepared were static frameworks using carboxylates, and early on it was recognized that increasing the pore size could be achieved by elongating the linker present between the metal centers.

Within the last decade, the number or MOF structures has increased dramatically, including structures that exhibit framework distortion based on external perturbation. Breathing, or dynamic MOFs, allow for these materials to be used in applications that allow for selectivity to be the central focus. Applications for these breathing materials include the separation of gases, which can be attained by a gate-

opening phenomenon within the breathing MOF. Our group has showcased breathing frameworks with a gate-opening effect by incorporating a triazole within the linker successfully.

Previous work within the Jenkins's group showcased a rotating aryl ring that rotated as a function of guest in a Cu 2D MOF. This MOF utilized a bis-triazole-based ligand, di-MTZ^{Ph}, and allowed for a family of 2D MOFs to be synthesized. Our work initially started with metal reactions utilizing di-MTZ^{Ph}. A Ag 2D MOF was formed from these combinatorial syntheses and demonstrated that the original synthesis of 2D MOFs with rotating aryl rings could be generalized. By incorporating a longer linker, di-MTZ^{Biph}, an expanded family of 2D MOFs with rotating aryl rings was synthesized, thus consisting of two gates for rotation instead of just one. An extended linker allowed for three separate states (open/open, open/closed, and closed/closed) to be observed within three separate MOFs. A Cu 2D MOF displayed the open/open state, which was observed clearly through single crystal X-ray diffraction. The initial Ag 2D MOF with the extended linker was made by using DMA and formed crystals after cooling the solution to room temperature. This original Ag MOF showed a closed/closed state observed in the crystal structure. Since these crystals formed as the solvent was cooling, other solvents were added in order to see if another state of rotation of the aryl rings could be realized. When NMP was added to the original Ag MOF solution while cooling, a third and final structure was obtained. Through single crystal X-ray diffraction, it was clearly observed that the phenyl rings showed the open/closed state. This was the first

example of an isostructurally designed family of gate-based breathing MOFs, with all possible states observed through single crystal X-ray diffraction.

Another way triazole-based ligands showed their versatility is with spin-crossover materials. By having SCO occur within a metal-organic framework, breathing could be achieved. Spin-crossover (SCO) employs an external perturbation, such as light, temperature or pressure that changes the metal-ligand bond distance. The use of triazoles and tetrazoles has previously been shown to facilitate SCO materials when iron is the metal center. A family of mixed triazole/tetrazole as well as bis-tetrazole ligands was synthesized in order to test with varying combinations of metal salts, ligand to metal ratios, temperature, and solvent. One reaction in particular proved successful, that of copper(II) nitrate and a mixed triazole/tetrazole ligand which formed a coordination polymer. Unfortunately, no other coordination polymers or MOFs were synthesized. The use of triazole and tetrazole ligands within SCO materials still remains a possible route for the synthesis of breathing metal-organic frameworks.

Dissertation Summation

Both 1,2,3- and 1,2,4-triazoles have been highlighted in the aforementioned chapters demonstrating that N-heterocyclic ligands can be employed to form a variety of structures. The inclusion of these moieties allowed for the synthesis of homoleptic complexes, coordination polymers, and metal-organic frameworks. By employing 1,2,3-

and 1,2,4-triazole based ligands, various binding modes were observed in the materials prepared. Incorporating the novel tris(1,2,3-triazolyl)borate exhibited binding through both the second and third nitrogen allowing for the synthesis of homoleptic complexes and a coordination polymer. The nitrene ligands could utilize the central nitrogen of the 1,2,3-triazole to bind to a metal center. In the metal-organic frameworks synthesized, both exodentate nitrogens in the bis-1,2,4-triazole ligand bound to the metal center in each example discussed in the previous chapter. These materials clearly exemplify multiple binding of triazoles and showcase the versatility of incorporating these moieties throughout coordination chemistry.

Potential Future Directions

The bis(1,2,3-triazolyl)borate ligand would be a candidate to spend further effort on to purify and isolate. With a pure product, this ligand could potentially lead to coordination complexes or polymers. Further research could also include the addition of another azolyl to the bis(1,2,3-triazolyl)borate to form a mixed triazolyl borate. This type of ligand could then be studied to first determine if any metal complexes or coordination polymers can be prepared, and if so, to evaluate the possible binding modes of mixed borate ligands.

The nitrenes may bind more effectively to metals by incorporating a negative charge on the ligand. This could be achieved by placing two separate boron groups

onto the 1,2,3-triazole. With one equivalent of the borane, as discussed in the previous chapter, the nitrene ligand was neutral having an improved charge over the cationic nitrene which required chelation from a pincer ligand. With the addition of two equivalents of borane, the first boron source would cancel the positive charge from the nitrogen and the second boron would contribute a negative charge to the nitrene. This negative charge should allow the central nitrogen to bind more efficiently to a positive metal salt.

LIST OF REFERENCES

1. (a) Al-Masoudi, I. A.; Al-Soud, Y. A.; Al-Salihi, N. J.; Al-Masoudi, N. A., 1,2,4-Triazoles: Synthetic approaches and pharmacological importance. (Review). *Chem. Heterocylc. Compd.* **2006**, *42*, 1377-1403; (b) Aromí, G.; Barrios, L. A.; Roubeau, O.; Gamez, P., Triazoles and tetrazoles: Prime ligands to generate remarkable coordination materials. *Coord. Chem. Rev.* **2011**, *255*, 485-546; (c) Haasnoot, J. G., Mononuclear, oligonuclear and polynuclear metal coordination compounds with 1,2,4-triazole derivatives as ligands. *Coord. Chem. Rev.* **2000**, *200–202*, 131-185; (d) Juricek, M.; Kouwer, P. H. J.; Rowan, A. E., Triazole: a unique building block for the construction of functional materials. *Chem. Commun.* **2011**, *47*, 8740-8749; (e) Schulze, B.; Schubert, U. S., Beyond click chemistry - supramolecular interactions of 1,2,3-triazoles. *Chem. Soc. Rev.* **2014**, *43*, 2522-2571.
2. Werner, A.; Stiasny, E., Ueber Nitroderivate des Azo-, Azoxy- und Hydrazo-Benzols. *Ber. Dtsch. Chem. Ges.* **1899**, *32*, 3256-3282.
3. Bladin, J. A., Ueber von Dicyanphenylhydrazin abgeleitete Verbindungen. *Ber. Dtsch. Chem. Ges.* **1885**, *18*, 1544-1551.
4. Tulchinsky, Y.; Kozuch, S.; Saha, P.; Mauda, A.; Nisnevich, G.; Botoshansky, M.; Shimon, L. J. W.; Gandelman, M., Coordination Chemistry of N-Heterocyclic Nitrenium-Based Ligands. *Chem. Eur. J.* **2015**, *21*, 7099-7110.
5. Maddila, S.; Pagadala, R.; Jonnalagadda, S. B., 1,2,4-Triazoles. A review of synthetic approaches and the biological activity. *Lett. Org. Chem.* **2013**, *10*, 693-714.
6. (a) Horike, S.; Umeyama, D.; Kitagawa, S., Ion Conductivity and Transport by Porous Coordination Polymers and Metal–Organic Frameworks. *Acc. Chem. Res.* **2013**, *46*, 2376-2384; (b) Roubeau, O., Triazole-Based One-Dimensional Spin-Crossover Coordination Polymers. *Chem. Eur. J.* **2012**, *18*, 15230-15244.
7. (a) Demessence, A.; D'Alessandro, D. M.; Foo, M. L.; Long, J. R., Strong CO2 Binding in a Water-Stable, Triazolate-Bridged Metal−Organic Framework Functionalized with Ethylenediamine. *J. Am. Chem. Soc.* **2009**, *131*, 8784-8786; (b) Kan, W.-Q.; Liu, B.; Yang, J.; Liu, Y.-Y.; Ma, J.-F., A Series of Highly Connected Metal–Organic Frameworks Based on Triangular Ligands and d10 Metals: Syntheses, Structures, Photoluminescence, and Photocatalysis. *Cryst. Growth Des.* **2012**, *12*, 2288-2298.
8. (a) Trofimenko, S., Boron-Pyrazole Chemistry. *J. Am. Chem. Soc.* **1966**, *88*, 1842-1844; (b) Trofimenko, S., Boron-pyrazole chemistry. II. Poly(1-pyrazolyl)-borates. *J. Am. Chem. Soc.* **1967**, *89*, 3170-3177; (c) Janiak, C.; Scharmann, T. G.; Albrecht, P.; Marlow, F.; Macdonald, R., [Hydrotris(1,2,4-triazolyl)borato]silver(I): Structure and Optical Properties of a Coordination Polymer Constructed from a Modified Poly(pyrazolyl)borate Ligand. *J. Am. Chem. Soc.* **1996**, *118*, 6307-6308; (d) Janiak, C.; Hemling, H., Linkage lsomerism in bis[hydrotris(1,2,4-triazolyl)borato]zinc from a molecular chelate complex to a three-dimensional co-ordination polymer. *J. Chem. Soc., Dalton Trans.* **1994**, 2947-2952; (e) Lobbia, G. G.; Pellei, M.; Pettinari, C.; Santini, C.; Somers, N.; White, A. H., Poly(1,2,3-benzotriazolyl)borate complexes with copper(I) and tri-organophosphane: an unprecedented κ1-coordination of $[H_2B(btz)_2]$ (btz=1,2,3-benzotriazolyl) in the X-ray crystal structure of $[Cu(PBn_3)2\{(btz)BH_2(btz)\}]$. *Inorg. Chim. Acta* **2002**, *333*, 100-108; (f) Lalor, F. J.; Miller, S. M.; Garvey, N., Poly(benzotriazolyl)borates—I. ligand synthesis and characterization. *Polyhedron* **1990**,

9, 63-68; (g) Santini, C.; Pellei, M.; Lobbia, G. G.; Papini, G., Synthesis and Properties of Poly(pyrazolyl)borate and Related Boron-Centered Scorpionate Ligands. Part A: Pyrazole-Based Systems. *Mini-Rev. Org. Chem.* **2010**, *7*, 84-124; (h) Pellei, M.; Lobbia, G. G.; Papini, G.; Santini, C., Synthesis and Properties of Poly(pyrazolyl)borate and Related Boron-Centered Scorpionate Ligands. Part B: Imidazole-, Triazole- and Other Heterocycle-Based Systems. *Mini-Rev. Org. Chem.* **2010**, *7*, 173-203; (i) Janiak, C.; Röhr, C.; Temizdemir, S., The Structure of Hydrotris(imidazolyl)boratothallium(I) – the First Structurally Authenticated Tris(imidazolyl)borate Metal Complex. *Z. Anorg. Allg. Chem.* **2000**, *626*, 1265-1267; (j) Onishi, M.; Kumagae, S.; Asai, K.; Kawano, H.; Shigemitsu, Y., Electrochemical Influence of Tridentate Polypyrazolylborate Ligands: Syntheses and Electrochemistry of Bis(η_3-polypyrazolylborato)ruthenium(II) Complexes. *Chem. Lett.* **2001**, 96-97; (k) Reger, D. L.; Huff, M. F.; Rheingold, A. L.; Haggerty, B. S., Control of structure in lead(II) complexes using poly(pyrazolyl)borate ligands. Stereochemically inactive lone pair in octahedral $[HB(3,5\text{-}Me_2pz)_3]_2Pb$ (pz = pyrazolyl ring). *J. Am. Chem. Soc.* **1992**, *114*, 579-584; (l) Santini, C.; Pellei, M.; Lobbia, G. G.; Alidori, S.; Berrettini, M.; Fedeli, D., New (diphenylphosphane)benzoic acid copper(I) derivatives of “scorpionate” ligands with superoxide scavenging activity. *Inorg. Chim. Acta* **2004**, *357*, 3549-3555; (m) Zaidi, S. A. A.; Khan, T. A.; Zaidi, S. R. A.; Siddiqi, Z. A., Transition metal complexes of hydrotris(imidazolyl)borate anion. *Polyhedron* **1985**, *4*, 1163-1166.

9. (a) Trofimenko, S., *Scorpionates. The Coordination of Polypyrazolylborate Ligands*. Imperical College Press: London, 1999; (b) Pettinari, C., *Scorpionates II: Chelating Borate Ligands*. Imperial College Press: London, 2008; (c) Smith, J. M., STRONGLY DONATING SCORPIONATE LIGANDS. *Comments Inorg. Chem.* **2008**, *29*, 189-233.

10. (a) Janiak, C., Clathrates and coordination polymers: new dimensions in poly(azolyl)borate chemistry with poly-(triazolyl)- and -(tetrazolyl)-borate ligands. *J. Chem. Soc., Chem. Commun.* **1994**, *0*, 545-547; (b) Janiak, C., Binary [Hydrotris(1,2,4-triazolyl)borate]metal Complexes $[M\{HB(C_2H_2N_3)_3\}_2]$ with M = Fe, Co, Cu, Zn: Synthesis, Characterization, Magnetochemistry, and X-ray Structure of $[Cu\{HB(C_2H_2N_3)_3\}_2 \cdot 4CH_3]$. *Chem. Ber.* **1994**, *127*, 1379-1385; (c) Hughes, B. C.; Lu, Z.; Jenkins, D. M., The final unadorned tris(azolyl)borate: finishing what Trofimenko started in 1966. *Chem. Commun.* **2014**, *50*, 5273-5275; (d) Ryu, D. W.; Lee, W. R.; Lim, K. S.; Phang, W. J.; Hong, C. S., Two Homochiral Bimetallic Metal–Organic Frameworks Composed of a Paramagnetic Metalloligand and Chiral Camphorates: Multifunctional Properties of Sorption, Magnetism, and Enantioselective Separation. *Cryst. Growth Des.* **2014**, *14*, 6472-6477.

11. (a) Herrmann, W. A., N-Heterocyclic Carbenes: A New Concept in Organometallic Catalysis. *Angew. Chem. Int. Ed.* **2002**, *41*, 1290-1309; (b) Bourissou, D.; Guerret, O.; Gabbaï, F. P.; Bertrand, G., Stable Carbenes. *Chem. Rev.* **2000**, *100*, 39-92; (c) Hahn, F. E.; Jahnke, M. C., Heterocyclic Carbenes: Synthesis and Coordination Chemistry. *Angew. Chem. Int. Ed.* **2008**, *47*, 3122-3172; (d) Arduengo, A. J. I.; Harlow, R. L.; Kline, M., A stable crystalline carbene. *J. Am. Chem. Soc.* **1991**, *113*, 361-363.

12. (a) Heims, F.; Pfaff, F. F.; Abram, S.-L.; Farquhar, E. R.; Bruschi, M.; Greco, C.; Ray, K., Redox Non-Innocence of a N-Heterocyclic Nitrenium Cation Bound to a Nickel–Cyclam Core. *J. Am. Chem. Soc.* **2014**, *136*, 582-585; (b) Tulchinsky, Y.; Iron, M. A.; Botoshansky, M.; Gandelman, M., Nitrenium ions as ligands for transition metals. *Nat. Chem.* **2011**, *3*, 525-531.
13. Batten Stuart, R.; Champness Neil, R.; Chen, X.-M.; Garcia-Martinez, J.; Kitagawa, S.; Öhrström, L.; O'Keeffe, M.; Paik Suh, M.; Reedijk, J., Terminology of metal–organic frameworks and coordination polymers (IUPAC Recommendations 2013). In *Pure Appl. Chem.*, 2013; Vol. 85, p 1715.
14. (a) Robin, A. Y.; Fromm, K. M., Coordination polymer networks with O- and N-donors: What they are, why and how they are made. *Coord. Chem. Rev.* **2006**, *250*, 2127-2157; (b) Wang, K.; Chen, Z.-L.; Zou, H.-H.; Zhang, Z.; Sun, W.-Y.; Liang, F.-P., Two Types of Cu-Ln Heterometallic Coordination Polymers with 2-Hydroxyisophthalate: Syntheses, Structures, and Magnetic Properties. *Cryst. Growth Des.* **2015**, *15*, 2883-2890.
15. Rowsell, J. L. C.; Spencer, E. C.; Eckert, J.; Howard, J. A. K.; Yaghi, O. M., Gas Adsorption Sites in a Large-Pore Metal-Organic Framework. *Science* **2005**, *309*, 1350-1354.
16. (a) Zhou, H.-C. J.; Kitagawa, S., Metal-Organic Frameworks (MOFs). *Chem. Soc. Rev.* **2014**, *43*, 5415-5418; (b) Meek, S. T.; Greathouse, J. A.; Allendorf, M. D., Metal-Organic Frameworks: A Rapidly Growing Class of Versatile Nanoporous Materials. *Adv. Mater.* **2011**, *23*, 249-267.
17. (a) Furukawa, H.; Cordova, K. E.; O'Keeffe, M.; Yaghi, O. M., The Chemistry and Applications of Metal-Organic Frameworks. *Science* **2013**, *341*; (b) Kitagawa, S.; Matsuda, R., Chemistry of coordination space of porous coordination polymers. *Coord. Chem. Rev.* **2007**, *251*, 2490-2509.
18. (a) Khan, N. A.; Hasan, Z.; Jhung, S. H., Adsorptive removal of hazardous materials using metal-organic frameworks (MOFs): A review. *J. Hazard. Mater.* **2013**, *244–245*, 444-456; (b) Murdock, C. R.; Hughes, B. C.; Lu, Z.; Jenkins, D. M., Approaches for synthesizing breathing MOFs by exploiting dimensional rigidity. *Coord. Chem. Rev.* **2014**, *258–259*, 119-136; (c) Kitagawa, S.; Kitaura, R.; Noro, S.-i., Functional Porous Coordination Polymers. *Angew. Chem. Int. Ed.* **2004**, *43*, 2334-2375; (d) Schneemann, A.; Bon, V.; Schwedler, I.; Senkovska, I.; Kaskel, S.; Fischer, R. A., Flexible metal-organic frameworks. *Chem. Soc. Rev.* **2014**, *43*, 6062-6096; (e) Ferey, G., Hybrid porous solids: past, present, future. *Chem. Soc. Rev.* **2008**, *37*, 191-214; (f) Ferey, G.; Serre, C., Large breathing effects in three-dimensional porous hybrid matter: facts, analyses, rules and consequences. *Chem. Soc. Rev.* **2009**, *38*, 1380-1399; (g) Fu, H.-R.; Zhang, J., Flexible Porous Zinc–Pyrazole–Adenine Framework for Hysteretic Sorption of Light Hydrocarbons. *Cryst. Growth Des.* **2015**, *15*, 1210-1213; (h) Li, X.-L.; Liu, G.-Z.; Xin, L.-Y.; Wang, L.-Y., A novel metal-organic framework displaying reversibly shrinking and expanding pore modulation. *CrystEngComm* **2012**, *14*, 5757-5760; (i) Murdock, C. R.; Lu, Z.; Jenkins, D. M., Effects of Solvation on the Framework of a Breathing Copper MOF Employing a Semirigid Linker. *Inorg. Chem.* **2013**, *52*, 2182-2187; (j) Murdock, C. R.; McNutt, N. W.; Keffer, D. J.; Jenkins, D. M., Rotating

Phenyl Rings as a Guest-Dependent Switch in Two-Dimensional Metal–Organic Frameworks. *J. Am. Chem. Soc.* **2014**, *136*, 671-678; (k) Seo, J.; Matsuda, R.; Sakamoto, H.; Bonneau, C.; Kitagawa, S., A Pillared-Layer Coordination Polymer with a Rotatable Pillar Acting as a Molecular Gate for Guest Molecules. *J. Am. Chem. Soc.* **2009**, *131*, 12792-12800; (l) Tanaka, D.; Nakagawa, K.; Higuchi, M.; Horike, S.; Kubota, Y.; Kobayashi, T. C.; Takata, M.; Kitagawa, S., Kinetic Gate-Opening Process in a Flexible Porous Coordination Polymer. *Angew. Chem. Int. Ed.* **2008**, *47*, 3914-3918; (m) Thallapally, P. K.; Tian, J.; Radha Kishan, M.; Fernandez, C. A.; Dalgarno, S. J.; McGrail, P. B.; Warren, J. E.; Atwood, J. L., Flexible (Breathing) Interpenetrated Metal−Organic Frameworks for CO_2 Separation Applications. *J. Am. Chem. Soc.* **2008**, *130*, 16842-16843; (n) Wang, C.; Li, L.; Bell, J. G.; Lv, X.; Tang, S.; Zhao, X.; Thomas, K. M., Hysteretic Gas and Vapor Sorption in Flexible Interpenetrated Lanthanide-Based Metal–Organic Frameworks with Coordinated Molecular Gating via Reversible Single-Crystal-to-Single-Crystal Transformation for Enhanced Selectivity. *Chem. Mater.* **2015**.

19. Kitagawa, S.; Uemura, K., Dynamic porous properties of coordination polymers inspired by hydrogen bonds. *Chem. Soc. Rev.* **2005**, *34*, 109-119.

20. (a) Bartual-Murgui, C.; Akou, A.; Thibault, C.; Molnar, G.; Vieu, C.; Salmon, L.; Bousseksou, A., Spin-crossover metal-organic frameworks: promising materials for designing gas sensors. *J. Mater. Chem. C* **2015**, *3*, 1277-1285; (b) Southon, P. D.; Liu, L.; Fellows, E. A.; Price, D. J.; Halder, G. J.; Chapman, K. W.; Moubaraki, B.; Murray, K. S.; Létard, J.-F.; Kepert, C. J., Dynamic Interplay between Spin-Crossover and Host−Guest Function in a Nanoporous Metal−Organic Framework Material. *J. Am. Chem. Soc.* **2009**, *131*, 10998-11009.

21. (a) Murray, K.; Kepert, C., Cooperativity in Spin Crossover Systems: Memory, Magnetism and Microporosity. In *Spin Crossover in Transition Metal Compounds I*, Gütlich, P.; Goodwin, H. A., Eds. Springer Berlin Heidelberg: 2004; Vol. 233, pp 195-228; (b) Halcrow, M. A., Iron(II) complexes of 2,6-di(pyrazol-1-yl)pyridines—A versatile system for spin-crossover research. *Coord. Chem. Rev.* **2009**, *253*, 2493-2514; (c) Craig, G. A.; Roubeau, O.; Aromí, G., Spin state switching in 2,6-bis(pyrazol-3-yl)pyridine (3-bpp) based Fe(II) complexes. *Coord. Chem. Rev.* **2014**, *269*, 13-31.

22. Li, J.-Y.; He, C.-T.; Chen, Y.-C.; Zhang, Z.-M.; Liu, W.; Ni, Z.-P.; Tong, M.-L., Tunable cooperativity in a spin-crossover Hoffman-like metal-organic framework material by aromatic guests. *J. Mater. Chem. C* **2015**.

23. Gutlich, P.; Garcia, Y.; Goodwin, H. A., Spin crossover phenomena in Fe() complexes. *Chem. Soc. Rev.* **2000**, *29*, 419-427.

24. Trofimenko, S., Recent advances in poly(pyrazolyl)borate (scorpionate) chemistry. *Chem. Rev.* **1993**, *93*, 943-980.

25. (a) Chisholm, M. H., Trispyrazolylborate ligands as ancillary ligands in the development of single-site metal alkoxide catalysts for ring-opening polymerization of cyclic esters. *Inorg. Chim. Acta* **2009**, *362*, 4284-4290; (b) Foley, N. A.; Lee, J. P.; Ke, Z.; Gunnoe, T. B.; Cundari, T. R., Ru(II) Catalysts Supported by Hydridotris(pyrazolyl)borate for the Hydroarylation of Olefins: Reaction Scope, Mechanistic Studies, and Guides for the Development of Improved Catalysts. *Acc. Chem. Res.* **2009**, *42*, 585-597; (c) Kumar, M.; DePasquale, J.; White, N. J.; Zeller, M.;

Papish, E. T., Ruthenium Complexes of Triazole-Based Scorpionate Ligands Transfer Hydrogen to Substrates under Base-Free Conditions. *Organometallics* **2013**, *32*, 2135-2144; (d) West, R.; Hill, A. F.; Fink, M. J., *Adv. Organomet. Chem*. Elsevier Inc.: 2008; Vol. 56.
26. (a) Basu, P.; Kail, B. W.; Adams, A. K.; Nemykin, V. N., Quantitation of the ligand effect in oxo-transfer reactions of dioxo-Mo(vi) trispyrazolyl borate complexes. *Dalton Trans.* **2013**, *42*, 3071-3081; (b) Ikeda, A.; Hoshino, K.; Komatsuzaki, H.; Satoh, M.; Nakazawa, J.; Hikichi, S., O_2 activation and external substrate oxidation capability of a Co(ii)-semiquinonato complex. *New J. Chem.* **2013**, *37*, 2377-2383; (c) Joslin, E. E.; McMullin, C. L.; Gunnoe, T. B.; Cundari, T. R.; Sabat, M.; Myers, W. H., Catalytic Hydroarylation of Ethylene Using TpRu(L)(NCMe)Ph (L = 2,6,7-Trioxa-1-phosphabicyclo[2,2,1]heptane): Comparison to TpRu(L′)(NCMe)Ph Systems (L′ = CO, PMe_3, $P(pyr)_3$, or $P(OCH_2)_3CEt$). *Organometallics* **2012**, *31*, 6851-6860; (d) Nakazawa, J.; Terada, S.; Yamada, M.; Hikichi, S., Structural Characterization and Oxidation Reactivity of a Nickel(II) Acylperoxo Complex. *J. Am. Chem. Soc.* **2013**, *135*, 6010-6013.
27. (a) Dixon, N. A.; McQuarters, A. B.; Kraus, J. S.; Soffer, J. B.; Lehnert, N.; Schweitzer-Stenner, R.; Papish, E. T., Dramatic tuning of ligand donor properties in (Ttz)CuCO through remote binding of H^+ (Ttz = hydrotris(triazolyl)borate). *Chem. Commun.* **2013**, *49*, 5571-5573; (b) Doonan, C. J.; Nielsen, D. J.; Smith, P. D.; White, J. M.; George, G. N.; Young, C. G., Models for the Molybdenum Hydroxylases: Synthesis, Characterization and Reactivity of cis-Oxosulfido-Mo(VI) Complexes. *J. Am. Chem. Soc.* **2005**, *128*, 305-316; (c) Eagle, A. A.; George, G. N.; Tiekink, E. R. T.; Young, C. G., Generation and biomimetic chemistry of tungsten–dithiolene complexes containing the hydrotris(3,5-dimethylpyrazol-1-yl)borate ligand. *J. Inorg. Biochem.* **1999**, *76*, 39-45; (d) Pellei, M.; Papini, G.; Lobbia, G. G.; Santini, C., Chemistry and relevant biomimetic applications of group 6 metals systems supported by scorpionates. *Curr. Bioact. Compd.* **2009**, *5*, 321-352.
28. Janiak, C.; Scharmann, T. G.; Hemling, H.; Lentz, D.; Pickardt, J., Transition-Metal Complexes with the Novel Poly (1,2,4-triazolyl)borate Ligands $[HnB(C_2H_2N_3)_4 - n]-$ (n = 1 and 2): Synthesis and Characterization of Metal Complexes of Dihydrobis(1,2,4-triazolyl)borate as One- or Two-Dimensional Coordination Polymers with Six-Membered Ring Water Substructures and the Structure of Two-Dimensional Liquid and Solid Water As Organized in the Intercalate $[Ni\{HB(C_2H_2N_3)_3\}_2] \cdot 6\ H_2O$ (X-ray Studies at 293 and 160 K). *Chem. Ber.* **1995**, *128*, 235-244.
29. (a) Janiak, C.; Scharmann, T. G.; Günther, W.; Hinrichs, W.; Lentz, D., Copper Coordination Polymers with Infinite Chloride Ion Channels and Different Directions of the Jahn-Teller Distortion, Built from Tris(1,2,4-triazolyl)borate as a Modified Tris(pyrazolyl)borate Ligand. *Chem. Ber.* **1996**, *129*, 991-995; (b) Youm, K.-T.; Kim, M. G.; Ko, J.; Jun, M.-J., 1D MnIII–FeII heterometallic coordination polymer built by an approach of metalloligand. *Polyhedron* **2007**, *26*, 929-932.
30. Snyder, C. J.; Martin, P. D.; Heeg, M. J.; Winter, C. H., Synthesis, Structure, and Properties of Group 1 Metal Complexes Containing Nitrogen-Rich Hydrotris(tetrazolyl)borate Ligands. *Chem. Eur. J.* **2013**, *19*, 3306-3310.

31. (a) Effendy; Gioia Lobbia, G.; Marchetti, F.; Pellei, M.; Pettinari, C.; Pettinari, R.; Santini, C.; Skelton, B. W.; White, A. H., Syntheses and spectroscopic and structural characterization of silver(I) complexes containing tris(isobutyl)phosphine and poly(azol-1-yl)borates. *Inorg. Chim. Acta* **2004**, *357*, 4247-4256; (b) Lobbia, G. G.; Pellei, M.; Pettinari, C.; Santini, C.; Skelton, B. W.; White, A. H., Silver(I) poly(1,2,3-benzotriazolyl)borate complexes containing mono- and bidentate phosphine coligands. *Inorg. Chim. Acta* **2005**, *358*, 3633-3641; (c) Shiu, K.-B.; Shen, F.-M.; Wang, S.-L.; Wei, S.-C., Organotransition-metal complexes of multidentate ligands: IX. Synthesis and structure of hydridotris(benzotriazol-l-yl) borate derivatives of the group VI metal carbonyls. *J. Organomet. Chem.* **1989**, *372*, 251-261.
32. Bucher, U. E.; Currao, A.; Nesper, R.; Rueegger, H.; Venanzi, L. M.; Younger, E., .kappa.2-.kappa.3 Isomerism in Rhodium(I) Tris(pyrazolyl)borate Complexes of the Type Tp_3R,4R,5RRh(LL) (LL = 2CO, COD, and NBD) and Their Dynamic Behavior in Solution. X-ray Crystal Structure of TpMeRh(NBD). *Inorg. Chem.* **1995**, *34*, 66-74.
33. (a) Bandoli, G.; Clemente, D. A.; Paolucci, G.; Doretti, L., Bis[Hydrotris(1-Pyrazolyl)Borato]Nickel(II), $C_{18}H_{20}B_2N_{12}Ni$. *Cryst. Struct. Comm.* **1979**, *8*, 965-970; (b) Churchill, M. R.; Gold, K.; Maw, C. E., Crystal structure and molecular geometry of bis[hydrotris(1-pyrazolyl)borato]cobalt(II). *Inorg. Chem.* **1970**, *9*, 1597-1604; (c) Oliver, J. D.; Mullica, D. F.; Hutchinson, B. B.; Milligan, W. O., Iron-nitrogen bond lengths in low-spin and high-spin iron(II) complexes with poly(pyrazolyl)borate ligands. *Inorg. Chem.* **1980**, *19*, 165-169.
34. Lipton, A. S.; Mason, S. S.; Myers, S. M.; Reger, D. L.; Ellis, P. D., ^{113}Cd Shielding Tensors of Monomeric Cadmium Compounds Containing Nitrogen Donor Atoms. 3. CP/MAS Studies on Five-Coordinate Cadmium Complexes Having N3X2 (X = H, N, O, and S) Donor Atoms. *Inorg. Chem.* **1996**, *35*, 7111-7117.
35. Zhang, J.; Wu, T.; Zhou, C.; Chen, S.; Feng, P.; Bu, X., Zeolitic Boron Imidazolate Frameworks. *Angew. Chem. Int. Ed.* **2009**, *48*, 2542-2545.
36. Lobbia, G. G.; Bovio, B.; Santini, C.; Cecchi, P.; Pettinari, C.; Marchetti, F., Tris(4-bromo-1H-pyrazol-1-yl)borato derivatives of first-row transition and group 12 and 14 metals. X-ray crystal structure of $[HB(4\text{-}Brpz)_3]_2$ Cd. 113Cd solution NMR study of bis[poly(pyrazolyl)borato]cadmium complexes. *Polyhedron* **1998**, *17*, 17-26.
37. (a) Arduengo, A. J.; Harlow, R. L.; Kline, M., A stable crystalline carbene. *J. Am. Chemi. Soc.* **1991**, *113*, 361-363; (b) Bellemin-Laponnaz, S.; Dagorne, S., Group 1 and 2 and Early Transition Metal Complexes Bearing N-Heterocyclic Carbene Ligands: Coordination Chemistry, Reactivity, and Applications. *Chem. Rev.* **2014**, *114*, 8747-8774; (c) Enders, D.; Niemeier, O.; Henseler, A., Organocatalysis by N-Heterocyclic Carbenes. *Chem. Rev.* **2007**, *107*, 5606-5655; (d) Glorius, F., *N-Heterocyclic Carbenes in Transition Metal Catalysis*. Springer: 2006; (e) Hopkinson, M. N.; Richter, C.; Schedler, M.; Glorius, F., An overview of N-heterocyclic carbenes. *Nature* **2014**, *510*, 485-496.
38. (a) Asay, M.; Jones, C.; Driess, M., N-Heterocyclic Carbene Analogues with Low-Valent Group 13 and Group 14 Elements: Syntheses, Structures, and Reactivities of a New Generation of Multitalented Ligands. *Chem. Rev.* **2011**, *111*, 354-396; (b) Denk, M.; Lennon, R.; Hayashi, R.; West, R.; Belyakov, A. V.; Verne, H. P.; Haaland, A.;

Wagner, M.; Metzler, N., Synthesis and Structure of a Stable Silylene. *J. Am.Chem. Soc.* **1994**, *116*, 2691-2692; (c) Denk, M. K.; Gupta, S.; Ramachandran, R., Aromatic phosphenium cations. *Tetrahedron Lett.* **1996**, *37*, 9025-9028; (d) Gudat, D.; Gans-Eichler, T.; Nieger, M., Synthesis and unprecedented oxidation of a cationic Sb-analogue of an Arduengo's carbene. *Chem. Commun.* **2004**, 2434-2435; (e) J. Carmalt, C.; Lomeli, V., Cyclic phosphenium and arsenium cations with 6[small pi] electrons and related systems. *Chem. Commun.* **1997**, 2095-2096; (f) Riener, K.; Haslinger, S.; Raba, A.; Högerl, M. P.; Cokoja, M.; Herrmann, W. A.; Kühn, F. E., Chemistry of Iron N-Heterocyclic Carbene Complexes: Syntheses, Structures, Reactivities, and Catalytic Applications. *Chem. Rev.* **2014**, *114*, 5215-5272.

39. (a) Baker, R. J.; Jones, C.; Platts, J. A., Analogies between the Reactivities of an Anionic Gallium(I) Heterocycle and N-Heterocyclic Carbenes Toward Metallocenes. *J. Am. Chem.Soc.* **2003**, *125*, 10534-10535; (b) Burck, S.; Daniels, J.; Gans-Eichler, T.; Gudat, D.; Nättinen, K.; Nieger, M., N-Heterocyclic Phosphenium, Arsenium, and Stibenium Ions as Ligands in Transition Metal Complexes: A Comparative Experimental and Computational Study. *Z. Anorg. Allg.Chem.* **2005**, *631*, 1403-1412; (c) Caputo, C. A.; Brazeau, A. L.; Hynes, Z.; Price, J. T.; Tuononen, H. M.; Jones, N. D., A Cation-Captured Palladium(0) Anion: Synthesis, Structure, and Bonding of $[PdBr(PPh_3)_2]^-$ Ligated by an N-Heterocyclic Phosphenium Cation. *Organometallics* **2009**, *28*, 5261-5265; (d) Day, G. S.; Pan, B.; Kellenberger, D. L.; Foxman, B. M.; Thomas, C. M., Guilty as charged: non-innocent behavior by a pincer ligand featuring a central cationic phosphenium donor. *Chem. Commun.* **2011**, *47*, 3634-3636; (e) Herrmann, W. A.; Denk, M.; Behm, J.; Scherer, W.; Klingan, F.-R.; Bock, H.; Solouki, B.; Wagner, M., Stable Cyclic Germanediyls ("Cyclogermylenes"): Synthesis, Structure, Metal Complexes, and Thermolyses. *Angew. Chem. Int. Ed.* **1992**, *31*, 1485-1488; (f) Schmidt, E. S.; Jockisch, A.; Schmidbaur, H., A Carbene Analogue with Low-Valent Gallium as a Heteroatom in a quasi-Aromatic Imidazolate Anion. *J. Am. Chem. Soc.* **1999**, *121*, 9758-9759; (g) Segawa, Y.; Yamashita, M.; Nozaki, K., Boryllithium: Isolation, Characterization, and Reactivity as a Boryl Anion. *Science* **2006**, *314*, 113-115; (h) Segawa, Y.; Yamashita, M.; Nozaki, K., Syntheses of PBP Pincer Iridium Complexes: A Supporting Boryl Ligand. *J. Am. Chem. Soc.* **2009**, *131*, 9201-9203; (i) Yoo, H.; Carroll, P. J.; Berry, D. H., Synthesis and Structure of Ruthenium−Silylene Complexes: Activation of Si−Cl Bonds in N-Heterocyclic Silanes. *J. Am. Chem. Soc.* **2006**, *128*, 6038-6039; (j) Zabula, A. V.; Hahn, F. E., Mono- and Bidentate Benzannulated N-Heterocyclic Germylenes, Stannylenes and Plumbylenes. *Eur. J. Inorg. Chem.* **2008**, *2008*, 5165-5179.

40. Ottosson, H.; Steel, P. G., Silylenes, Silenes, and Disilenes: Novel Silicon-Based Reagents for Organic Synthesis? *Chem. Eur. J.* **2006**, *12*, 1576-1585.

41. Liao, W.; Chen, Y.; Liu, Y.; Duan, H.; Petersen, J. L.; Shi, X., 1,2,3-triazole-boranes: stable and efficient reagents for ketone and aldehyde reductive amination in organic solvents or in water. *Chem. Commun.* **2009**, 6436-6438.

42. Seefeld, M. A.; Rouse, M. B.; Heerding, D. A.; Peace, S.; Yamashita, D. S.; McNulty, K. C. Preparation of novel heterocyclic carboxamides as inhibitors of Akt activity. WO2008098104A1, 2008.

43. Koren, A. O., Acid-mediated regioselective alkylation of 1,2,3-triazole. *J. Heterocycl. Chem.* **2002**, *39*, 1111-1112.
44. (a) Taddei, M.; Costantino, F.; Ienco, A.; Comotti, A.; Dau, P. V.; Cohen, S. M., Synthesis, breathing, and gas sorption study of the first isoreticular mixed-linker phosphonate based metal-organic frameworks. *Chem. Commun.* **2013**, *49*, 1315-1317; (b) Sanda, S.; Parshamoni, S.; Konar, S., Third-Generation Breathing Metal–Organic Framework with Selective, Stepwise, Reversible, and Hysteretic Adsorption Properties. *Inorg. Chem.* **2013**, *52*, 12866-12868; (c) Walton, K. S., Metal-organic frameworks: Recognizing the unrecognizable. *Nat. Chem.* **2014**, *6*, 277-278; (d) Banerjee, D.; Cairns, A. J.; Liu, J.; Motkuri, R. K.; Nune, S. K.; Fernandez, C. A.; Krishna, R.; Strachan, D. M.; Thallapally, P. K., Potential of Metal–Organic Frameworks for Separation of Xenon and Krypton. *Acc. Chem. Res.* **2015**, *48*, 211-219; (e) Li, J.-R.; Kuppler, R. J.; Zhou, H.-C., Selective gas adsorption and separation in metal-organic frameworks. *Chem. Soc. Rev.* **2009**, *38*, 1477-1504; (f) Schneemann, A.; Henke, S.; Schwedler, I.; Fischer, R. A., Targeted Manipulation of Metal–Organic Frameworks To Direct Sorption Properties. *ChemPhysChem* **2014**, *15*, 823-839.
45. (a) Alaerts, L.; Kirschhock, C. E. A.; Maes, M.; van der Veen, M. A.; Finsy, V.; Depla, A.; Martens, J. A.; Baron, G. V.; Jacobs, P. A.; Denayer, J. F. M.; De Vos, D. E., Selective Adsorption and Separation of Xylene Isomers and Ethylbenzene with the Microporous Vanadium(IV) Terephthalate MIL-47. *Angew. Chem. Int. Ed.* **2007**, *46*, 4293-4297; (b) Alaerts, L.; Maes, M.; Giebeler, L.; Jacobs, P. A.; Martens, J. A.; Denayer, J. F. M.; Kirschhock, C. E. A.; De Vos, D. E., Selective Adsorption and Separation of ortho-Substituted Alkylaromatics with the Microporous Aluminum Terephthalate MIL-53. *J. Am. Chem. Soc.* **2008**, *130*, 14170-14178; (c) Finsy, V.; Verelst, H.; Alaerts, L.; De Vos, D.; Jacobs, P. A.; Baron, G. V.; Denayer, J. F. M., Pore-Filling-Dependent Selectivity Effects in the Vapor-Phase Separation of Xylene Isomers on the Metal−Organic Framework MIL-47. *J. Am. Chem. Soc.* **2008**, *130*, 7110-7118; (d) Maes, M.; Vermoortele, F.; Alaerts, L.; Couck, S.; Kirschhock, C. E. A.; Denayer, J. F. M.; De Vos, D. E., Separation of Styrene and Ethylbenzene on Metal−Organic Frameworks: Analogous Structures with Different Adsorption Mechanisms. *J. Am. Chem. Soc.* **2010**, *132*, 15277-15285; (e) Moreira, M. A.; Santos, J. C.; Ferreira, A. F. P.; Loureiro, J. M.; Rodrigues, A. E., Influence of the Eluent in the MIL-53(Al) Selectivity for Xylene Isomers Separation. *Ind. Eng. Chem. Res.* **2011**, *50*, 7688-7695; (f) Finsy, V.; Kirschhock, C. E. A.; Vedts, G.; Maes, M.; Alaerts, L.; De Vos, D. E.; Baron, G. V.; Denayer, J. F. M., Framework Breathing in the Vapour-Phase Adsorption and Separation of Xylene Isomers with the Metal–Organic Framework MIL-53. *Chem. Eur. J.* **2009**, *15*, 7724-7731.
46. Wang, X.; Eckert, J.; Liu, L.; Jacobson, A. J., Breathing and Twisting: An Investigation of Framework Deformation and Guest Packing in Single Crystals of a Microporous Vanadium Benzenedicarboxylate. *Inorg. Chem.* **2011**, *50*, 2028-2036.
47. (a) Sareeya, B.; Satoru, S.; Susumu, K., Chemistry and application of flexible porous coordination polymers. *Sci. Tech. Adv. Mater.* **2008**, *9*, 014108; (b) Bureekaew, S.; Sato, H.; Matsuda, R.; Kubota, Y.; Hirose, R.; Kim, J.; Kato, K.; Takata, M.; Kitagawa, S., Control of Interpenetration for Tuning Structural Flexibility Influences

Sorption Properties. *Angew. Chem. Int. Ed.* **2010**, *49*, 7660-7664; (c) Demessence, A.; Long, J. R., Selective Gas Adsorption in the Flexible Metal–Organic Frameworks Cu(BDTri)L (L=DMF, DEF). *Chem. Eur. J.* **2010**, *16*, 5902-5908; (d) Kole, G. K.; Vittal, J. J., Solid-state reactivity and structural transformations involving coordination polymers. *Chem. Soc. Rev.* **2013**, *42*, 1755-1775; (e) Fairen-Jimenez, D.; Moggach, S. A.; Wharmby, M. T.; Wright, P. A.; Parsons, S.; Düren, T., Opening the Gate: Framework Flexibility in ZIF-8 Explored by Experiments and Simulations. *J. Am. Chem. Soc.* **2011**, *133*, 8900-8902; (f) Aijaz, A.; Barea, E.; Bharadwaj, P. K., Diamondoid Three-Dimensional Metal-Organic Framework Showing Structural Transformation with Guest Molecules. *Cryst. Growth Des.* **2009**, *9*, 4480-4486; (g) Dybtsev, D. N.; Chun, H.; Kim, K., Rigid and Flexible: A Highly Porous Metal–Organic Framework with Unusual Guest-Dependent Dynamic Behavior. *Angew. Chem. Int. Ed.* **2004**, *43*, 5033-5036.

48. Ferey, G., Swelling Hybrid Solids. *Z. Anorg. Allg. Chem.* **2012**, *638*, 1897-1909.

49. (a) Gould, S. L.; Tranchemontagne, D.; Yaghi, O. M.; Garcia-Garibay, M. A., Amphidynamic Character of Crystalline MOF-5: Rotational Dynamics of Terephthalate Phenylenes in a Free-Volume, Sterically Unhindered Environment. *J. Am. Chem. Soc.* **2008**, *130*, 3246-3247; (b) Horike, S.; Matsuda, R.; Tanaka, D.; Matsubara, S.; Mizuno, M.; Endo, K.; Kitagawa, S., Dynamic Motion of Building Blocks in Porous Coordination Polymers. *Angew. Chem. Int. Ed.* **2006**, *45*, 7226-7230; (c) Horike, S.; Shimomura, S.; Kitagawa, S., Soft porous crystals. *Nat. Chem.* **2009**, *1*, 695-704; (d) Husain, A.; Ellwart, M.; Bourne, S. A.; Öhrström, L.; Oliver, C. L., Single-Crystal-to-Single-Crystal Transformation of a Novel 2-Fold Interpenetrated Cadmium-Organic Framework with Trimesate and 1,2-Bis(4-pyridyl)ethane into the Thermally Desolvated Form Which Exhibits Liquid and Gas Sorption Properties. *Cryst. Growth Des.* **2013**, *13*, 1526-1534; (e) Park, I.-H.; Lee, S. S.; Vittal, J. J., Guest-Triggered Supramolecular Isomerism in a Pillared-Layer Structure with Unusual Isomers of Paddle-Wheel Secondary Building Units by Reversible Single-Crystal-to-Single-Crystal Transformation. *Chem. Eur. J.* **2013**, *19*, 2695-2702; (f) Winston, E. B.; Lowell, P. J.; Vacek, J.; Chocholousova, J.; Michl, J.; Price, J. C., Dipolar molecular rotors in the metal-organic framework crystal IRMOF-2. *Phys. Chem. Chem. Phys.* **2008**, *10*, 5188-5191.

50. (a) Bernardo, P.; Drioli, E.; Golemme, G., Membrane Gas Separation: A Review/State of the Art. *Ind. Eng. Chem. Res.* **2009**, *48*, 4638-4663; (b) Zhang, M.; Bosch, M.; Gentle Iii, T.; Zhou, H.-C., Rational design of metal-organic frameworks with anticipated porosities and functionalities. *CrystEngComm* **2014**, *16*, 4069-4083; (c) Yin, Z.; Zhou, Y.-L.; Zeng, M.-H.; Kurmoo, M., The concept of mixed organic ligands in metal-organic frameworks: design, tuning and functions. *Dalton Trans.* **2015**, *44*, 5258-5275; (d) Chen, T.-H.; Popov, I.; Kaveevivitchai, W.; Miljanić, O. Š., Metal–Organic Frameworks: Rise of the Ligands. *Chem. Mater.* **2014**, *26*, 4322-4325; (e) Wang, C.; Liu, D.; Lin, W., Metal–Organic Frameworks as A Tunable Platform for Designing Functional Molecular Materials. *J. Am. Chem. Soc.* **2013**, *135*, 13222-13234.

51. (a) Venna, S. R.; Carreon, M. A., Metal organic framework membranes for carbon dioxide separation. *Chem. Eng. Sci.* **2015**, *124*, 3-19; (b) Li, B.; Wen, H.-M.; Zhou, W.; Chen, B., Porous Metal–Organic Frameworks for Gas Storage and Separation: What, How, and Why? *J. Phys. Chem. Lett.* **2014**, *5*, 3468-3479; (c) Qiu, S.;

Xue, M.; Zhu, G., Metal-organic framework membranes: from synthesis to separation application. *Chem. Soc. Rev.* **2014**, *43*, 6116-6140.
52. (a) Renz, F., Physical and chemical induced spin crossover. *J. Phys. Conf. Ser.* **2010**, *217*, 012022; (b) Gutlich, P.; Garcia, Y.; Goodwin, H. A., Spin crossover phenomena in Fe(II) complexes. *Chem. Soc. Rev.* **2000**, *29*, 419-427; (c) Kahn, O.; Martinez, C. J., Spin-Transition Polymers: From Molecular Materials Toward Memory Devices. *Science* **1998**, *279*, 44-48.
53. (a) Naik, A. D.; Dîrtu, M. M.; Railliet, A. P.; Marchand-Brynaert, J.; Garcia, Y., Coordination Polymers and Metal Organic Frameworks Derived from 1,2,4-Triazole Amino Acid Linkers. *Polymers* **2011**, *3*, 1750-1775; (b) Bräunlich, I.; Sánchez-Ferrer, A.; Bauer, M.; Schepper, R.; Knüsel, P.; Dshemuchadse, J.; Mezzenga, R.; Caseri, W., Polynuclear Iron(II)–Aminotriazole Spincrossover Complexes (Polymers) In Solution. *Inorg. Chem.* **2014**, *53*, 3546-3557; (c) Ahrens-Botzong, A.; Muffler, K.; Stuppy, S. M.; Rackwitz, S.; Rüffer, R.; Schünemann, V.; Wolny, J. A., Mössbauer spectroscopy, Raman- and IR- microscopy studies of hysteretic behaviour in spincrossover systems. *J. Phys. Conf. Ser.* **2010**, *217*, 012033; (d) Tao, J.; Ma, Z.-J.; Huang, R.-B.; Zheng, L.-S., Synthesis and Characterization of a Tetrazolate-Bridged Coordination Framework Encapsulating D2h-Symmetric Cyclic $(H_2O)_4$ Cluster Arrays. *Inorg. Chem.* **2004**, *43*, 6133-6135; (e) Gaponik, P. N.; Karavai, V. P.; Davshko, I. V.; Degtyarik, M. M.; Bogatikov, A. N., ChemInform Abstract: Synthesis and Properties of Phenylenebis-1H-tetrazoles. *ChemInform* **1992**, *23*.
54. Halcrow, M. A., Structure:function relationships in molecular spin-crossover complexes. *Chem. Soc. Rev.* **2011**, *40*, 4119-4142.
55. Halder, G. J.; Kepert, C. J.; Moubaraki, B.; Murray, K. S.; Cashion, J. D., Guest-Dependent Spin Crossover in a Nanoporous Molecular Framework Material. *Science* **2002**, *298*, 1762-1765.
56. Southon, P. D.; Liu, L.; Fellows, E. A.; Price, D. J.; Halder, G. J.; Chapman, K. W.; Moubaraki, B.; Murray, K. S.; Létard, J.-F. o.; Kepert, C. J., Dynamic Interplay between Spin-Crossover and Host−Guest Function in a Nanoporous Metal−Organic Framework Material. *J. Am. Chem. Soc.* **2009**, *131*, 10998-11009.
57. Ohba, M.; Yoneda, K.; Agustí, G.; Muñoz, M. C.; Gaspar, A. B.; Real, J. A.; Yamasaki, M.; Ando, H.; Nakao, Y.; Sakaki, S.; Kitagawa, S., Bidirectional Chemo-Switching of Spin State in a Microporous Framework. *Angew. Chem. Inter. Ed.* **2009**, *48*, 4767-4771.
58. Naik, A. D.; Marchand-Brynaert, J.; Garcia, Y., A Simplified Approach to N- and N,N′-Linked 1,2,4-Triazoles by Transamination. *Synthesis* **2008**, *2008*, 149-154.
59. Bondar, O. A.; Lukashuk, L. V.; Lysenko, A. B.; Krautscheid, H.; Rusanov, E. B.; Chernega, A. N.; Domasevitch, K. V., New microporous copper(II) coordination polymers based upon bifunctional 1,2,4-triazole/tetrazolate bridges. *CrystEngComm* **2008**, *10*, 1216-1226.
60. (a) Czaja, A. U.; Trukhan, N.; Muller, U., Industrial applications of metal-organic frameworks. *Chem. Soc. Rev.* **2009**, *38*, 1284-1293; (b) Rowsell, J. L. C.; Yaghi, O. M., Metal-organic frameworks: a new class of porous materials. *Microporous Mesoporous Mater.* **2004**, *73*, 3-14.

61. Dincă, M.; Yu, A. F.; Long, J. R., Microporous Metal−Organic Frameworks Incorporating 1,4-Benzeneditetrazolate: Syntheses, Structures, and Hydrogen Storage Properties. *J. Am. Chem. Soc.* **2006**, *128*, 8904-8913.

VITA

Brianna Celiese Hughes was born on September 19, 1986 in Douglas, Georgia to Jamie and Leland Hughes. She was raised in Hazlehurst, Georgia, where she graduated from Jeff Davis High School in 2005, third in her class, and extended her education by attending Georgia Southern University in Statesboro, Georgia. Initially majoring in biology, plans changed quickly after having a glimpse into the world of chemistry and she hasn't looked back. Brianna graduated in 2010 with a B.S. in chemistry and a minor in biology keeping her HOPE scholarship the entire duration of her collegiate education.

During the months leading up to graduation, Brianna began applying to graduate schools in chemistry. After visiting University of Tennessee - Knoxville for their open house, she knew that Rocky Top would become her new home for the next few years. Brianna began a summer program at the University of Tennessee with Dr. David Jenkins before starting her graduate degree in the fall of 2010. During her time in the Ph.D. program at UTK, Brianna published papers, attended a national ACS conference, and attained multiple departmental achievement awards for her accomplishments.